uOttawa

L'Université canadienne
Canada's university

FACULTÉ DES ÉTUDES SUPÉRIEURES ET POSTOCTORALES

uOttawa

L'Université canadienne
Canada's university

FACULTY OF GRADUATE AND POSDOCTORAL STUDIES

Saeed Al-Marzoug

AUTEUR DE LA THÈSE / AUTHOR OF THESIS

Ph.D. (Physics)

GRADE / DEGREE

Department of Physics

FACULTÉ, ÉCOLE, DÉPARTEMENT / FACULTY, SCHOOL, DEPARTMENT

Luus-Jaakola optimization procedure for some problems in optics

TITRE DE LA THÈSE / TITLE OF THESIS

Richard Hodgson

DIRECTEUR (DIRECTRICE) DE LA THÈSE / THESIS SUPERVISOR

CO-DIRECTEUR (CO-DIRECTRICE) DE LA THÈSE / THESIS CO-SUPERVISOR

EXAMINATEURS (EXAMINATRICES) DE LA THÈSE / THESIS EXAMINERS

David Arsner

Andrzej Czajkowski

Liang Chen

Christian Jacob

Gary W. Slater

Le Doyen de la Faculté des études supérieures et postdoctorales / Dean of the Faculty of Graduate and Postdoctoral Studies

Luus-Jaakola optimization procedure for some problems in optics

Saeed M. Al-Marzoug
B.Sc. University 1997
M.Sc. University 2003

THESIS SUBMITTED IN PARTIAL FULFILLMENT
OF THE REQUIREMENTS FOR THE DEGREE OF
DOCTOR OF PHILOSOPHY IN PHYSICS

Ottawa,Ontario
June,2008

Your file Votre référence
ISBN: 978-0-494-52328-5
Our file Notre référence
ISBN: 978-0-494-52328-5

SUMMARY

In today's technology an increasing use is made of materials consisting of thin layers with thicknesses in the range of a few nanometers. Applications of these types of materials can be found in integrated circuits, magnetic heads and tapes, solid-state lasers, X-ray mirrors and coated window glass, etc. They are used for their mechanical, magnetic, optical and/or electrical properties. These properties are related to the structural parameters of these materials, such as the elemental composition, thickness, roughness and number of layers in the material. The first part of this thesis explores both the thickness of layers and the number of layers in x-ray multilayer mirrors by using the Luus-Jaakola optimization procedure in order to achieve a desired reflectivity. The reflectivity of multilayer coatings shows a strong dependence on the thickness of each layer and the number of layers. In the first chapter we present and modify the Luus-Jaakola algorithm to design optical th in-film systems by optimizing the thickness of the layers as well as the number of layers. We show that the optimization model can improve the results using fewer layers of material with the Luus-Jaakola method for the design of x-ray multilayer mirrors in both the angular and spectral domains. Numerical results indicate that the proposed approach performs very competitively with other approaches. It has become possible to design optical coatings with fewer layers. This opens a new opportunity for the design of high quality optical coatings. We then apply this technique to help in the design of multilayer mirrors for a target application, such as an astronomical grazing-incidence hard X-ray telescope. These designs are compared with other author's results. Further, we present a computational study of a modification of the Luus-Jaakola method that could be used in multilayer mirrors with more than two components. Then we apply this method to determine the optical constants, thickness and root mean square roughens of the layers. Finally, in the last part of the thesis we present optimization results of phase-only sampled fiber Bragg gratings by using the modified Luus-Jaakola method. We show that it is able to produce a high number of channels with less refractive-index modulation, high reflectivity, as well as requiring fewer segments.

SOMMAIRE

De nos jours, les usages de matériaux en couches minces de l'ordre du nanomètre se multiplient dans diverses sphères technologiques. Par exemple, on retrouve ces types de matériaux dans les circuits intégrés, les têtes et cassettes magnétiques, les sources de laser à l'état solide, les miroirs pour rayon X, et l'enduit de certaines fenêtres. Ce sont leurs propriétés mécaniques, magnétiques, électriques et/ou optiques qui sont recherchées, propriétés qui sont liées aux paramètres structuraux de ces matériaux, tels la composition, l'épaisseur, la rugosité, et le nombre de couches. La première partie de cette thèse vise une meilleure compréhension du rôle de l'épaisseur et du nombre de couches dans les miroirs multicouches sensibles aux rayons X en utilisant la procédure d'optimisation de Luus-Jaakola pour obtenir la réflexivité désirée qui dépend fortement de ces paramètres. Le premier chapitre présente une version modifiée de l'algorithme de Luus-Jakola permettant la conception de films en couches minces où les deux paramètres sont optimisés. Nous démontrons que notre méthode permet d'améliorer les propriétés de miroirs multicouches sensibles aux rayons X autant dans le domaine angulaire que spectral tout en réduisant le nombre de couches nécessaires. Les résultats numériques montrent que notre approche se compare avantageusement aux autres. Il devient alors possible de créer des films optiques avec moins de couches ouvrant la porte à l'innovation dans le domaine de l'optique de haute qualité. Nous avons par ailleurs utilisé notre technique pour aider à la conception d'un télescope à incidence rasante pour rayons X (“*grazing-incidence hard X-ray telescope*”). Nos résultats se comparent à ceux de l'auteur. Nous présentons ensuite une étude numérique de ! la méthode Luus-Jaakola modifiée permettant l'usage de plus de deux composantes dans les miroirs multicouches. Nous employons ensuite cette nouvelle méthode pour déterminer les constantes optiques, l'épaisseur, et la moyenne des carrés de la rugosité des couches. Enfin, dans la dernière partie de cette thèse, nous utilisons cet algorithme modifié de Luus-Jaakola pour optimiser les réseaux de Bragg à fibres échantillonnés exclusivement dans la phase. Nous pouvons ainsi produire une grande quantité de canaux qui comportent moins de modulation dans l'index de réfraction, possèdent une forte réflexivité, et requièrent moins de segments.

STATEMENT OF ORIGINALITY

The work presented in this thesis is, to the best of my knowledge, new and original. I developed all the original ideas, with crucial input from my supervisor Richard Hodgson. I wrote the computer codes and all the papers, with again some critical proof reading by Prof. Hodgson.

ACKNOWLEDGEMENTS

This thesis arose in part out of years of research that has been done since I came to the University of Ottawa. During this time, I have worked with a great number of people whose contributions have helped in assorted ways to the research and the production of this thesis. They deserve special mention, and it is a pleasure to convey my gratitude to them all in my humble acknowledgments.

In the first place I would like to record my gratitude to Professor Richard Hodgson for his supervision, advice, and guidance from the very early stages of this research, as well as giving me extraordinary experiences throughout the work. Above all and the most needed, he provided me unflinching encouragement and support in various ways. His truly scientific intuition has made him a constant oasis of ideas and passions in science, which exceptionally inspire and enrich my growth as a student, a researcher and the scientist that I want to be. I am indebted to him more than he knows.

I gratefully acknowledge Martin for his translation of my summary into French, and discussions about the thesis style.

Words fail me to express my appreciation to my wife Nawal whose dedication, love and persistent confidence in me, has taken the load off my shoulder. I owe her for unselfishly letting her intelligence, passions, and ambitions collide with mine. Also, I am glad that my children Mohammed, Ebraheem and Zahraa can now finally read about what I have been doing all these years.

Finally, thanks are also given to King Fahd University of Petroleum and Minerals (KFUPM). This thesis would have never been completed without the research scholarships that it provided.

Table of Content

1

Background Theory

By definition, x-rays are a form of electromagnetic radiation produced following the ejection of an inner orbital electron and subsequent transition of atomic orbital electrons from states of high to low energy [1]. According to this definition, the wavelength of x-ray radiation ranges from 0.01 to 23 nm. X-rays with a wavelength longer than 0.1 nm are called soft x-rays. At wavelengths shorter than this, they are called hard x-rays. Hard x-rays overlap the range of gamma rays, which are generated by transitions within atomic nuclei. At the long wavelength side x-rays are adjacent to Extreme Ultra Violet (E/XUV) radiation. Also on this side an overlap between two regions exists, although this overlap is not based on any physical argument: wavelengths longer than 10 nm are usually referred to as XUV. Notably the term EUV, mostly used to indicate the wavelength of 13.4 nm, has been proposed for EUV lithography.

For normal incidence the reflection of electromagnetic radiation with energy less than 25eV($\approx 50nm$)at a single surface can result in reflectivities of between 10 and 80%. For energies larger than 2.5 keV ($\approx 0.5nm$) natural crystals can be used as reflectors. Reflections from different crystal layers, also named Multilayer Optical Coatings, obeying Bragg's law can result in reflectivity values higher than 80% [2]. Artificially layered structures have been of considerable interest during the last decades. Their use in visible optics is widely known. Application of these structures having nanometer periods can be found in superconductivity [3], magnetism [4] and optics in the regime from far UV to X-rays. The high reflectivity as well as the dispersive character of multilayer coatings has opened new possibilities for applications in X-ray optics [5, 6], X-ray tele-

scopes [7, 8] and spectroscopy [9]. Such coatings are basically stacks of thin films, composed of two materials with alternately high and low scattering power or equivalently, optical densities. In principle all material combinations are possible, but in order to obtain stable structures, materials have to be chosen that do not interdiffuse.

The reflectivity of the multilayer coatings is based on interference and depends primarily on the optical properties of materials, the thickness of each layer and the total number of layers.

The reflection at a single interface of two materials can be described using two approaches: an atomic and a macroscopic approach. In the atomic approach [2], each atom in the material is considered to scatter and absorb the radiation. The interaction takes place with the electrons and is strongly dependent on the frequency or wavelength of the incoming wavefront. The reflection is calculated by summing the partially scattered waves. In the macroscopic approach a complex refractive index n is attributed to each material [10]. The reflectivity is then calculated using Fresnel's equations. Because the atomic and macroscopic approach describe the same phenomena, a relation between the refractive index and the atomic scattering factors can be found [2]. In the case of wavelengths larger than 1000Å, which is in the near UV region, interaction with the nearly free electrons in the conduction band of metals is very strong, so reflection at normal incidence can be obtained at smoothly polished metal surfaces. For wavelengths smaller than 100Å, the interaction cross-section is low and decreases rapidly for shorter wavelength X-rays, so normal incidence reflectors consisting of a single interface with vacuum are not efficient.

As a result of interference of waves, reflected from many interfaces, a strongly improved normal incidence reflector with dispersive character can be obtained. Theoretically the reflectivity of multilayer optical coatings depends on the reflectivity of each interface in combination with absorption and extinction of the whole stack. Deviation from the theoretical reflectivity is caused by thickness errors of the individual layers and the character of the interfaces [11]. Thickness errors are increasingly difficult to control for growing numbers of layers in the stack.

Transition layers due to interdiffusion, giving rise to less sharp boundaries, reduce the reflectivity of the interface [12]. For a transition layer consisting of graded composition the reduced reflection is compensated by an enhanced transmission. As more layers take part in the reflection process, an improved energy resolution can be expected, limited by the total absorption or extinction of the whole stack. Due to interface roughness, reflection at each interface is reduced due to scattering. This results in reduced reflected intensity in the specular direction. As scattering can

be considered as a loss and does not give rise to an enhanced transmission, no improvement of the energy resolution can be expected. In the high spatial frequency range, interface roughness behaves as a transition layer for X-rays, where it can give rise to reduced reflectivity and enhanced transmission.

It can be concluded that, in order to produce a multilayer mirror with high reflectivity, the multilayer stack should be made with suitable materials, a proper thickness of each layer, limited interface roughness, and also the most suitable number of layers in the stack.

Nowadays, many different approaches have been proposed for designing multilayer optical coatings. They roughly include analytical, graphical, and numerical methods [13, 14]. The numerical methods are particularly powerful because they can be applied to the design of coatings with complicated properties. In most numerical methods the design of optical coatings is formulated as an optimization problem, based on the use of merit functions, which are often extremely difficult due to the large number of local minima [15], and so it is hard to find feasible solutions efficiently no matter what methods are applied. These numerical approaches can be classified into refinement methods [16, 17] and synthesis methods [18, 19].

Refinement methods, such as damped least square, modified gradient, golden section, Hook and Jeeves search [20], and simplex methods, normally require a starting design that is close to the desired performance. Then, a desired solution is achieved by gradually modifying the starting design. Unfortunately, to choose a starting design is a time-consuming and difficult task in complex systems and the performance of refinement methods is very sensitive to the choice of starting points. On the other hand, the synthesis method, such as gradient evolution and simulated annealing, can generate their own starting designs. Unfortunately, the quality of many synthesis approaches are not satisfactory, so that they need a refinement method to refine their obtained solutions. Many of the above approaches require the determination of first and second derivatives of the merit function or require other limitations. The objective of these approaches is to find the thickness of layers of a multilayer coating and none of these approaches can be used to optimize the number of layers of a multilayer coating system at the same time. Therefore, to develop a good synthesis method which is capable of optimization the layer thicknesses as well as the number of layers is an important research topic.

Luus and Jaakola [21] successfully showed that their method could be used to solve difficult optimization problems with functions having large numbers of local minima. This procedure uses

random search points and systematic contraction of the search region. Luus [22, 23] introduced a multipass formulation for the procedure with the region size between each pass to be changed according to the extent to which each variable changes with respect to the previous pass. With this method, Luus et al.[24] were able to solve the complex cancer chemotherapy optimization problem of high dimension that involved 84 variables and several state constraints. The Luus-Jaakola optimization procedure was successfully employed to solve multiphase equilibrium calculations involving both phase as well as chemical equilibrium [25]. In article I, we modified the Luus-Jaakola method to allow the number of layers in the multilayer mirror structure to be one of the variables that can be optimized, along with the layer thicknesses.

Now I briefly outline the structure of the present thesis. This thesis consists of five published articles related to some problems of optimization in optics. The first three articles [Chapters two,three and four] are part of a series that examines the modification of the Luus-Jaakola optimization procedure as applied to multilayer optical coatings. Some examples are demonstrated in Chapter two. Another application in Hard X-rays is posed in Chapter three. The effect of adding a third material to multilayer stacks is studied in the following article. Finding the optical constants and some information about each layer by using the Luus-Jaakola optimization method is presented in Chapter five. The last chapter of the thesis presents the phase-only sampling fiber Bragg gratings technique for producing channels in optical fibers. Here we used the modification of the Luus-Jaakola method to model this technique.

The remainder of this chapter is organized as follows: section 1 provides a short overview of multilayer theory, and outlines some of the techniques that have been used to calculate the multilayer reflectivity. Section 2 overviews the fiber Bragg gratings and the numerical technique is summarized. The Luus-Jaakola optimization procedure is introduced in section 3, and application of the algorithm to the optimization of Lennard-Jones clusters is also investigated. In section 3.3, we apply the Luus-Jaakola method to a test function, and compare it in several dimensions against the well-known Particle Swarm optimization algorithm.

Theory of Multilayer reflectivity

Several methods are available in the literature for the estimation of the reflectivity of a multilayer stack [26]. Such methods can be grouped according to the theory, kinematical or dynamical, on which they are based. In the kinematical theory, multiple reflections and depletion of the incident

beam are neglected if the reflectivity at each boundary, absorption, and the total reflectivity of the structure are small. In these approximations, the multilayer reflectivity is the vector sum of the reflected amplitudes of the single boundaries [26]. Instead, the dynamical theory takes into full consideration the multiple reflections at each interface and provides an exact determination of the amplitude and phase of the reflected beam. For each theory, two formalisms are available for evaluating the reflectivity performance of multilayers: the recurrence formalism derived by Parrat and the matrix formalism introduced by Abèles [27].

Recursive method

A two-material multilayer coating deposited on a substrate is considered as pictorially shown in Fig 1.1. The stack has N layers counted from the top, so that layer 1 is close to the coating surface and layer N is close to the substrate. The j^{th} layer has a thickness t_j and a complex index of refraction $n_j = 1 - \delta_j - i\beta_j$, where the real term δ_j is associated with dispersion and the imaginary term β_j with absorption. Both parameters can be calculated when the atomic scattering factors f_1 and f_2, the material density and the radiation energy are known [26]. The reflection coefficient of the electric field at the j^{th} interface is defined as:

$$R_j = e^{-ik_j t_j}.(\frac{E_{r,j}}{E_{i,j}}), \tag{1.1}$$

where $E_{i,j}$ and $E_{r,j}$ are the incident and reflected electrical fields in the j^{th} layer, respectively and t_j is the thickness of its layer. In equation 1.1,k_j is the component of the wave vector normal to the coating surface in the j-th layer. Since the parallel component of the wave vector is conserved and equal to $2\pi n_0 \sin\theta_0/\lambda$, k_j is given by:

$$k_j = \frac{2\pi}{\lambda}\sqrt{n_j^2 - n_0^2 sin^2\theta_0}, \tag{1.2}$$

where θ_0 is the incident angle at the interface between air and the first layer and n_0 is the index of refraction of air. In the Parrat formalism, the reflection coefficients at two adjacent interfaces are related by the following relation [28],

$$R_j = e^{-2ik_j t_j}.\frac{R_{j+1} + r_j}{R_{j+1}.r_j + 1}, \tag{1.3}$$

where r_j is the Frensel reflection at the j-th interface. The expression for r_j depends on the polarization of the electromagnetic wave. For s-polarization (electric field perpendicular to the

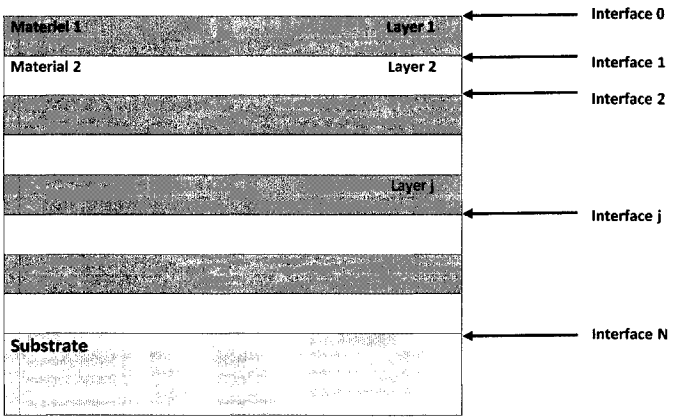

FIGURE 1.1 Pictorial cross-section of a multilayer stack

plane of incidence), r_j is given by :

$$r_j = e^{-2\sigma_j^2 k_j k_{j+1}} \cdot \frac{k_j - k_{j+1}}{k_j + k_{j+1}}, \tag{1.4}$$

whereas,for p-polarization (electric field in the plane of incidence), the Fresnel reflection is :

$$r_j = e^{-2\sigma_j^2 k_j k_{j+1}} \cdot \frac{k_j n_j^{-2} - k_{j+1} n_{j+1}^{-2}}{k_j n_j^{-2} + k_{j+1} n_{j+1}^{-2}}. \tag{1.5}$$

The exponential term in 1.4 and 1.5 is the Nevot-Croce factor modeling roughness and inter-diffusion, assumed to have a Gaussian distribution with vertical rms value σ_j [29].

The reflection coefficient $R \equiv R_0$ of the whole stack can be calculated by recursive application of 1.3. To this end, one starts from the N-th interface where $R_N = r_N$ and then applies relation 1.3 N times up to the topmost interface. Once the electric field reflection coefficient R is calculated, the intensity reflectivity is obtained as $|R|^2$. For un-polarized fields $|R|^2$ must be computed as the average value of the two orthogonal polarizations. Finally, the multilayer performance is evaluated through a figure of merit (FOM) calculated by integrating the reflectivity over either a wavelength or angular range. More precisely, the FOM is defined as :

$$FOM = \sqrt{[\frac{1}{N}\sum_{i=1}^{N}(R(\lambda_i) - R_{des}(\lambda))^2]} \tag{1.6}$$

where R_{des} is the design reflectance.

Matrix method

Using the matrix method , one relates the incident E_i and reflected E_r electrical fields on each side of the multilayer to each other using 2×2 matrix $\mathbf{S}$ [30]:

$$\begin{bmatrix} E_i(z) \\ E_r(z) \end{bmatrix} = \begin{bmatrix} S_{11} & S_{12} \\ S_{21} & S_{22} \end{bmatrix} \begin{bmatrix} E_i(z+t) \\ E_r(z+t) \end{bmatrix}, \tag{1.7}$$

or

$$\mathbf{E}(z) = \mathbf{S}\mathbf{E}(z+t), \tag{1.8}$$

where t equals the thickness of the structure. The scattering matrix $\mathbf{S}$ represents the overall reflection and transmission characteristics of the multilayer and can be composed of a product of the interface and layer matrices $\mathbf{I}$ and $\mathbf{L}$:

$$\mathbf{S} = \prod_{l=1}^{N} \mathbf{I}_l \mathbf{L}_l, \tag{1.9}$$

where N equals the number of layers, and $\mathbf{I}_l$ equals the interface matrix between layer *l* and *l-1*:

$$\mathbf{I}_l = \frac{1}{t_{l-1,l}} \begin{bmatrix} 1 & r_{l-1,l} \\ r_{l-1,l} & 1 \end{bmatrix}, \tag{1.10}$$

where t_{l-1} and r_{l-1} are the Fresnel coefficients for the interface *l-1* and *l*. $\mathbf{L}_l$ describes the effect of propagation through the homogeneous layer *l* alone, and is given by:

$$\mathbf{L}_l = \begin{bmatrix} e^{i\beta_l} & 0 \\ 0 & e^{-i\beta_l} \end{bmatrix}, \tag{1.11}$$

where the phase shift is $\beta_l = \frac{2\pi}{\lambda} n_l t_l cos\theta_l$. The reflectivity R of the multilayer structure can easily be calculated using:

$$R = \frac{S_{21}}{S_{11}}. \tag{1.12}$$

The main advantage of this calculation method is the ability to perform fast calculations of systems with many periods, since one can calculate a matrix describing one period, and then raise this matrix to the power of the number of periods to obtain the result for the full multilayer stack.

Bilayer thickness distribution

Broadband reflectivity is achieved with multilayer coatings by varying the bilayer thicknesses throughout the coating. Methods for specifying the bilayer thickness distribution generally fall into two categories: power-law distributions and "needle variation" derived distributions.

Power law distributions are motivated by the fact that more bilayers are needed to achieve a given level of reflectance for high energy photons than are needed for low energy photons. The use of power law bilayer thickness distributions originated with F. Mezei [31], who was also the first to propose the use of multilayer coatings for the reflection of thermal neutrons. Mezei's approach to power-law parameterizations is outlined in Jonesen [32] and will not be repeated here. Mezei (1976) derives a power law formula for flat response, broadband neutron mirrors assuming that N, the number of bilayers, is large and ignoring multiple reflections and absorption/extinction. The Mezei formula is

$$d(k) = d_c/k^{0.25}, \tag{1.13}$$

where k is the index of the bilayer consisting of layers $j = 2k-1$ and $j = 2k$, and $d_c = \lambda/2sin\theta$. Note also that his definition for the maximum bilayer thickness (d_c) does not include any refraction corrections to the Bragg formula.

Other power-law parameterizations have been developed [33, 34, 35] but will not be expanded upon, with the exception of Jonesen's parameterizations. In his thesis, Jonesen proposes an empirical distribution formula which is a generalization of the Mezei formula:

$$d(k) = \frac{a}{(b+k)^c} \tag{1.14}$$

with $a, c > 0$ and $b > -1$. Using the energy weighted average reflectance at a single incidence angle as his figure of merit, Jonesen finds superior performance with his parameterizations when compared against those of Mezei et al.[31], Schelten and Mika et al.[33], Hayter and Mook et al.[34], and Yamada et al.[35].

The other major class of multilayer designs involves the needle variation technique, where a merit function is used to predict locations in the coating design where the addition or subtraction of bilayers will improve the desired reflectance response. This technique was pioneered in the 1980s by Tikhonoravov [36] and Baskakov [37]. The needle variation method is potentially very

useful for solving the inverse of the Fresnel formulae, i.e., calculating a bilayer distribution from a desired reflectance profile. For example, in the work of Kozhevnikov et al. [38, 39], a recursion relation has been developed to calculate an initial distribution for a given reflectance profile. Standard minimization techniques (Newton-Raphson, Levenberg-Marquadt, simplex) are then used to minimize the mean square difference between the calculated reflectance and the desired profile. The limitation to Kozhevnikov's present method is that the number of bilayers is fixed, narrowing the search space considerably, but also, very likely, missing the true optimal design. It is possible that the needle variation technique, in conjunction with Kozhevnikov's recursion relation, would be a very powerful technique for solving the "inverse problem".

Fiber Bragg gratings

In 1978, at the Canadian Communication Research Center (CRC), Ottawa, Ontario, Canada [40], K. O. Hill et al first demonstrated refractive index changes in a germanosillica optical fiber by launching a beam of intense light into a fiber. Three years later, Lam and Garside [41] showed the relationship between the photoinduced refractive index and the power of the exposed UV light. This led to the discovery of a new writing technology for fiber Bragg gratings. The ultraviolet(UV)light side-written technology, was demonstrated by Meltz et al. [42] in 1989. Fiber Bragg grating technology developed rapidly after UV light side-written technology was developed. Since then, much research has been done to improve the quality and durability of fiber Bragg gratings. Fiber gratings are the keys to modern optical fiber communications and sensory systems. The commercial products of fiber Bragg gratings have been available since early 1995. FBGs have found applications in wavelength stabilization of semiconductor lasers [43]. They are also used in dispersion compensation of long-haul transmission systems [44]. Add/drop multplexers of dense wavelength division multiplexed (WDM) networks have been designed cost effectively using FBGs [45]. For sensor applications, complete discussions on the use of FBGs for temperature, strain and pressure sensors are given by Kersey et al. [46] and Kashyap [47]. Further uses in communications include: gain flattening for erbium-doped fiber amplifiers [48]; wavelength tuning for optical sources [49]; and temperature sensors for wavelength routers in WDM passive optical networks [50]. Recently high channel-count fiber Bragg gratings, as one of the fiber based promising solutions to the broad-band chromatic dispersion compensation for the existing fiber line, has attracted great interest [51, 52, 53, 54, 55]. However, with an increasing number of wavelength-division-multiplex (WDM) channels to cover the full C-band, high channel-count FBG devices become

extremely difficult to realize due to the requirements of a considerably high index modulation and the tremendous precision of the FBG writing tools. To date, three main methods have been proposed trying to make FBG based broad-band devices realizable. One is the utilization of a long-length fiber as reported in [54], where a nonlinearly chirped FBG was demonstrated as a simultaneously chromatic dispersion and slope dispersion compensator, but the grating length is 1 meter - too long to be used in a practical system due to the effects of the package, temperature and uniformity. The second one is to overwrite the gratings with different central wavelengths in the same length of fiber[56], but exactly matching the channel central wavelengths to the ITU grids is a challenge, and the writing time for a high channel-count FBG is too long to be acceptable. The third one is the utilization of various advanced sampling functions [57, 55, 58, 59, 52, 53] to construct a multiple identical FBG in the same length of fiber as that of a one-channel FBG. Of all the sampling methods the phase-only sampling seems to be the most promising one, because it can reduce the index change required for 40- or 80-channel sampled FBGs to practical levels[59, 52]. Furthermore, phase-only sampling has no modulation in its amplitude such that the apodization profile for a multi-channel FBG is the same as that of the seed grating, which thus makes the multi-channel gratings particularly suitable to be fabricated with robust side-writing phase-mask techniques [60].

This section will discuss the fundamentals of fiber Bragg gratings. This will be followed by a discussion the principle of phase-only sampling FBGs. A numerical technique used to simulate the properties of FBGs will be presented.

Fundamentals of Fiber Bragg gratings

The Bragg grating is defined as a perturbation to the effective index of refraction, n_{eff}, of the optical fiber core described by,

$$\delta n_{eff}(z) = \overline{\delta n_{eff}}(1 + \nu \cos[\frac{2\pi}{\Lambda_0} z + \phi(z)]) \tag{1.15}$$

where ν is the fringe visibility, Λ_0 the nominal period, $\phi(z)$ the grating chirp, and $\overline{\delta n_{eff}}$ the "dc" index change spatially averaged over a grating. When light propagates through the periodically alternating regions of higher and lower refractive index within the fiber, it is reflected by successive, coherent scattering from the index variations. When the reflection from a crest in the index modulation is in phase with the next one, we have maximum mode coupling or reflection. The

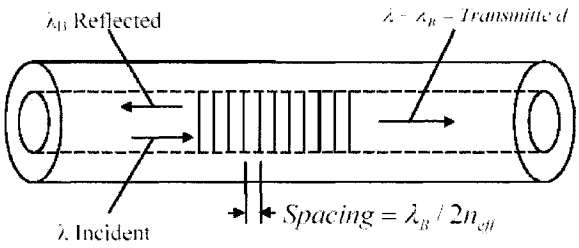

FIGURE 1.2 Bragg resonance for the reflection

strongest mode coupling occurs at the Bragg wavelength, λ_B, (see figure 1.2) given by,

$$\lambda_B = 2n_{eff}\Lambda \tag{1.16}$$

where n_{eff} is the effective mode index of refraction of the fiber. Coupled mode theory is an excellent tool for obtaining quantitative information about the spectral response of fiber Bragg gratings [61, 60]. The assumptions are made that the optical fiber is weakly guiding and no energy is coupled to radiation modes. Using coupled mode theory with the above assumptions, one obtains the following coupled first order differential equations describing mode propagation through the grating (z is the coordinate in the direction of propagation)[62]:

$$\begin{aligned} \frac{dR(z)}{dz} &= i\hat{\sigma}R(z) + i\kappa S(z) \\ \frac{dS(z)}{dz} &= -i\hat{\sigma}S(z) - i\kappa R(z) \end{aligned} \tag{1.17}$$

where $R(z)$ and $S(z)$ are the amplitudes of the forward and backward propagating modes. $\hat{\sigma}$ is the general "dc" self-coupling coefficient as a function of the propagating wavelength, λ, defined as

$$\hat{\sigma} = 2\pi n_{eff}(\frac{1}{\lambda} - \frac{1}{\lambda_D}) + \frac{2\pi}{\lambda}\overline{\delta n_{eff}} - \frac{1}{2}\phi(z)' \tag{1.18}$$

where $\phi(z)' = d\phi/dz$, and $\lambda_D = 2n_{eff}\Lambda_0$ is the design wavelength. κ is the "ac" coupling coefficient defined as

$$\kappa = \frac{\pi}{\lambda}\nu\overline{\delta n_{eff}} \tag{1.19}$$

We define the limits of the grating to be $(-L/2) \leq z \leq (L/2)$. Equation 1.17 can be solved exactly for a uniform grating (i.e. $\Lambda(z)' = \phi(z)' = 0$) with the following boundary conditions:

$R(-L/2) = 1$ and $S((L/2) = 0$. In order to model the physical conditions of the grating, we then transfer the boundary conditions into $R(-L/2) = 1$ and $S(L/2) = 0$ [62].

Principles of phase-only sampled FBG (WDM)

For phase-only sampled fiber Bragg gratings (PSFBG), the effective index modulation can be written by using Fourier analysis as [53] :

$$\delta n_{eff} = \overline{\delta n_{eff}}(1 + \nu Re\{\sum_{m} F_m \exp[i(2\pi z/\Lambda + 2\pi m z/\Lambda_s)]\}) \tag{1.20}$$

$$F_m = \frac{1}{M}\sum_{k=0}^{N-1}[\exp(i2\pi\phi(k))\exp(-ik2\pi m/M)], m = 0, 1, 2, ..., M. \tag{1.21}$$

where Λ_s is the period of the sampling function which contains N segments per sampling period and M is the number of Fourier coefficients which is assumed to be equal to the number of segments N. F_m is the Fourier coefficient which is linearly dependent on the coupling coefficient κ_m as $\kappa_m = F_m\pi\overline{\delta n_{eff}}/\lambda_B$. The channel spacing Δf of the sampled gratings is determined by the sampling period Λ_s through the following expression [63]:

$$\Delta f = \frac{c}{2n_{eff}\Lambda_s}. \tag{1.22}$$

The reflected spectrum for a PSFBG can be calculated by using the transfer matrix method as will be discussed in the next subsection . One begins by defining a fitness function E. In this case, for the minimization problem, the function E provides a measurement of the deviation between the target reflection spectrum and the calculated reflectivity:

$$E = \sum_{i} |R_{calc}(\lambda_i) - R_{targ}(\lambda_i)| \tag{1.23}$$

where $\{\lambda_i\}$ is the discrete set of wavelengths where the reflection spectra are evaluated. This function E becomes the figure-of-merit (FOM) function for the optimization algorithm.

Simulation of fiber Bragg gratings

For non-uniform gratings equation 1.17 can be solved numerically using different techniques. Equation 1.17 can be transformed into the Ricatti differential equation by substituting $\rho(z) = S(z)/R(z)$. Differentiating ρ with respect to z and substituting into equation 1.17 yields

$$\frac{d\rho(z)}{dz} = -i\kappa - 2i\hat{\sigma}\rho(z) - i\kappa\rho(z)^2 \tag{1.24}$$

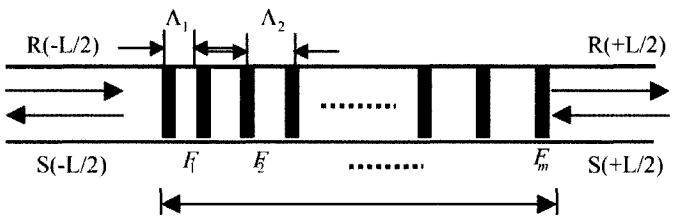

FIGURE 1.3 Principle of the T-matrix approximation

The boundary conditions are then transformed to $\rho(L/2) = 0$. Fourth order Runge-Kutta numerical integration with adaptive step size can be used to solve the equation 1.17 or 1.24 by integrating backwards from $z = L/2$ to $z = -L/2$. The reflectivity $r(\lambda)$ of the Bragg grating can then be calculated as a function of wavelength as

$$r(\lambda) = |\frac{S(-L/2)}{R(-L/2)}|^2 = |\rho(-L/2)|^2 \tag{1.25}$$

However, each of these methods is computationally intensive and therefore not practical for analyzing large amounts of experimental data. For this reason, T-matrix approximations have been developed.

The T-matrix approximation, first introduced by Yamada nad Sakuda, is widely used to model Bragg gratings with non-constant properties [64]. This approach divides the grating into M smaller sections each with uniform coupling properties as illustrated in Fig. 1.3. Defining R_i and S_i to be the field amplitudes after traversing the i^{th} section, the propagation through this uniform section is described by the 2×2 matrix F_i defined as

$$\begin{bmatrix} R_i \\ S_i \end{bmatrix} = F_i \begin{bmatrix} R_{i-1} \\ S_{i-1} \end{bmatrix} \tag{1.26}$$

The components of F_i are given by

$$F_i = \begin{bmatrix} cosh(\gamma_B \Delta z) - i\frac{\widehat{\sigma}}{\gamma_B} sinh(\gamma_B \Delta z) & -i\frac{\kappa}{\gamma_B} sinh(\gamma_B \Delta z) \\ i\frac{\kappa}{\gamma_B} sinh(\gamma_B \Delta z) & cosh(\gamma_B \Delta z) + i\frac{\widehat{\sigma}}{\gamma_B} sinh(\gamma_B \Delta z) \end{bmatrix} \tag{1.27}$$

where, $\gamma_B = \sqrt{\kappa^2 - \hat{\sigma}^2}$, and Δz is the length of the section [62]. For the entire grating, the

transfer matrix, F can be written,

$$\begin{bmatrix} R(-L/2) \\ S(-L/2) \end{bmatrix} = F \begin{bmatrix} R(L/2) \\ S(L/2) \end{bmatrix} \tag{1.28}$$

where, $F = F_M.F_{M-1}.\ldots.F_1$. The reflectivity as a function of wavelength can then be calculated using equation 1.25.

The primary advantage of the T-matrix method is that it is computationally efficient as compared to direct numerical integration of equation 1.17. Typically, $M \cong 100$ is more than sufficient to accurately model chirped gratings. A limitation of the T-matrix approximation is that the number of sections M can not be arbitrarily large since several grating periods are required for complete coupling. Therefore, we require that [60] ,

$$M \ll \frac{2n_{eff}L}{\lambda_D} \tag{1.29}$$

The Luus-Jaakola optimization procedure

The Luus-Jaakola method

As stated by Liao and Luus [65], the idea behind the Luus-Jaakola algorithm is very simple: random solutions are selected over a region that is decreased in size as iterations proceed. The convergence properties of the Luus-Jaakola optimization method has been studied theoretically and some of the conditions for convergence of the algorithm are given[66]. It is shown that the global minimum can be found even if the performance function is multimodal (has several local minima) because searches are made in random directions.

The optimization process is described by a vector x consisting of a set of real numbers. The idea of the optimization is then very simple, so the standard LJ algorithm may be summarized most conveniently in the following [65]:

1. Choose some reasonable initial point x^*; a reasonable initial region size r; and choose the number R of random points to be used at each iteration; and the number of iterations M to be used in a pass.

2. Choose R test points through the equation $x = x^* + Dr$ where D is a diagonal matrix of randomly chosen points from the interval [-0.5, 0.5], and r is the region size vector.
3. Check each of the R test points with respect to feasibility from the domain of variables.
4. For each feasible point evaluate the FOM.
5. Replace x^* by the test point that gives the smallest value for the FOM.
6. Repeat steps 2-5 for M iterations.
7. Reduce the region size vector r by γ through $r^{j+1} = \gamma r^j$ where γ is a region contraction factor such as 0.95, and j is the iteration index.
8. Go to step 2 and continue for M iterations to finish a pass and examine the results.

Optimization Of Lennard-Jones clusters

Determining the global minima of Lennard-Jones clusters poses a challenging task of numerical optimization techniques as the number of local minima on the potential energy surface grows exponentially with the number of atoms N in the cluster [67]. Global optimization techniques to minimize the potential usually combine global and local search algorithms: a global search algorithm, e.g., genetic algorithm [68, 69, 70], simulated annealing [71], or Monte Carlo suggests points from where a local optimization (e.g., conjugate gradient method) is started. The Lennard-Jones potential models van der Waals interactions between noble gas atoms. The Lennard-Jones potential is given by

$$E = 4\epsilon \sum_{i=1}^{N-1} \sum_{j>i}^{N} [(\frac{\sigma}{r_{ij}})^{12} - (\frac{\sigma}{r_{ij}})^{6}] \tag{1.30}$$

where ϵ is the pair well depth and σ is the pair separation at equilibrium. r_{ij} is the distance between atoms i and j. Throughout this section, reduced units $\epsilon = 1$ and $\sigma = 1$ are used. Thus, the potential can be expressed as

$$E = 4 \sum_{i=1}^{N-1} \sum_{j>i}^{N} g_{ij} \tag{1.31}$$

$$g_{ij} := [(\frac{1}{r_{ij}})^{12} - (\frac{1}{r_{ij}})^{6}]. \tag{1.32}$$

The aim is to find a spatial distribution of atoms with minimal energy. The atomic coordinates r_{ij} are the optimization parameters and the number of atoms is N which results in $n = 3N$

parameters. Table 1.1 shows optimized energies for Lennard Jones clusters $N = 2 - 13$ by Luus-Jaakola optimization method over 100 runs, along with the average outcome over the successful runs (global minima are found) out of 100 runs. Also shown is V_{min} , the global minimum published in the literatures [72]. For 2-6 atom clusters, in each case 100% of the runs are successful, for the others, more than 50% on average of the runs are successful. It can be seen that all the optimizations succeeded and compare well with the published results.

TABLE 1.1 Optimized Lennard Jones energy by Luus-Jaakola optimization method over 100 runs (Unit: ϵ)

N	Dimension	V_{min}	Lowest energy	Average energy	Successful runs
2	6	-1.000	-1.000	-1.000	100
3	9	-3.000	-3.000	-3.000	100
4	12	-6.000	-6.000	-6.000	100
5	15	-9.103	-9.103	-9.103	100
6	18	-12.712	-12.712	-12.712	100
7	21	-16.505	-16.505	-16.107	68
8	24	-19.982	-19.982	-18.914	79
9	27	-24.113	-24.113	-23.854	62
10	30	-28.422	-28.422	-27.107	71
11	33	-32.765	-32.765	-28.541	57
12	36	-37.976	-37.966	-32.874	51
13	39	-44.326	-44.326	-37.147	53

Comparing the LJ method with other optimization algorithms

Genetic algorithm

Liao and Luus [65] found that the Luus-Jaakola method is advantageous over the genetic algorithm in test problems. In this subsection, we will summarize the advantages as follows:

- The LJ method is faster than GA.
- Using a center point of the possible solution region in the LJ method is more convenient

to using an initial population randomly chosen over the whole possible region in GA to introduce diversity into the population.

- The number of parameters in the LJ method is less than in the GA, so the LJ optimization procedure is easier to use than the GA.
- The LJ procedure was found to be more reliable than the GA for getting the global optimum.

Particle Swarm optimization

In order to test the capability of the LJ method in comparison to the Particle Swarm optimization, a test problem that is commonly used in the evolutionary computation literature is used. In this subsection, the Particle Swarm Optimization is introduced. Both the LJ method and the Particle Swarm Optimization methods are compared on a test problem function.

Particle Swarm Optimization (PSO) is a metaheuristic based on auto-organizing structures inspired by biological systems. The analysis of bird flock behavior, similar to fish school behavior and swarm insect behavior made researchers try to develop an algorithm able to describe this dynamic [73]. Instead of birds in the sky looking for food, or fish looking for a safe place in the ocean, there is a group of data structures, the particles, "flying" in an n-dimensional search space looking for optima, or for the near-optimal region. PSO is similar to the other evolutionary algorithms in that the system is initialized with a population of random solutions. However, each potential solution is also assigned a randomized velocity, and potential solutions, called particles, corresponding to individuals. Each particle in PSO flies in a D-dimensional problem space with a velocity which is dynamically adjusted according to the flying experiences of its own and its colleagues. The location of the i^{th} particle is represented as $X_i = (x_{i1}, \ldots, x_{id}, \ldots, x_{iD})$,where $x_{id} \in [l_d, u_d], d \in [1, D], l_d, u_d$ are the lower and upper bounds for the d^{th} dimension, respectively. The best previous position (which gave the best fitness value) of the i^{th} particle is recorded and represented as $P_i = (p_{i1}, \ldots, p_{id}, \ldots)$, which is also called *pbest*. The index of the best particle among all the particles in the population is represented by the symbol g. The location P_g is also called *gbest*. The velocity for the i^{th} particle is represented as $V_i = (v_{i1}, \ldots, v_{id}, \ldots, v_{iD})$. The particle swarm optimization concept consists of, at each time step, changing the velocity and

location of each particle toward its *pbest* an *gbest* locations according the equations 1.33 and 1.34, respectively:

$$v_{id} = \omega v_{id} + c_1 \text{rand}()(p_{id} - x_{id}) + c_2 \text{rand}()(p_{gd} - x_{id}) \tag{1.33}$$

$$x_{id} = x_{id} + v_{id} \tag{1.34}$$

where ω is an inertial weight [74], c_1 and c_2 are acceleration constants [75], and *rand()* is a random function in the range [0,1]. For equation 1.33, the first part represents the inertia of the previous velocity; the second part is the "cognition" part, which represents the private thinking by itself; the third part is the "social" part, which represents the cooperation among the particles [76]. The process for implementing PSO is as follows:

1. Initialize a population (array) which includes m particles.
2. Evaluate the desired optimization fitness function for each particle.
3. Compare the evaluated fitness value of each particle with its *pbest*. If current value is better than *pbest*, then set the current location as the *pbest* location. Furthermore, if current value is better than *gbest*, then reset *gbest* to the current index in the particle array.
4. Change the velocity and location of the particle according to the equation 1.33 and 1.34, respectively.
5. Loop to step 2 until a stop criterion is met.

The parameters of a standard PSO include: number of particles m, inertial weight ω, acceleration constants c_1 and c_2.

The Rosenbrock function is our test function, which is also known as the banana function or the second function of De Jong. Figure 1.4 is a plot of the Rosenbrock funtion in 2D. The global optimum lies inside a long, narrow, parabolic shaped flat valley. To find the valley is trivial, however, convergence to the global optimum is difficult and hence this problem has been used in comparing both algorithms. The function has the following definition:

$$f(x) = \sum_{j=1}^{n/2} [100(x_{2j} - x_{2j-1}^2)^2 + (1 - x_{2j-1})^2] \tag{1.35}$$

with any dimension D. Here $x_j \in [-2.048, 2.048]$, and the global minimum is given by $f^*(\mathbf{x}) = 0$ at the point $(1, \ldots, 1)$.

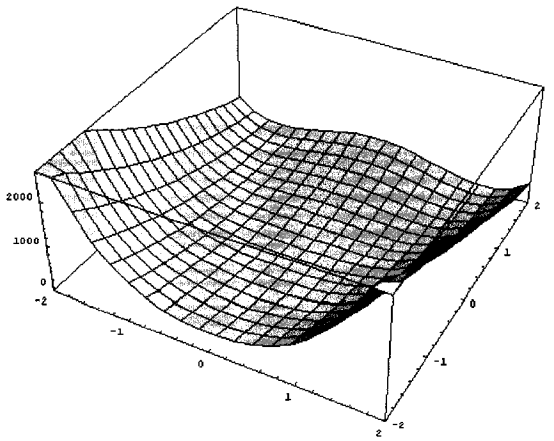

FIGURE 1.4 Rosenbrock function in 2D

We executed the PSO using the following parameter values: 10,000 objective function evaluations, 20 and 50 particles (in configuration #1 and #2 respectively), $\omega = 1$, $c_1 = 2.0$ and $c_2 = 2.0$. As the purpose of this section is to compare the Luus-Jaakola method against the widely-employed PSO, we executed the Luus-Jaakola algorithm using more configurations than the PSO, as presented in Table 1.1. Note that in all configurations the product pass*iteration is equal to 10,000, so that the computational effort is the same as in PSO.

TABLE 1.2 Parameters for each Luus-Jaakola algorithm configuration

Configuration	No. of pass	No. of iteration	γ
#1	40	250	0.97
#2	20	500	0.97
#3	50	200	0.95
#4	10	1000	0.99

Tables 1.3, 1.4, 1.5 and 1.6 show the average best results achieved over 100 runs by both algorithms for 3-D, 6-D, 9-D and 12-D.

Examining the tables, one can note that LJ method performed better than PSO in higher dimensions as well as lower dimensions.

TABLE 1.3 Average best results in 3-D

Algorithm	Configuration	Average Best Result
PSO	#1	3.613e-5
	#2	9.947e-6
LJ	#1	0.000
	#2	0.000
	#3	0.000
	#4	0.000

TABLE 1.4 Average best results in 6-D

Algorithm	Configuration	Average Best Result
PSO	#1	0.026
	#2	0.014
LJ	#1	6.453e-29
	#2	1.117e-19
	#3	2.299e-24
	#4	8.110e-21

Presentation of the thesis

This thesis is composed of five articles published in scientific journals during the course of my Ph.D. degree. Below is a list of these articles, with a few additional notes.

1) S M Al-Marzoug, R J W Hodgson. *Luus-Jaakola optimization procedure for multilayer optical coatings.* ***Opt. Commun. 265***, 234–240 (2006).

   The Luus-Jaakola optimization procedure for global optimization of the reflectivity of multilayer coatings in the extreme-ultra-violet and soft-Xray wavelength ranges has been implemented as a new technique. It shows how the LJ algorithm can evolve the design for better performance. Examples of designs obtained by LJ optimization techniques are given.

2) S M Al-Marzoug, R J W Hodgson. *Optimization of platinum-carbon multilayer mirrors for hard X-ray optics.* ***Opt. Commun. 268***, 84–89 (2006).

TABLE 1.5 Average best results in 9-D

Algorithm	Configuration	Average Best Result
PSO	#1	4.311
	#2	0.357
LJ	#1	1.537e-19
	#2	8.358e-12
	#3	1.028e-16
	#4	5.522e-8

TABLE 1.6 Average best results in 12-D

Algorithm	Configuration	Average Best Result
PSO	#1	3.895
	#2	5.350
LJ	#1	9.685e-11
	#2	0.001
	#3	3.095e-6
	#4	1.198e-5

In this article, Pt/C multilayer coatings have been designed and characterized for use in the Hard X-ray region. By numerically simulating the reflection from a multilayer mirror during the optimization procedure based on Luus-Jaakola algorithm, we obtain optimized layer designs.

3) S M Al-Marzoug, R J W Hodgson. *Optimization of multilayer mirrors at 13.4nm with more than two materials* ***Appl. Opt. 47***, 2155–2160 (2008).

In this article, we study the increase of normal incidence reflectivity generated by the addition of a third material in the period of a standard periodic multilayer, for a wavelength of 13.4 nm. The nature and thickness of the three materials and the number of layers has been optimized to provide the best enhancement of reflectivity. By adding Be layers and C layers in different orders in a Si/Mo stack, we have observed enhancements of the reflectivity and a reduction in the number of layers compared with different orders.

4) S M Al-Marzoug, R J W Hodgson. *Determination of optical constants in the EUV/soft X-ray*

region using the Luus-Jaakola optimization procedure. ***Opt. Commun. 280***, 110–113 (2007).

The present paper considers the calculation of the absorption coefficient, the index of refraction, the root mean square roughness, and the thickness of thin films using optical reflectivity data only. To solve the problem, The Luus-Jaakola optimization approach is used. Examples are presented and discussed.

5) S M Al-Marzoug, R J W Hodgson.. *Luus-Jaakola optimization procedure for phase-only sampled fiber Bragg gratings.****Appl. Opt. 47***, 2275–2280 (2008).

Phase-only sampling functions are proposed for the sampled fiber Bragg gratings (FBGs) with high channel count, which require significantly less refractive-index modulation. The design using the Luus-Jaakola optimization results in high channel uniformity, a high number of channels, with a minimum of segments required.

Other contributions

In the course of my Ph.D. studies, I presented the results of my work at various conferences. Below is a summary of these research related activities

1) Saeed Almarzoug, Richard Hodgson.*Application of Luus-Jaakola optimization method to the design of optical coatings.* ***The World Scientific and Engineering Academy and Society***, Vancouver, Canada (2007).

2) Saeed Almarzoug, Richard Hodgson. *Luus-Jaakola optimization procedure for multilayer optical coatings..* ***Canadian Association of Physicists*** , Brock University, St. Catharines, Canada (2006).

2

Luus-Jaakola optimization procedure for multilayer optical coatings

S M Al-Marzoug, R J W Hodgson. *Opt. Commun* **265**, 234 (2006)

Corrections

1. On page 26, after the equation 3 of the first column. " with $k_j = \frac{2\pi}{\lambda}\sqrt{n_j - n_0^2 cos^2\theta_0}$." shuld read "$k_j = \frac{2\pi}{\lambda}\sqrt{n_j^2 - n_0^2 cos^2\theta_0}$".

2. Equation 5 should read:

$$F_j = F_0 e^{-2k_j k_{j+1}\sigma_j^2}$$

Available online at www.sciencedirect.com
ScienceDirect
Optics Communications 265 (2006) 234–240
OPTICS COMMUNICATIONS
www.elsevier.com/locate/optcom

Luus–Jaakola optimization procedure for multilayer optical coatings

S.M. Al-Marzoug, R.J.W. Hodgson *

Department of Physics, University of Ottawa, ON, Canada K1N 6N5

Received 10 February 2006; accepted 8 March 2006

Abstract

Designing multilayer optical coatings is a difficult optimization problem because of the huge size of the search space. In the present paper, the Luus–Jaakola (LJ) optimization procedure, a new optimization algorithm, is employed to model multilayer optical coatings in the X-ray domain. With this algorithm it is not necessary to specify initially the number of layers present in a design. Only an upper limit needs to be defined. The algorithm has been used to maximize the reflectivity over a range of incident angles at a fixed wavelength, and over a wavelength range at a fixed incident angle. The results show that the LJ algorithm can be effectively applied to the design of multilayer optical coatings resulting in fewer layers than obtained using alternative optimization methods.

PACS: 41.5; 61.10.Kw; 95.55.Ka; 2.30.Zz; 2.60.Pn

Keywords: Luus–Jaakola optimization; Multilayer mirrors; Reflectivity; Depth-graded X-ray optics

1. Introduction

The Luus–Jaakola (LJ) optimization procedure [1] has enabled several difficult optimization problems to be solved, and has provided a means to solve a wide variety of problems in optimal control, such as singular time optimal control [2]. This optimization procedure has been used effectively for the optimization of complex systems such as heat exchanger networks [3], and it has successfully been employed for the minimization of the Gibbs free energy for single phase situations [4]. The LJ method and Genetic algorithm have been compared [5]. It was found that the LJ method is faster and is more reliable in achieving the global optimum.

To improve the convergence rate of the LJ optimization procedure, Luus [6] suggested using a multipass procedure, where at the beginning of the process, the region size for each variable is chosen to be the range over which the variable has moved during the previous pass. If the range is smaller than some tolerance ϵ, then the region size would be set equal to that tolerance.

The goal of this paper is to test the reliability of the LJ optimization procedure by optimizing the reflectivity profile of multilayer coatings both over a range of wavelengths at a fixed incident angle, or over a range of incident angles at a fixed wavelength. The LJ method also has the advantage of allowing the number of layers in the mirror to be one of the variables that can be optimized.

2. Multilayer reflectivity calculation

A basic understanding of multilayer structures for X-ray and extreme-ultraviolet (EUV) optics has grown significantly in the last decade. Multilayer structures based on X-ray and EUV optical systems are in an advanced stage of development in many laboratories. In most of these systems the basic requirements are the highest possible reflection efficiency, moderate energy resolution, and high-imaging characteristics. Therefore, to increase the reflection efficiency, periodic multilayers are prepared as artificial structures where not a single surface but many interfaces reflect the incoming beam and under a

* Corresponding author. Tel.: +1 613 562 5758; fax: +1 613 562 5190.
E-mail addresses: salma224@science.uottawa.ca (S.M. Al-Marzoug), rhodgson@physics.uottawa.ca (R.J.W. Hodgson).

0030-4018/$ - see front matter © 2006 Elsevier B.V. All rights reserved.
doi:10.1016/j.optcom.2006.03.039

convenient angle of incidence, the beams reflected from individual interfaces combine together in phase to produce an intense reflected beam.

A multilayer coating for X-ray mirrors consists of a stack of alternating layers of two materials, an absorber and a spacer. The reflectivity of the multilayer coating depends on several parameters: the pair of materials used, the d-spacing, the thickness ratio, the number of bilayers, and the root-mean-square interface roughness.

If the multilayer optics coatings can be considered as a stratified continuous medium, we may use the optical method to calculate its reflectivity. In this approach, a complex refractive index $n = 1 - \delta - i\beta$ is attributed to each layer, where δ and β are, as usual, the refractive decrement and the absorption coefficients, respectively. We calculate δ and β from the atomic scattering factors f_1 and f_2 using well known relationships, $\delta = Kf_1$ and $\beta = Kf_2$, with

$$K = \frac{r_0 \lambda^2 N_A}{2\pi A}\rho \tag{1}$$

Here r_0 is the classical electron radius, N_A is Avogadro's number, λ is the photon wavelength, A is the atomic weight and ρ is the mass density. The optical constants for the materials are entered from external files which can be loaded from a database [7].

Therefore, the reflectance of a multilayer system, consisting of N layers can be calculated using a recursive formalism given by Parratt [8]. For s-polarized radiation where the electrical field vector is perpendicular to the plane of incidence, the Fresnel coefficient for reflection from the interface between the j and $j+1$ layer is given by

$$F_j = \frac{k_j - k_{j+1}}{k_j + k_{j+1}} \tag{2}$$

and for p-polarized radiation where the electrical field vector is parallel to the plane of incidence it is

$$F_j = \frac{k_j n_j^{-2} - k_{j+1} n_{j+1}^{-2}}{k_j n_j^{-2} + k_{j+1} n_{j+1}^{-2}} \tag{3}$$

with $k_j = \sqrt{n_j - \cos^2\theta_0}$. Here θ_0 and λ are the incident angle and its wavelength, respectively. The recursion relation for reflection is given by:

$$R_j = e^{-2ik_j d_j}\frac{R_{j+1} + F_j}{1 + R_{j+1}F_j} \tag{4}$$

where d_j is the thickness of jth layer. The calculation takes into account the decrease of the specular reflectivity due to the interfacial roughness by the modification of the Fresnel coefficients according to

$$F_j = F_0 e^{2k_j k_{j+1}\sigma_j} \tag{5}$$

where F_0 is the reflection coefficient from an ideal interface for either s- or p-polarization and σ is the root-mean-square deviation of the interface atoms with respect to a smooth interface. Thus, the procedure to compute the net reflection R_0 coefficients for the multilayer stack is to apply Eq. (4) recursively, starting at the bottom layer with the assumption that $R_N = 0$, since there is no reflection from an infinitely thick substrate. The final reflectivity from the multilayer system can by obtained from $|R_0|$. For unpolarized radiation the reflectivity is given by the average value of the two polarizations. Finally, the desired spectral reflectance profiles are fitted by minimizing a suitable merit function that is composed of an appropriate function of R defined within the wavelength range or incident angle range. For that we can define the typical figure-of-merit (FOM):

$$\mathrm{FOM} = \sqrt{\left[\frac{1}{N}\sum_{i=1}^{N}(R - R_{des})^2\right]} \tag{6}$$

where R_{des} is the design reflectance.

3. Algorithm of Luus–Jaakola (LJ) optimization procedure

Let us now consider an optimization procedure that does not require any auxiliary variables to be introduced in order to solve the above parameter estimation problem. The set of variables in the optimization process are described by a vector x consisting of a set of real numbers. The idea of the optimization is then very simple, so the standard LJ algorithm may be summarized most conveniently in the following [5]:

1. Choose some reasonable initial point x^*; a reasonable initial region size r; and choose the number R of random points to be used at each iteration; and the number of iterations M to be used in a pass.
2. Choose R test points through the equation $x = x^* + Dr$ where D is a diagonal matrix of randomly chosen points from the interval $[-0.5, 0.5]$, and r is the region size vector.
3. Check each of the R test points with respect to feasibility from the domain of variables.
4. For each feasible point evaluate the FOM as give by Eq. (6).
5. Replace x^* by the test point that gives the smallest value for the FOM.
6. Repeat steps 2–5 for M iterations.
7. Reduce the region size vector r by γ through $r^{j+1} = \gamma r^j$ where γ is a region contraction factor such as 0.95, and j is the iteration index.
8. Go to step 2 and continue for M iterations to finish a pass and examine the results.

The modification of the LJ optimization procedure for multilayer optics coatings may be given by the followings steps:

1. Choose a reasonable initial number of layers ι^*, for example $\iota^* = 0.5(l_{max} + l_{min})$, where l_{max} is the maximum number of layers and l_{min} is the minimum number of layers allowed.

2. Choose a reasonable initial region size for the number of layers r_{layer}, for example $r_{\text{layer}} = 10(l_{\max} - l_{\min})$.
3. Choose some reasonable initial thickness d^*, for example $d^* = 0.5(d_{\min} + d_{\max})$, where $d_{\min}$ is the minimum thickness and $d_{\max}$ is the maximum thickness.
4. Choose a reasonable initial region size r, for example $r = 4(d_{\max} - d_{\min})$.
5. Choose the number R of random points to be used at each iteration; the number of iterations M to be used in a pass; and the number of passes Q.
6. Choose a test point R through the equation $\iota = \iota^* + Dr_{\text{layer}}$ where D is a diagonal matrix with randomly chosen elements from the interval $[-0.5, 0.5]$.
7. Check each of the R test points with respect to feasibility with the domain of layers.
8. For every R points, choose the thickness point through the equation $d = d^* + Dr$.
9. Check each of the R test points with respect to feasibility for the domain of thicknesses.
10. For each feasible point evaluate the FOM as give by Eq. (6).
11. Replace ι^* by the test point that gives the smallest value for the FOM.
12. Replace d^* by the test point that gives the smallest value for the FOM.
13. Repeat steps 2–12 for M iterations.
14. Reduce the region size vector r by γ through $r^{j+1} = \gamma r^j$ where γ is a region contraction factor of thicknesses such as 0.95, and j is the iteration index; reduce the region size for the number of layers by $r^{j+1}_{\text{layer}} = \alpha r^j_{\text{layer}}$, where α is a region contraction factor for layers, such as 0.96.
15. Go to step 6 and continue for M iterations to finish a pass.
16. At the end of the pass determine the region size to be used at the beginning of the next pass from the size of the variation of each variable as suggested by Luus [5], i.e., choose

$$r_i^{k+1} = |d_i^*(k) - d_i^*(k-1)|, \quad i = 1, 2, \ldots, N \tag{7}$$

where $d_i^*(k)$ is the best value of d_i after k passes and $d_i^*(k-1)$ is the best value of d_i after $k-1$ passes and N is the number of layers. To prevent the region becoming zero, if the region size as calculated from Eq. (7) is less than the region collapse parameter ε, set the region size at the beginning of the pass for that variable equal to ε.
17. If r_{layer} is less than some parameter η put the region size for the next pass equal to some integer value, for Example 10.
18. Continue the procedure for Q passes.
19. Run the algorithms many times and examine the results.

4. Examples and numerical results

Initially the algorithm was used to design multilayer stack structures for high reflectivity in the wavelength range 16–19 nm at normal incidence. Note that for X-ray mirrors this is a sufficiently wide range of wavelengths. On the one hand it is required that the mean reflectance in the target wavelength range is a high value, wherever possible. On the other hand it is also desirable to have the smallest possible number of layers. It is also required that variations of the reflectance from the mean value in the target wavelength be small enough.

Along with the above target demands there are a number of additional feasibility demands. The thicknesses of each layer should be in the range from 0.8 to 12 nm. Also the roughness was taken to be $\sigma = 0.3$ nm.

The layer materials were chosen to be Mo and Si, which are known to be suitable materials for the construction of high reflectivity mirrors in this region of the soft X-ray spectrum. For the absorber we have selected Mo and the spacer is Si. The multilayer consists of alternating absorber and spacer layers. The target reflectances for the wavelength region from 16–19 nm was chosen to be 0.2, 0.25, and 0.3. The optimization process adjusts the thickness of each layer, as well as the total number of layers in the stack, in order to achieve the best value for the FOM.

The results are shown in Figs. 1–3. In each case the left panel shows the optimized reflectivity. The design values for the reflectivity R_0 are 0.2, 0.25, and 0.3, respectively. The reflectance shown in Fig. 1 was achieved with a stack having 22 layers. Its reflectance features an excellent uniformity ($\Delta R = 0.002$). The best results as shown in Fig. 2 were achieved with a 32-layer stack. The mean reflectance ($\overline{R} = 0.252$) in this case is very good, but the reflectance uniformity in the target region is slightly worse than in the previous case ($\Delta R = 0.004$). Fig. 3 shows that the response is less uniform when $R_0 = 0.3$ and more layers were required to achieve the desired reflectivity (34 layers). The bilayer thicknesses for each design are shown in the right panel in each of the figures.

The effectiveness of the LJ optimization procedure is confirmed by comparing the above results with those of other authors. Table 1 presents the reflectance of Mo/Si mirrors from Ref. [9] in the same wavelength range. The number of layers, mean reflectance values, and deviations are compared. For the first case ($R_0 = 0.2$), the mean reflectance is the same as the result from our LJ calculation, however the uniformity in our case is much better than obtained in Ref. [9]. In the second case ($R_0 = 0.25$), the LJ method gives an excellent result for both the mean reflectance and the deviation from the mean. The average reflectivity in the $R_0 = 0.3$ case is much better than in Ref. [9]. In all three cases the LJ calculations led to better results with far fewer layers. We reduced the number of layers by 64% in the first design, whereas in the second and third designs they were reduced by 50%.

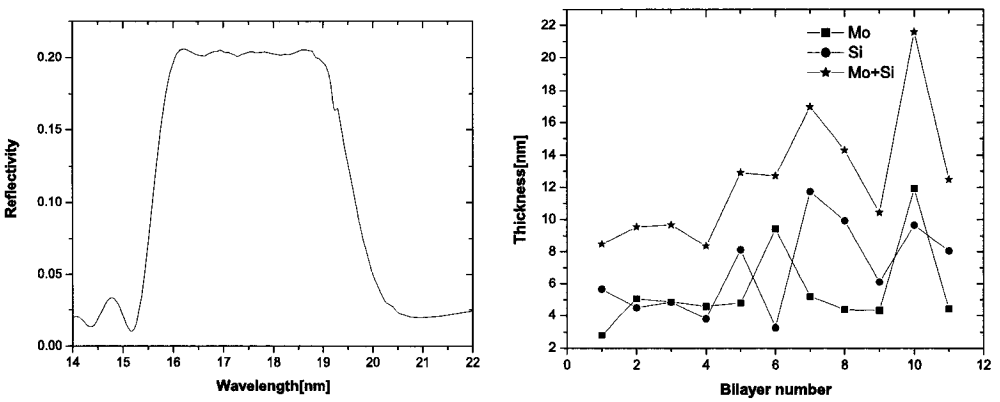

Fig. 1. Optimized reflectivity (left) of broadband multilayer mirror Mo/Si in the wavelength range from 16 to 19 nm and the thickness (right) of each bilayer for design $R_0 = 0.2$.

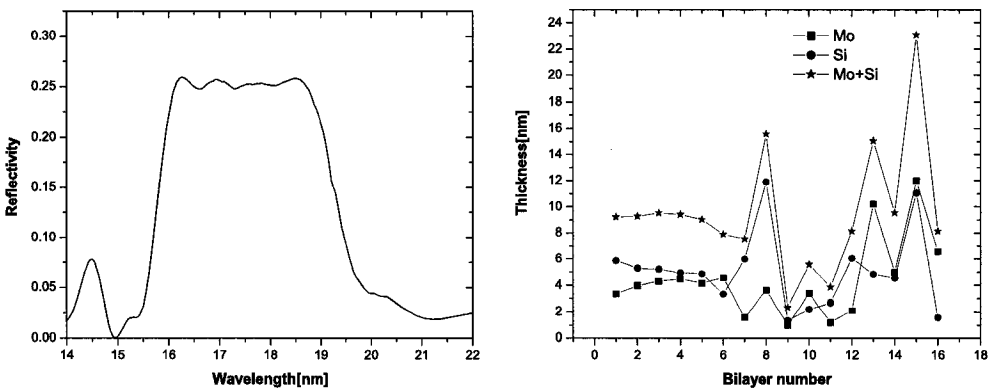

Fig. 2. Optimized reflectivity (left) of broadband multilayer mirror Mo/Si in the wavelength range from 16 to 19 nm and the thickness (right) of each bilayer for design $R_0 = 0.25$.

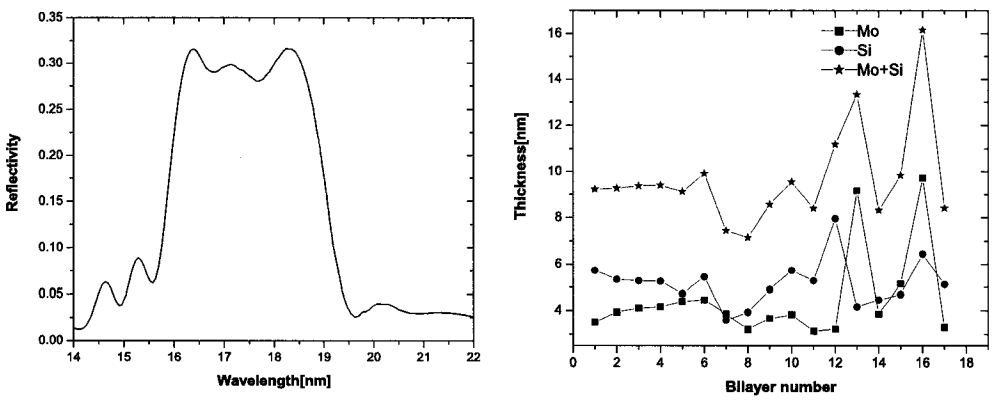

Fig. 3. Optimized reflectivity (left) of broadband multilayer mirror Mo/Si in the wavelength range from 16 to 19 nm and the thickness (right) of each bilayer for design $R_0 = 0.3$.

The LJ optimization procedure was also tested by applying it to Pt/C multilayer mirrors over the energy range 20–30 keV. In this case the incident radiation struck the mirror at a glancing angle of 0.2°, and a roughness of 0.5 nm was assumed. The results of the optimization for this mirror are shown in Fig. 4. This same example was optimized using a

Table 1
Parameters of multilayer mirror Mo/Si for normal incidence with rms roughness 0.3 nm

Design R_0	No. of layers		$\overline{R}$		ΔR	
	Ref. [9]	LJ	Ref. [9]	LJ	Ref. [9]	LJ
0.2	60	22	0.20	0.20	0.04	0.002
0.25	60	32	0.225	0.253	0.08	0.004
0.3	60	34	0.23	0.288	0.14	0.027

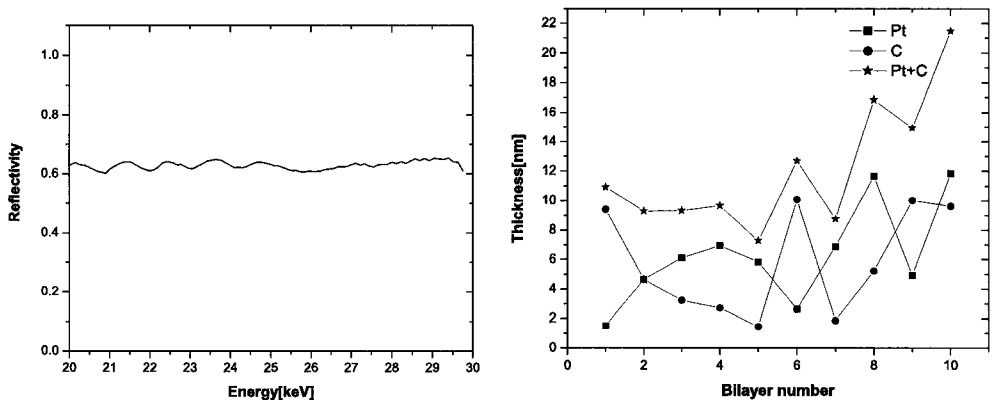

Fig. 4. Optimized reflectivity (left) of broadband multilayer mirror Pt/C in the energy range from 20 to 30 keV and the thickness (right) of each bilayer.

Table 2
Parameters of multilayer mirror Pt/C for angular incidence 0.2° and rms roughness 0.5 nm

Optimization algorithm	No. of layers	$\overline{R}$	ΔR
Genetic algorithm	20	0.6079	0.0293
Luus–Jaakola method	20	0.62836	0.01281

Genetic algorithm in Ref. [10]. Table 2 shows the results of both the Genetic algorithm and the LJ method for the Pt/C multilayer. In the case of the Genetic algorithm, the number of layers was fixed, whereas in the LJ case, the number of layers was variable. It is interesting to see that in the latter case the optimum number of layers turned out to be the same as for the Genetic algorithm. However the LJ optimization procedure resulted in a lower standard deviation and a higher average reflectivity.

The LJ procedure was also applied to an example with a fixed wavelength, but with a range of angles for the incident radiation. A W/C multilayer coating at a wavelength of 0.154 nm was studied over three different angular ranges. Typical thicknesses of layers are from 0.8 to 10 nm. The root-mean-square surface roughness σ was estimated to be 0.3 nm. The left panels in Figs. 5–7 show the optimized reflectivity spectra in different angular ranges

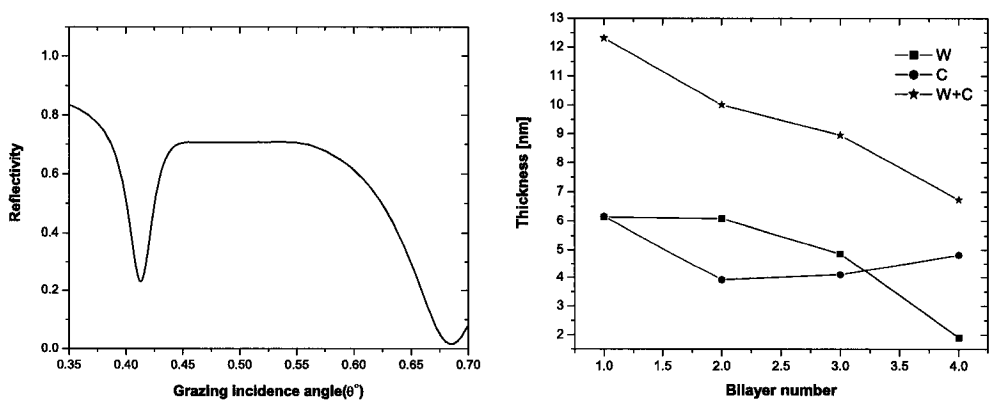

Fig. 5. Optimized reflectivity (left) of broadband multilayer mirror W/C in angular range from 0.45° to 0.55°, and the thickness (right) of each bilayer.

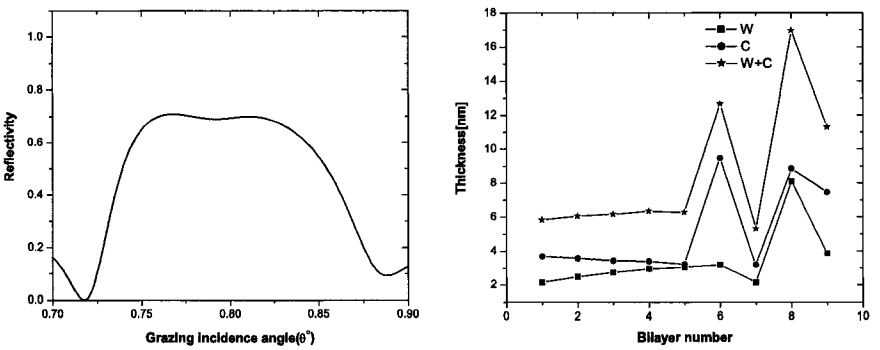

Fig. 6. Optimized reflectivity (left) of broadband multilayer mirror W/C in angular range from 0.75° to 0.84° and the thickness (right) of each bilayer.

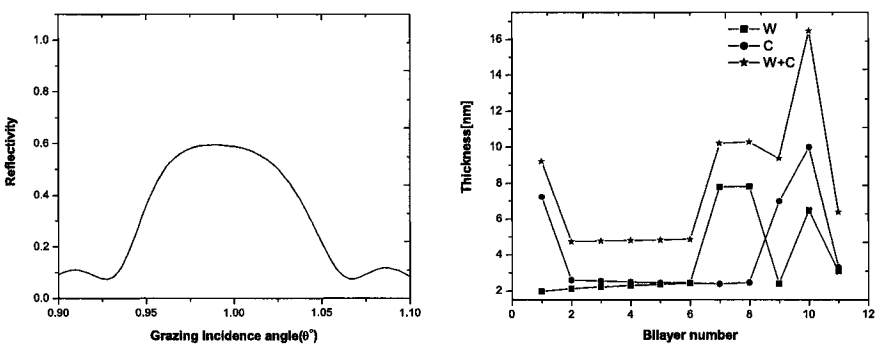

Fig. 7. Optimized reflectivity (left) of broadband multilayer mirror W/C in angular range from 0.96° to 1.03° and the thickness (right) of each bilayer.

Table 3
Parameters of multilayer mirror W/C for $\lambda = 0.154$ nm, with rms roughness $\sigma = 0.3$ nm

Angular range	No. of layers		$\overline{R}$		ΔR	
	Ref. [11]	LJ	Ref. [11]	LJ	Ref. [11]	LJ
0.45–0.55	12	8	0.706	0.706	0.006	0.0016
0.75–0.84	20	18	0.668	0.689	0.017	0.018
0.96–1.03	24	22	0.548	0.563	0.008	0.0324

after applying the LJ method. The performance parameters of these figures are compared with results from Ref. [11], and are listed in Table 3.

From Table 3 we see that both results have the same mean reflectivity in the angular range 0.45°–0.55°, but the LJ method gives a more uniform reflectivity (standard deviation = 6 times lower) and uses fewer layers (33% less). In the angular range 0.75°–0.84°, both results have the same standard deviation, but the LJ result has a 3% higher average reflectivity and 10% fewer layers. Finally, the result in Ref. [11] has a smaller deviation in the angular range 0.96°–1.03° than the LJ method. However, the LJ method gives a higher average reflectivity with fewer layers. The bilayer thicknesses for each angular range are shown in the right panel of each figure.

5. Conclusion

The Luus–Jaakola optimization procedure proves to be a very successful optimization scheme for the design of multilayer mirrors. Like the Genetic Algorithm (GA), and other stochastic methods, no derivatives of the figure-of-merit function are required. The prime advantage of the LJ algorithm over the GA is that one can mix integer and real variables in the scheme so that the number of layers can be optimized at the same time as the thicknesses of the layers

are being adjusted to achieve an optimum reflectivity. This should prove to be a useful tool for this type of design.

Acknowledgments

The authors acknowledge the financial support from the government of Saudi Arabia for this study.

References

[1] R. Luus, THI. Jaakola, AIChE J. 19 (1973) 760.
[2] R. Luus, Nonlinear Anal. 47 (2001) 5647.
[3] R. Luus, Ind. Eng. Chem. Res. 32 (1993) 2633.
[4] Y.P. Lee, G.P. Rangahiah, R. Luus, Comp. Chem. Eng. 23 (1999) 1183.
[5] B. Liao, R. Luus, Eng. Optimiz. 37 (4) (2005) 381.
[6] R. Luus, Hung. J. Ind. Chem. 26 (1998) 281.
[7] Lawrence Livermore National Laboratory optical constants database ftp://www-phys.llnl.gov/pub/rayleigh.
[8] M. Born, E. Wolf, Principles of Optics, seventh ed., Cambridge University Press, Cambridge, 1999.
[9] A. Michette, Z. Wang, Opt. Commun. 177 (2000) 47.
[10] P. Binda, F. Zocchi, Proc. SPIE 5536 (2000) 97.
[11] Z. Wang, J. Cao, A. Michette, Opt. Commun. 177 (2000) 25.

3

Optimization of platinum-carbon multilayer mirrors for hard X-ray optics

S M Al-Marzoug, R J W Hodgson. *Opt. Commun* **268**, 84 (2006)

Available online at www.sciencedirect.com
ScienceDirect
Optics Communications 268 (2006) 84–89
OPTICS COMMUNICATIONS
www.elsevier.com/locate/optcom

Optimization of platinum–carbon multilayer mirrors for hard X-ray optics

S.M. Al-Marzoug, R.J.W. Hodgson *

Department of Physics, University of Ottawa, 50 Louis Pasteur, ON, Canada K1N 6N5

Received 19 April 2006; received in revised form 30 June 2006; accepted 30 June 2006

Abstract

The design of hard X-ray optics for astrophysical technology is one of the key technologies for investigating active galaxies and clusters of galaxies. In the present paper, we have optimized multilayer mirrors of platinum–carbon layer pairs for the hard X-ray region at different grazing angles. The Luus–Jaakola optimization procedure has been implemented for the global optimization of multialyer mirrors. With this algorithm it is not necessary to specify initially the number of layers present in a design.

PACS: 41.5; 61.10.Kw; 95.55.Ka; 2.30.Zz; 2.60.Pn

Keywords: Luus–Jaakola optimization; Multilayer mirrors; Reflectivity; Hard X-ray optics

1. Introduction

Designing X-ray multilayer mirrors is the enabling technology for a new generation of astronomical space telescopes working above $E = 10$ keV, including the high-energy focusing telescope (HEFT) [1] and InFocus [2] balloon instruments. The multilayer coatings are designed to provide broadband X-ray reflectance at grazing incidence. The multilayer mirrors used for a hard X-ray telescopes must satisfy many requirements, such as: (1) high reflectivity in the 20–40 keV band with grazing angles of 0.107–0.358° to get a large effective area for the telescope, (2) a flat and broad energy response, and (3) a minimum number of layer pairs N in order to shorten the time for their mass production [3–7].

Several methods of designing multilayer stacks have been studied for astronomical applications, such as Genetic algorithms [8], multi-block methods [9], simplex methods [10], and simulated annealing methods [11]. Most of these methods optimized the multilayer stack by varying the thicknesses of the layers for a fixed number of layers. However, the Luus–Jaakola (LJ) optimization procedure [12] allows the number of layers in the mirror to be one of the variables in the optimization algorithm that can be optimized. This optimization procedure has been used effectively for optimization of complex systems such as heat exchanger networks [13,14], and it has successfully been employed for the minimization of the Gibbs free energy for single phase situations [15]. The LJ method and Genetic algorithm have been compared [16]. It was found that the LJ method is faster and offers a higher reliability in achieving the global optimum.

To improve the convergence rate of the LJ optimization procedure, Luus [17] suggested using a multi-pass procedure, where at the beginning of the process, the region size for each variable is chosen to be the range over which the variable has moved during the previous pass. If the range is smaller than some tolerance ϵ, then the region size would be set equal to that tolerance. In this paper, we make use of the Luus–Jaakola optimization procedure to find the maximum reflectivity of Pt/C mirrors in a given energy band with the minimum number layer pairs to be used in hard X-ray telescopes.

* Corresponding author. Tel.: +1 6135625758; fax: +1 6135625190.
E-mail address: rhodgson@physics.uottawa.ca (R.J.W. Hodgson).

0030-4018/$ - see front matter © 2006 Elsevier B.V. All rights reserved.
doi:10.1016/j.optcom.2006.06.081

2. Multilayer reflectivity calculation

A basic understanding of multilayer structures for X-ray and extreme-ultraviolet (EUV) optics has grown significantly in the last decade. Multilayer structures based on X-ray and EUV optical systems are in an advanced stage of development in many laboratories. In most of these systems the basic requirements are the highest possible reflection efficiency, moderate energy resolution and high-imaging characteristics. Therefore, to increase the reflection efficiency, periodic multilayers are prepared as artificial structures where not a single surface but many interfaces reflect the incoming beam and under a convenient angle of incidence, the beams reflected from individual interfaces combine together in phase to produce an intense reflected beam.

A multilayer coating for X-ray mirrors consists of a stack of alternating layers of two materials, an absorber and a spacer. The reflectivity of the multilayer coating depends on several parameters: the pair of materials used, the d-spacing, the thickness ratio, the number of bilayers, and the root-mean-square interface roughness.

If the multilayer optics coatings can be considered as a stratified continuous medium, we may use the optical method to calculate its reflectivity. In this approach, a complex refractive index $n = 1 - \delta - i\beta$ is attributed to each layer, where δ and β are, as usual, the refractive decrement and the absorption coefficients, respectively. We calculate δ and β from the atomic scattering factors f_1 and f_2 using well known relationships, $\delta = Kf_1$ and $\beta = Kf_2$, with

$$K = \frac{r_0 \lambda^2 N_A}{2\pi A}\rho \tag{1}$$

Here r_0 is the classical electron radius, N_A is Avogadro's number, λ is the photon wavelength, A is the atomic weight and ρ is the mass density. The optical constants for the materials are entered from external files which can be loaded from a database [18].

Therefore, the reflectance of a multilayer system, consisting of N layers can be calculated using a recursive formalism given by Parratt [19]. For s-polarized radiation where the electrical field vector is perpendicular to the plane of incidence, the Fresnel coefficient for reflection from the interface between the j and $j+1$ layer is given by

$$F_j = \frac{k_j - k_{j+1}}{k_j + k_{j+1}} \tag{2}$$

and for p-polarized radiation where the electrical field vector is parallel to the plane of incidence it is

$$F_j = \frac{k_j n_j^{-2} - k_{j+1} n_{j+1}^{-2}}{k_j n_j^{-2} + k_{j+1} n_{j+1}^{-2}} \tag{3}$$

with $k_j = \sqrt{n_j^2 - \cos^2\theta_0}$. Here θ_0 and λ are the incident angle and its wavelength, respectively. The recursion relation for reflection is given by

$$R_j = e^{-2ik_j d_j}\frac{R_{j+1} + F_j}{1 + R_{j+1}F_j} \tag{4}$$

where d_j is the thickness of jth layer. The calculation takes into account the decrease of the specular reflectivity due to the interfacial roughness by the modification of the Fresnel coefficients according to

$$F_j = F_0 e^{-2k_j k_{j+1}\sigma_j^2} \tag{5}$$

where F_0 is the reflection coefficient from an ideal interface for either s or p polarization and σ is the root mean square deviation of the interface atoms with respect to a smooth interface. Thus, the procedure to compute the net reflection R_0 coefficients for the multilayer stack is to apply Eq. (4) recursively, starting at the bottom layer with the assumption that $R_N = 0$, since there is no reflection from an infinitely thick substrate. The final reflectivity from the multilayer system can by obtained from $|R_0|$. For unpolarized radiation the reflectivity is given by the average value of the two polarizations. Finally, the desired spectral reflectance profiles are fitted by minimizing a suitable merit function that is composed of an appropriate function of R defined within the wavelength range or incident angle range. For that we can define the typical figure of merit (FOM):

$$\mathrm{FOM} = \sqrt{\left[\frac{1}{N}\sum_{i=1}^{N}(R(\lambda_i) - R_{\mathrm{des}}(\lambda))^2\right]} \tag{6}$$

where R_{des} is the design reflectance.

3. Algorithm of Luus–Jaakola (LJ) optimization procedure

The problem of maximizing the reflectivity of the multilayer structure reduces to that of determining the layer thicknesses and the number of layers in the structure. The optimization procedure that is employed here does not require any auxiliary variables to be introduced in order to solve this parameter estimation problem. The set of variables in the optimization process, i.e., the layer thicknesses and the number of layers, are described by a vector x consisting of a set of real numbers. The idea of the optimization is then very simple, so the standard LJ algorithm may be summarized most conveniently in the following [16]:

(1) Choose some reasonable initial point x^*; a reasonable initial region size r; and choose the number R of random points to be used at each iteration; and the number of iterations M to be used in a pass.
(2) Choose R test points through the equation $x = x^* + Dr$ where D is a diagonal matrix of randomly chosen points from the interval $[-0.5, 0.5]$, and r is the region size vector.
(3) Check each of the R test points with respect to feasibility from the domain of variables.
(4) For each feasible point evaluate the FOM as given by Eq. (6).

(5) Replace x^* by the test point that gives the smallest value for the FOM.
(6) Repeat Steps 2–5 for M iterations.
(7) Reduce the region size vector r by γ through $r^{j+1} = \gamma r^j$ where γ is a region contraction factor such as 0.95, and j is the iteration index.
(8) Go to Step 2 and continue for M iterations to finish a pass and examine the results.

The modification of the LJ optimization procedure for multilayer optics coatings may be given by the followings steps:

(1) Choose a reasonable initial number of layers ι^*, for example $\iota^* = 0.5(l_{max} + l_{min})$, where l_{max} is the maximum number of layers and l_{min} is the minimum number of layers allowed.
(2) Choose a reasonable initial region size for the number of layers r_{layer}, for example, $r_{layer} = 10(l_{max} - l_{min})$.
(3) Choose some reasonable initial thickness d^*, for example, $d^* = 0.5(d_{min} + d_{max})$, where d_{min} is the minimum thickness and d_{max} is the maximum thickness.
(4) Choose a reasonable initial region size r, for example, $r = 4(d_{max} - d_{min})$.
(5) Choose the number R of random points to be used at each iteration; the number of iterations M to be used in a pass; and the number of passes Q.
(6) Choose a test point R through the equation $\iota = \iota^* + Dr_{layer}$ where D is a diagonal matrix with randomly chosen elements from the interval $[-0.5, 0.5]$.
(7) Check each of the R test points with respect to feasibility with the domain of layers.
(8) For every R points, choose the thickness point through the equation $d = d^* + Dr$.
(9) Check each of the R test points with respect to feasibility for the domain of thicknesses.
(10) For each feasible point evaluate the FOM as given by Eq. (6).
(11) Replace ι^* by the test point that gives the smallest value for the FOM.
(12) Replace d^* by the test point that gives the smallest value for the FOM.
(13) Repeat Steps 2–12 for M iterations.
(14) Reduce the region size vector r by γ through $r^{j+1} = \gamma r^j$ where γ is a region contraction factor of thicknesses such as 0.95, and j is the iteration index; reduce the region size for the number of layers by $r^{j+1}_{layer} = \alpha r^j_{layer}$, where α is a region contraction factor for layers, such as 0.96.
(15) Go to Step 6 and continue for M iterations to finish a pass.
(16) At the end of the pass determine the region size to be used at the beginning of the next pass from the size of the variation of each variable as suggested by Luus [17], i.e., choose

$$r_i^{k+1} = |d_i^*(k) - d_i^*(k-1)|, \quad i = 1, 2, \ldots, N \tag{7}$$

where $d_i^*(k)$ is the best value of d_i after k passes and $d_i^*(k-1)$ is the best value of d_i after $k-1$ passes and N is the number of layers. To prevent the region becoming zero, if the region size as calculated from Eq. (7) is less than the region collapse parameter ε, set the region size at the beginning of the pass for that variable equal to ε.
(17) If r_{layer} is less than some parameter η put the region size for the next pass equal to some integer value, for example 10.
(18) Continue the procedure for Q passes.
(19) Run the algorithms many times and examine the results.

4. Optimization results and discussion

The algorithm was used to design multilayer stack structures for high reflectivity in the energy range 20–40 keV over a range of incident angles from 0.1° to 0.358°. The calculations were divided into 13 groups according to the grazing angle. On the one hand, it is required that the mean reflectance in the target energy range has a high value, wherever possible. On the other hand, it is also desirable to have the smallest possible number of layers. It is also required that the variations of the reflectance from the mean value in the target energy are sufficiently small.

Along with the above target demands there are a number of additional feasibility demands. The thicknesses of each layer should be in the range from 1 to 10 nm. For all the mirror groups, the interfacial roughness of two materials is estimated to be 0.3 nm.

The layer materials were chosen to be Pt and C, which are known to be suitable materials for the construction of high reflectivity mirrors in this region of the hard X-ray spectrum [20,21]. Both materials have no absorption edges in the hard X-ray region concerned. Long term chemical stability and its ease of thin film deposition are also preferable characteristics of platinum. For the absorber we have selected Pt while the spacer is C. The multilayer mirror consists of alternating absorber and spacer layers. The optimization process adjusts the thickness of each layer, as well as the total number of layers in the stack, in order to achieve the best value for the FOM.

The optimization results for the Pt/C mirrors studied are summarized in Table 1. Fig. 1 also shows calculated reflectivities of all groups. From Table 1, the reflectance at incidence angle 0.11° was achieved with a stack having only 10 layers. Its reflectance features an excellent uniformity ($\Delta R = 0.006$). At incident angles of 0.123° and 0.135°, the average reflectivities are above 80% and the standard deviation is less than 4% while the numbers of layers required are less than 20. At incidence angles between 0.152° and 0.187°, the standard deviations are the same ($\Delta R = 0.09$) and the average reflectivity is more than 60%. However,

Table 1
Pt/C Mirror design for broad band energy 20–40 keV

Group	Angles ($\theta°$)	Total number of layers	Total d (nm)	Average reflectivity	Standard deviation
1	0.11	10	52.1	0.90	0.006
2	0.123	14	87.8	0.88	0.02
3	0.135	18	92.3	0.83	0.04
4	0.152	18	86.2	0.75	0.09
5	0.169	24	108.3	0.69	0.09
6	0.187	28	110.7	0.62	0.09
7	0.208	42	203.9	0.55	0.139
8	0.219	44	176.5	0.532	0.140
9	0.23	46	181.1	0.492	0.133
10	0.253	50	182.4	0.422	0.1355
11	0.28	60	231.5	0.345	0.156
12	0.31	68	241.3	0.28	0.151
13	0.342	76	270.3	0.241	0.156

the number of layers are increased up to 28 in order to achieve the higher reflectivity. The angles chosen for these calculations are the same as those used by other authors [22]. Even though the critical angle for Pt is 0.161°, the inclusion of absorption and the roughness at the interfaces results in non-perfect reflection at angles below this.

When the gazing angle is more than 0.2°, the reflectance uniformity in the target region is less than for the smaller angles. The average reflectivity is in the range 30–55%, and the number of layers needed is between 40 and 60. For angles larger than 0.3°, the reflectivity becomes less uniform and more layers are required to achieve a higher reflectivity (more than 68 layers). The bilayer thicknesses of some designs are shown in Fig. 2. The effectiveness of the LJ optimization procedure is confirmed by comparing the above results with those of other authors. Table 2 presents the reflectance of Pt/C mirrors from Ref. [22] in the same energy range. The number of layers, mean reflectance values, and total thicknesses of the stack are compared. From grazing angles 0.11° to 0.187°, the mean reflectance obtained using the LJ procedure is higher than that found in Ref. [22] and requires fewer layers. It also results in a reduced total thickness of the stack. For example, at 0.123°,

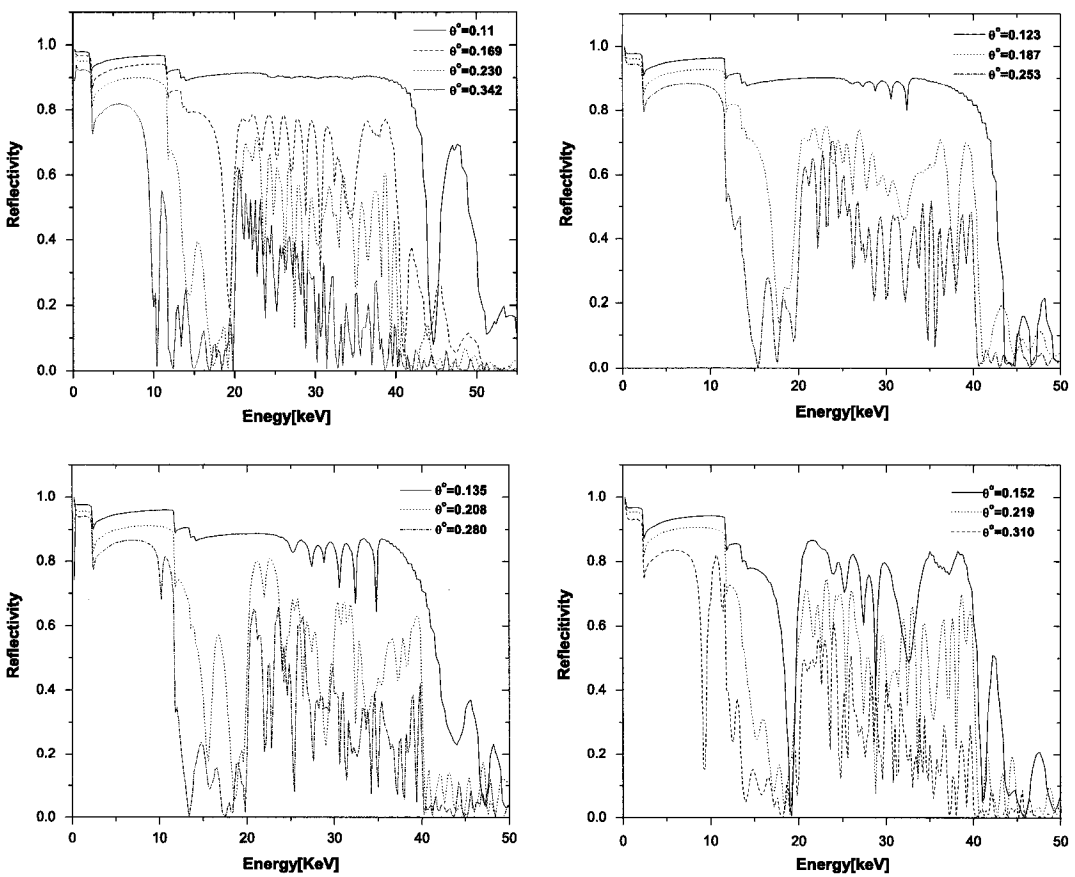

Fig. 1. Optimized reflectivity curves of broadband multilayer mirror Pt/C in the energy range from 20 to 40 keV at grazing angle from 0.11 to 0.342.

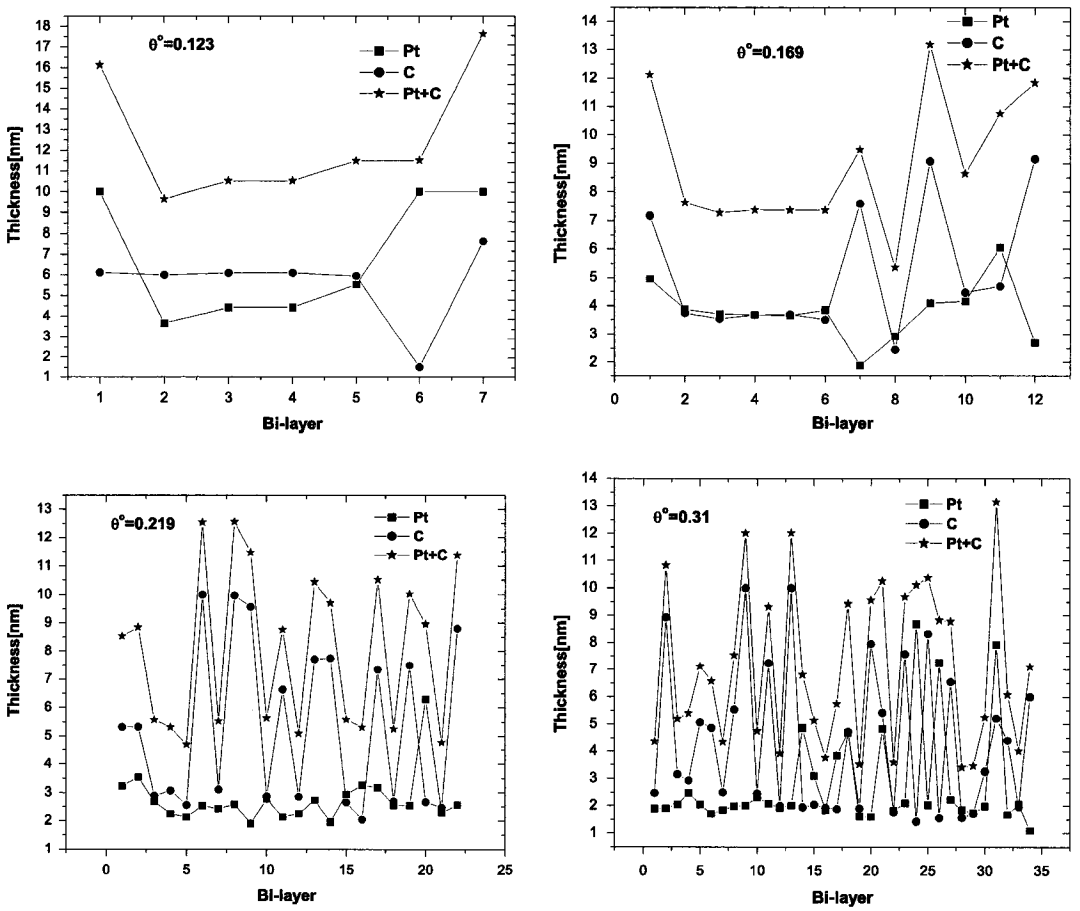

Fig. 2. Layer thicknesses as a function of the bilayer number for grazing angles 0.123°, 0.169°, 0.219° and 0.31°.

Table 2
Comparison between LJ method design and Ref. [22] design of Pt/C mirrors for broad band energy 20–40 keV

Angles (θ°)	Number of layers		Average reflectivity (%)		Total d (nm)	
	LJ	Ref. [22]	LJ	Ref. [22]	LJ	Ref. [22]
0.11	10	50	90	80	52.1	152.4
0.123	14	50	88	80	87.8	152.4
0.135	18	50	83	75	92.3	152.4
0.187	28	82	62	50	110.7	190.9
0.208	42	82	55	40	203.9	188.5
0.28	60	126	34	20	231.5	178.9
0.31	68	126	28	20	241.3	178.9
0.342	76	130	24	20	270.3	217.8

the LJ method gives a higher reflectivity (by more than 8%) and requires fewer layers (70% less). In addition, the total thickness of the stack is reduced by 40%. However, when the grazing angle is larger than 0.2°, the total thickness of the stacks in Ref. [22] is less than that found using the LJ method. However, the LJ result has a higher average reflectivity and a reduced number of layers needed. Also, in the LJ method, at 0.28°, the average reflectivity is increased by 70% over that of Ref. [22] while the total thickness is also larger by more than 30%.

5. Conclusion

The Luus–Jakkola optimization procedure proves to be a very successful optimization scheme for the design of multilayer mirrors in the hard X-ray region. We have applied this optimization method to the design of multilayer mirrors using Pt/C layers. In this design, the average reflectivities obtained fell in the range 25–90% for grazing angles in the range 0.1–0.34°, which for most cases was larger than that obtained in previous calculations. It was also found that the number of layers and the total thickness of the stack was less than that obtained by other methods.

Acknowledgement

The authors acknowledge the financial support from the government of Saudi Arabia for this study.

References

[1] C. Hailey, S. Abdali, F. Christensen, W. Craige, T. Decker, F. Harison, M. Jimmenez-garate, Proc. SPIE 3114 (1997) 535.
[2] K. Yamashita, P. Serlemitsos, J. Tueller, S. Barthelmy, L. Bartlett, K. Chan, A. Furuzawa, N. Nakajo, N. Nakamura, Y. Namba, Y. Okajima, D. Palmer, A. Parsons, Y. Soong, S. Stahl, H. Takata, K. Tamura, Y. Tawara, B. Teegarden, Appl. Opt. 37 (1998) 8067.
[3] T. Okajima, K. Tamura, Y. Ogasaka, K. Haga, S. Takahashi, S. Ichimaru, H. Kito, S. Fukuda, A. Goto, K. Nomoto, H. Satake, S. Kato, Y. Kamata, A. Furuzawa, F. Akimoto, T. Yoshioka, K. Kondo, Y. Haba, T. Tanaka, K. Wada, N. Hamada, M. Hudaverdi, Y. Tawara, K. Yamashita, P. Serlemitsos, Y. Soong, K. Chan, S. Owens, F. Berendse, J. Tueller, K. Misaki, R. Shibata, H. Mori, K. Itoh, H. Kunieda, Y. Namba, Appl. Opt. 41 (25) (2002) 5417.
[4] S.M. Owens, F. Berendse, T. Okajima, K. Misaki, Y. Ogasaka, K. Tamura, Y. Tawara, H. Kunieda, K.W. Chan, Y. Soong, W.H. Baumgartner, H. Krimm, J. Tueller, P.J. Serlemitsos, K. Yamashita, K. Haga, S. Ichimaru, S. Takahashi, A. Gotou, H. Kitou, S. Fukuda, Y. Kamata, A. Furuzawa, F. Akimoto, T. Yoshioka, K. Kondou, Y. Haba, T. Tanaka, Proc. SPIE 4496 (2002) 115.
[5] F. Berendse, S.M. Owens, P.J. Serlemitsos, J. Tueller, K.W. Chan, Y. Soong, H. Krimm, W.H. Baumgartner, H. Kunieda, K. Misaki, Y. Ogasaka, T. Okajima, K. Tamura, Y. Tawara, K. Yamashita, K. Haga, S. Ichimuru, S. Takahashi, A. Gotou, H. Kitou, S. Fukuda, Y. Kamata, A. Furuzawa, F. Akimoto, T. Yoshioka, K. Kondou, Y. Haba, T. Tanaka, Appl. Opt. 42 (10) (2003) 1856.
[6] K. Yamashita, P. Serlemitsos, J. Tueller, S. Barthelmy, L. Bartlett, K.W. Chan, A. Furuzawa, N. Gehrels, K. Haga, H. Kunieda, P. Kurczynski, G. Lodha, N. Nakajo, N. Nakamura, Y. Namba, Y. Ogasaka, T. Okajima, D. Palmer, A. Parsons, Y. Soong, C.M. Stahl, H. Takata, K. Tamura, Y. Tawara, B.J. Teegarden, Appl. Opt. 37 (34) (1998) 8067.
[7] T. Okajima, Y. Ogasaka, K. Tamura, A. Furuzawa, Y. Tawara, K. Yamashita, H. Kunieda, Proc. SPIE 4851 (2003) 716.
[8] P. Binda, F. Zocchi, Proc. SPIE 5536 (2004) 97.
[9] Y. Yamashita, K. Akiyama, K. Haga, H. Kunieda, G. Lodaha, N. Nakago, N. Nakamura, T. Okajima, K. Tamura, Y. Tawara, J. Synchrotron Radiat. 5 (1998) 711.
[10] V. Cotroneo, G. Pareschi, Proc. SPIE 5536 (2004) 49.
[11] T. Boudet, P. Chaton, L. Herault, G. Gonon, L. Jouanet, P. Keller, Appl. Opt. 35 (1996) 6219.
[12] R. Luus, Thi. Jaakola, AIChe 19 (1973) 760.
[13] R. Luus, Nonlinear Anal. 47 (2001) 5647.
[14] R. Luus, Ind. Eng. Chem. Res. 32 (1993) 2633.
[15] Y.P. Lee, G.P. Rangahiah, R. Luus, Comp. Chem. Eng. 23 (1999) 1183.
[16] B. Liao, R. Luus, Eng. Optimiz. 37 (4) (2005) 381.
[17] R. Luus, Hung. J. Ind. Chem. 26 (1998) 281.
[18] Lawrence Livermore National Laboratory optical constants database. Available from: <ftp://www-phys.llnl.gov/pub/raylcigh>.
[19] M. Born, E. Wolf, Principles of Optics, seventh ed., Cambridge University Press, Cambridge, 1999.
[20] G. Lodha, K. Yamashita, T. Suzuki, I. Hatsukade, K. Tamura, T. Ishigami, S. Takahama, Y. Namba, Appl. Opt. 33 (1994) 5869.
[21] K. Tamura, C. Sakai, N. Yamada, Y. Ogasaka, R. Shibata, Proc. SPIE 5900 (2005) 23.
[22] K. Yamashita, Nucl. Instrum. Methods 529 (2004) 59.

4

Optimization of multilayer mirrors at 13.4nm with more than two materials

S M Al-Marzoug, R J W Hodgson. *Appl. Opt.* **47**, 2155 (2008)

Optimization of multilayer mirrors at 13.4 nm with more than two materials

S. M. Al-Marzoug* and R. J. W. Hodgson

Department of Physics, University of Ottawa, Ontario K1N 6N5, Canada

*Corresponding author: salma044@uottawa.ca

Received 28 March 2007; revised 31 January 2008; accepted 1 February 2008; posted 4 February 2008 (Doc. ID 81613); published 18 April 2008

The design of multilayer mirrors with more than two materials is one of the key technologies for investigating lithography. We study a new procedure for optimizing multilayer mirrors of different combinations of materials at a wavelength of 13.4 nm. By adding Be and C layers in different orders to a Si/Mo stack, we have observed enhancement of the reflectivity and a reduction in the number of layers. The Luus–Jaakola optimization procedure has been implemented for the global optimization of the multilayer mirrors. With this algorithm it is not necessary to specify initially the number of layers present in a given design. © 2008 Optical Society of America

OCIS codes: 310.0310, 340.0340.

1. Introduction

The wavelength region ranging from 10 to 15 nm is of particular importance for extreme ultraviolet (EUV) lithography [1–3]. For high reflectivity at normal incidence, in the EUV spectral region, mirrors are necessarily multilayered thin film designs. So far most multilayer coatings have been constructed by alternating layers of two materials with optimized thicknesses at every layer in order to provide the highest possible reflectance for a given wavelength. An example of high-reflectivity EUV mirrors for normal incidence is the Si/Mo stack that shows high reflectivity in the 13.4 nm spectral region [4]. The typical designs that have been created so far use 50–60 periods of Si/Mo. These designs yield a maximum theoretical reflectivity of $R = 0.73$. Small improvements in the reflectivity are significant when several such mirrors are combined in instrumentation. However, only a few studies have attempted to calculate reflectances for mirrors having more than two materials [5,6]. It has been shown that for both intermixing zones and barrier-layer designs, the reflectance is slightly increased with designs ignoring the intermixing zones or the barrier layers. Larruquert [6] has developed a theory of quasi-periodic multicomponent multilayers made of highly absorbing materials and obtained a selection rule for the materials to be used with a period to optimize the reflectivity. However, most materials are moderately absorbing in the EUV range, so this theory is no longer valid in this range [6].

Several methods of designing multilayer stacks have been studied for lithography applications. These include multiparameter optimization methods such as genetic algorithms [7], simplex methods [8], and simulated annealing methods [9]. Most of these methods optimized the multilayer stack by varying the thicknesses of the layers for a fixed number of layers. Other approaches include the layer-by-layer scheme [10] and the use of optimal control theory [11]. However, the Luus–Jaakola (LJ) optimization procedure [12] allows the number of layers in the mirror to be one of the variables in the optimization algorithm that can be optimized. This optimization procedure has been used effectively for the optimization of complex systems such as heat exchanger networks [13,14], and it has successfully been employed for the minimization of the Gibbs free energy for single-phase situations [15]. The results of [16] show that the LJ algorithm can be effectively applied to the design of standard multilayer optical coatings, resulting

0003-6935/08/122155-06$15.00/0

in fewer layers than are obtained by using alternative optimization methods. The LJ method and genetic algorithms have been compared [17], and it was found that the LJ method is faster and offers a higher reliability in achieving the global optimum.

To improve the convergence rate of the LJ optimization procedure, Luus [18] suggested using a multipass procedure, where at the beginning of the process the region size for each variable is chosen to be the range over which the variable has moved during the previous pass. If the range is smaller than some tolerance ϵ, then the region size would be set equal to that tolerance. In this computational study, we make use of this variation of the LJ optimization procedure to improve the reflectivity of the standard Si/Mo stacks at 13.4 nm by adding another material and manipulating the ordering, the thickness, and the number of layers.

2. Multilayer Reflectivity Calculation

A basic understanding of multilayer structures for x-ray and EUV optics has grown significantly in the past decade. Multilayer structures based on x-ray and EUV optical systems are in an advanced stage of development in many laboratories. In most of these systems the basic requirements are the highest possible reflection efficiency, moderate energy resolution, and high-quality imaging characteristics. Therefore, to increase the reflection efficiency, periodic multilayers are prepared as artificial structures where not a single surface but many interfaces reflect the incoming beam, and under a convenient angle of incidence the beams reflected from individual interfaces combine together in phase to produce an intense reflected beam.

A multilayer coating for x-ray mirrors typically consists of a stack of alternating layers of two materials, an absorber and a spacer. The reflectivity of the multilayer coating depends on several parameters: the pair of materials used, the d spacing, the thickness ratio, the number of bilayers, and the root-mean-square interface roughness.

If the multilayer optics coatings can be considered a stratified continuous medium, we may use the optical method to calculate its reflectivity. In this approach, a complex refractive index $\hat{n} = n - ik$ is attributed to each layer, where n and k are, as usual, the refractive decrement and the extinction coefficients, respectively. The optical constants for the materials are entered from external files that can be loaded from a database [19].

Therefore, the reflectance of a multilayer system consisting of N layers can be calculated by using a recursive formalism given, for example, by Parratt [20]. Details of the basic theory have been presented in earlier work by the authors [16]. The net reflection coefficients are computed by using the well-known recursion relation for each layer, starting at the bottom layer where it is assumed that the reflectivity is zero from an infinitely thick substrate. The average reflectivity coming from the s- and p-polarizations is used in this study.

Finally, the desired spectral reflectance profiles are fitted by minimizing a suitable merit function that is composed of an appropriate function of the reflectivity R defined within the wavelength range or incident angle range. For that, we can define the typical figure of merit function (FOM):

$$\mathrm{FOM} = \sqrt{\frac{1}{N}\sum_{i=1}^{N}[R(\lambda_i) - R_{\mathrm{des}}(\lambda)]^2} \qquad (1)$$

where R_{des} is the design reflectance. The computed value of R is a function of the number of layers of material in the mirror, as well as the thickness of each layer.

3. Algorithm of Luus–Jaakola Optimization Procedure

The problem of maximizing the reflectivity of the multilayer structure, for a given set of materials, reduces to that of determining the layer thicknesses and the number of layers in the structure. The optimization procedure that is employed here does not require any auxiliary variables to be introduced in order to solve this parameter estimation problem. The only parameters required are those associated with the optimization procedure. The set of variables in the optimization process, i.e., the layer thicknesses and the number of layers, are described by a vector x consisting of a set of real numbers. The idea of the optimization is then very simple; the standard LJ algorithm as described in [17] has been summarized in our earlier work [16]. It is important to emphasize that the number of layers, in the multilayer stack, is one of the variables that is free to change in the optimization calculation, as opposed to the normal procedure where a fixed number of layers is chosen. This differs from the common procedure of fixing the number of layers (or periods) and then performing the optimization on the layer thicknesses.

The modification of the LJ optimization procedure for multilayer optical coatings as employed in the current study have been summarized by the 19-step algorithm described in our previous work [16]. Minimization of the figure-of-merit function FOM will yield the best values for the thickness of each layer in the mirror, as well as the total number of layers. The optimization variables that are chosen at the outset include R, the number of random points in each iteration; M, the number of iterations in a pass; and Q, the number of passes. The complete algorithm is run 50 times in order to determine the optimum solution.

4. Optimization Results and Discussion

The above algorithm was utilized to design multilayer stack structures for high reflectivity at the wavelength 13.4 nm at normal incidence. This wavelength, above the Si L edge, is important in the design of optics for EUV lithography. On the one hand,

it is required that the reflectance at the target wavelength have a high value, wherever possible. On the other hand, it is also desirable to have the smallest possible number of layers. Along with target demands there are a number of additional feasibility demands. The thickness of each layer should be in the range from 0.1 to 4 nm. The number of layers of each stack should be in the range from 4 to 400 layers. Table 1 lists the parameters of the LJ algorithm used in the following simulations. For all stacks we have assumed that there is no intermixing between the materials, so that there is a clean distinction where one material ends and the other starts. The basic layer materials were chosen to be Mo and Si, which are known to be suitable materials for the construction of high-reflectivity mirrors in this region of the soft-x-ray spectrum. We chose Be and C as third materials. The optical constants, n and k, of these materials at a wavelength of 13.4 nm are depicted in Fig. 1.

The notation that we adopted to represent a period in a multicomponent stack is based on the commonly used notation for a two-component stack, e.g., Si/Mo, where Si is the high-refractive-index and Mo is the low-refractive-index material. For the three component stacks, we used two methods (Fig. 2): (1) multilayers with barrier zones, e.g., Si/Be/Mo/Be, where Be is deposited as Si on Mo and Mo on Si interfaces; (2) multilayers with three-component stacks in periodic structures, e.g., Si/Mo/C multilayers formed with Si as the outermost layer, a Mo layer underneath, and a C layer for a complete period, followed by the second period starting a new Si layer, and so on.

Table 1. Parameters for LJ Optimization

Parameter	Value
No. of test points (R)	35
No. of iterations (M)	80
No. of passes (Q)	12
Region contraction factor (γ)	0.95

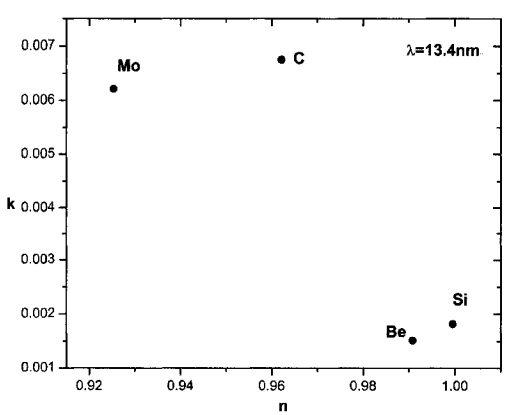

Fig. 1. Optical constants for Si, Mo, Be, and C at 13.4 nm.

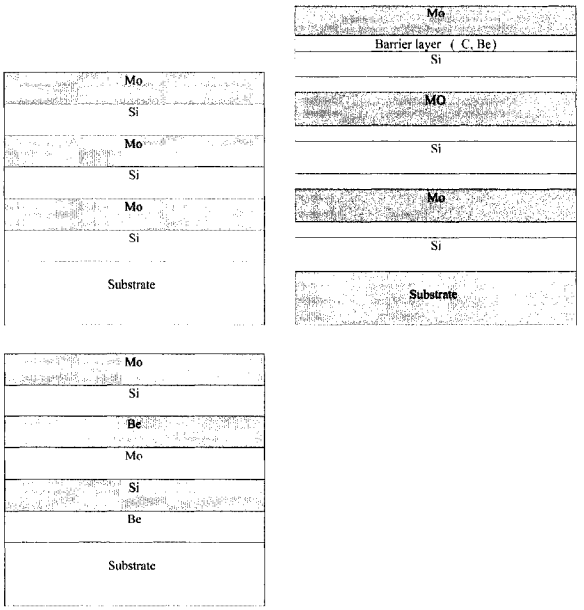

Fig. 2. Ideal standard Mo/Si multilayers (top left) consist of alternating Mo and Si layers. Three-component multilayer mirror (right) consists of Mo and Si layers separated with barriers. Three-component multilayers (bottom left) consists of three Mo, Si, and Be layers.

Standard mirrors having two materials for components are considered for optimization first. The calculated reflectances of optimized multilayers are shown in Table 1 for combinations of different materials. Data are shown for the combinations for materials that provide the highest possible reflectance. The best results, as shown in Table 2, were achieved with a 150-layer stack of Si/Mo and Mo/Si multilayers. The reflectance in these cases is very good, with the total thickness of the Mo/Si stack 10% higher than that of the Si/Mo stack. The Mo/Be multilayer combination is also shown to have a high reflectivity, but less than the Si–Mo combination. Also, the number of layers is 20% more than for the Si–Mo combination. Choosing C as a second material of a bilayer combination is not a good choice to get high reflectivity. Again, the Si/Be combination shows a worse response for both reflectivity, the number of layers, and the total thickness of the stack. The reflectivity response from the bilayer stacks of Table 2 is shown in the left-hand panel of Fig. 3. The right-hand panel of Fig. 3 shows

Table 2. Optimized Normal Incidence Reflectances of Standard Multilayer Mirrors at 13.4 nm

Mirrors	No. of layers	Total d (nm)	$R_{13.4\,nm}$
Si/Mo	150	376.7	0.7455
Mo/Be	180	451.1	0.7326
Si/Be	256	638.2	0.1701
Mo/Si	150	416.0	0.7464
Si/C	178	474.1	0.5130
Mo/C	162	462.6	0.3561

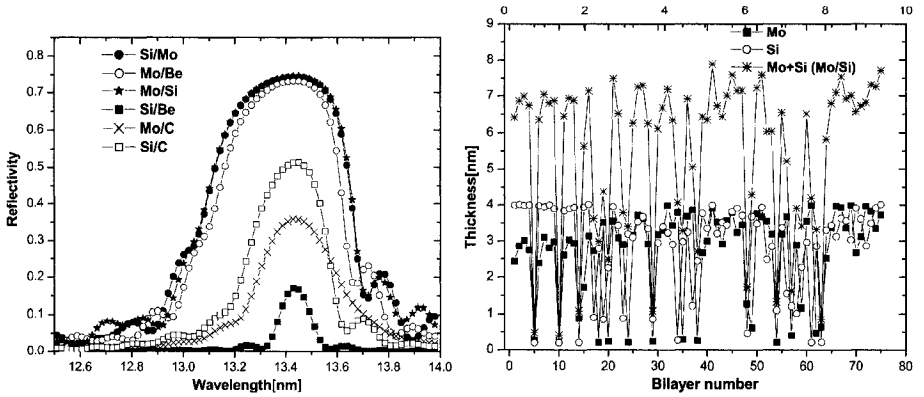

Fig. 3. Optimized reflectivity (left) of multilayer mirrors from Table 1 at a wavelength of 13.4 nm and using the thickness design of a Mo/Si bilayer.

the bilayer thickness for the Mo/Si design. It is to be noted that there is considerable variability of the thickness of each material as a function of the layer number. This is in contrast to some other studies carried out with fixed numbers of layers, where the thickness of the layers tends to vary smoothly with layer number [10,11].

The three-component system in Table 3 is set as a two-component stack with the third material interleaved between the two layers. These barrier layers are often introduced to prevent mixing of the materials on either side. In other studies using barrier layers, the thicknesses of these layers are held fixed, whereas in this study we allow the thickness of each barrier layer to vary as well. C and Be were used as the barrier materials in this study. The results of optimization of the reflectivity with inclusion of the barrier layers at different stacks are shown in Fig. 4. From these optimizations, it appears that Be barrier layers are more suitable for the Si-on-Mo boundaries. On optimization of the stack with C barriers for Si-on-Mo boundaries, the peak reflectivity decreases by 5%, whereas the number of layers and the total thickness increases by 36%. Comparing Mo/C/Si/C multilayers with the Mo/C/Si/C interface-engineered multilayers in [21], the number of layers of Mo/C/Si/C engineered multilayers is 240 with a fixed thickness of Mo (2.6 nm), Si (4.4 nm) and C (0.4 nm), which is 35% more than the optimized multilayer in this study. However, the reflectivity of the engineered multilayer is 0.696, which is 1% more than the optimized structure found here. The thicknesses of barrier layers for the Si/Be/Mo/Be stack is shown in Fig. 5, showing considerable variability through the stack.

Table 3. Optimized Normal Incidence Reflectance of Multilayer Mirrors, Barrier at 13.4 nm

Mirrors	No. of layers	Total d (nm)	$R_{13.4\,\mathrm{nm}}$
Mo/Be/Si/Be	176	358.3	0.7294
Si/Be/Mo/Be	156	286.6	0.7310
Mo/C/Si/C	176	312.2	0.6887
Si/C/Mo/C	212	399.2	0.6810

The results for the optimization of the multilayer mirrors composed of three materials per period is shown in Table 4. In this table, we selected C and Be as the additional third material in the standard multilayer (Si–Mo combination). With these selected

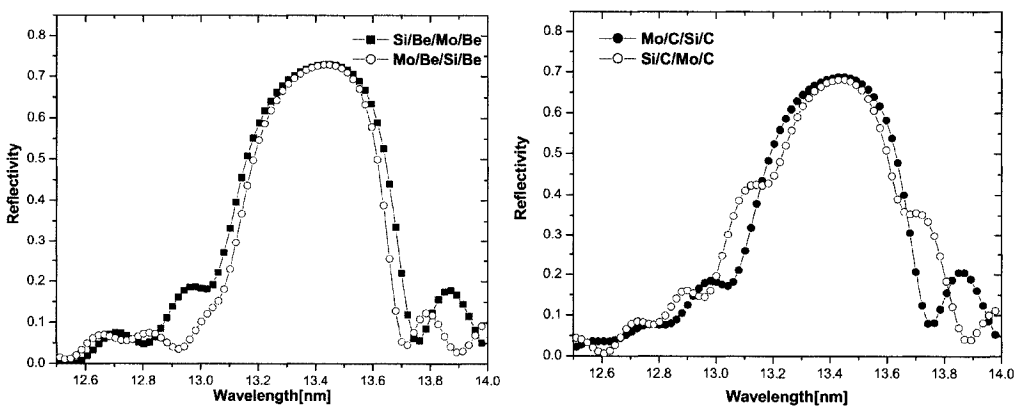

Fig. 4. Optimized reflectivity of multilayer mirrors with barrier layer Be (left) and with barrier layer C (right) at the wavelength 13.4 nm.

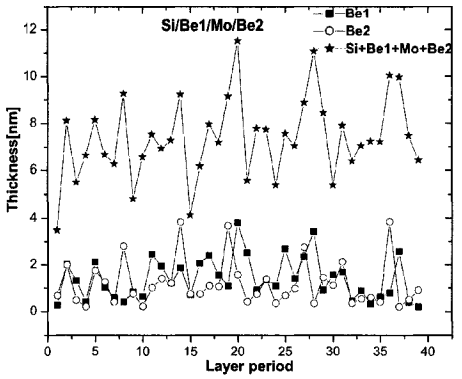

Fig. 5. Thickness design of Si/Be/Mo/Be stack.

materials, we have six structure possibilities per third material. For example, with the Be component as the third material, we can realize six multilayers, noted as Si/Mo/Be, Si/Be/Mo, Mo/Si/Be, Mo/Be/Si, Be/Si/Mo, and Be/Mo/Si. In the notation Si/Mo/Be, the first material (Si) is on the top of the multilayer, and the last one (Be) is next to the substrate. For each combination the algorithm numerically optimizes the thickness of each material and the number of layers (see Fig. 6).

From Table 4, we can see that the addition of Be or C on top of the Si/Mo combination results in an increase in the reflectivity over that of two materials on their own. Also, when compared with the standard multilayer results in Table 2, the addition of Be between Mo and Si (Be deposited on Si) yields a decrease of the total thickness of multilayers by up to 30%, and the reflectivity decreases by 3%, whereas the addition of C between Mo and Si (C deposited on Si) results in a lowering of the reflectivity by 52%, while the number of layers is increased by 18%.

Also, when the Be layer is between Si and Mo (Be deposited on Mo) the reflectivity is increased slightly by 1%. However, the reflectivity is 30% less when adding the C layer between Si and Mo (C deposited on Mo). Hence the Si/Be/Mo stack and C layer as a bottom layer give the best results for the reflectivity. Choosing C as the top layer in the Mo–Si combination and Be on top of the Si/Mo stack, the reflectivity is decreased.

Table 4. Optimized Normal Incidence Reflectance of Multilayer Mirrors, Three-Component Materials at 13.4 nm

Mirrors	No. of layers	Total d (nm)	$R_{13.4\,nm}$
Si/Mo/Be	141	327.7	0.7480
Mo/Si/Be	126	273.7	0.7395
Be/Mo/Si	147	343.0	0.7329
Mo/Be/Si	138	289.5	0.7199
Si/Be/Mo	177	401.2	0.7551
Be/Si/Mo	177	398.6	0.1084
Si/Mo/C	177	389.2	0.7494
Mo/Si/C	147	339.4	0.7379
Si/C/Mo	156	350.4	0.5006
C/Si/Mo	150	340.8	0.4931
Mo/C/Si	177	406.1	0.3568
C/Mo/Si	177	394.6	0.3554

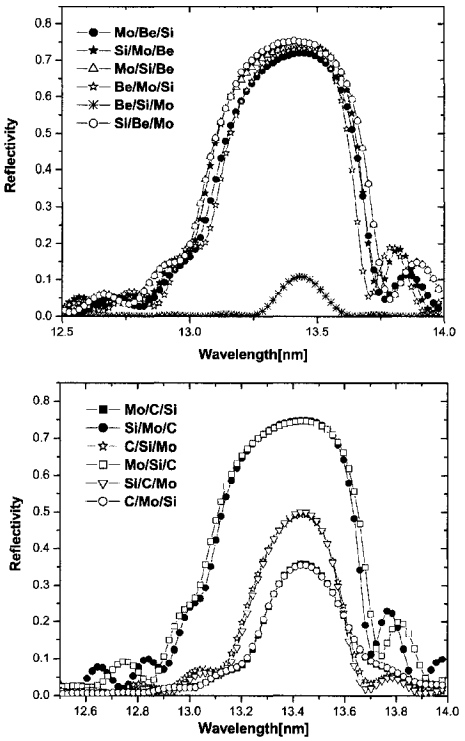

Fig. 6. Optimized reflectivity of multialyer mirrors with a third layer Be (top) and with a third layer C (bottom) at the wavelength 13.4 nm.

5. Conclusion

The technique of Luus–Jaakola optimization has been successfully applied to the design of multilayer mirrors showing improved reflectance at 13.4 nm for more than two materials. Instead of using the standard two-layer multilayers, we designed multilayer systems in which Mo and Si layers are separated with C and Be materials. In addition, we studied different combinations of three-component multilayer systems for their reflectance, total thickness of the stack, and the total number of layers. The approach employed in this study offers a simple tool to investigate the effects of varying the number of layers in a multilayer mirror, as well as determining the layer thicknesses.

The authors acknowledge financial support from the government of Saudi Arabia for this study.

References

1. S. Bajt, J. Alameda, T. Barbee, W. M. Clift, J. A. Folta, B. Kaufmann, and E. Spiller, "Improved reflectance and stability of Mo/Si multilayers," Proc. SPIE **4506**, 65–75 (2001).
2. S. P. Vernon, D. G. Stearns, and R. S. Rosen, "Ion-assisted sputter deposition of molybdenum-silicon multilayers," Appl. Opt. **32**, 6969–6974 (1993).

3. J. Folta, S. Bajt, T. Barbee Jr., R. Grabner, P. Mirkarimi, T. Nguyen, M. Schmidt, E. Spiller, C. Walton, M. Wedowski, and C. Montcalm, "Advances in multilayer reflective coatings for extreme-ultraviolet lithography," Proc. SPIE **3676**, 702–709 (1999).
4. K. M. Skulina, C. S. Alford, R. M. Bionta, D. M. Makowiecki, E. M. Gullikson, R. Soufli, J. B. Kortright, and J. H. Underwood, "Molybdenum/beryllium multilayer mirrors for normal incidence in the extreme ultraviolet," Appl. Opt. **34**, 3727–3730 (1995).
5. K. Powell, J. Tait, and A. Michette, "Simulated annealing in the design of broadband multilayers containing more than two materials," Proc. SPIE **4145**, 254–256 (2001).
6. J. Larruquert, "Reflectance enhancement in the extreme ultraviolet and soft x rays by means of multilayers with more than two materials," J. Opt. Soc. Am. A **19**, 391–397 (2002).
7. P. Binda and F. Zocchi, "Genetic algorithm optimization of x-ray multilayer coatings," Proc. SPIE **5536**, 97–108 (2004).
8. V. Cotroneo and G. Pareschi, "Global optimization of x-ray multilayer mirrors with iterated simplex method," Proc. SPIE **5536**, 49–60 (2004).
9. T. Boudet, P. Chaton, L. Herault, G. Gonon, L. Jouanet, and P. Keller, "Thin-film designs by simulated annealing," Appl. Opt. **35**, 6219–6226 (1996).
10. J. Larruquert, "New layer-by-layer multilayer design method," J. Opt. Soc. Am. A **19**, 385–390 (2002).
11. M. Singh and J. J. M. Braat, "Design of multilayer extreme-ultraviolet mirrors for enhanced reflectivity," Appl. Opt. **39**, 2189–2197 (2000).
12. R. Luus and T. Jaakola, "Optimization by direct search and systematic reduction of the size of search region," AIChE. J. **19**, 760–766 (1973).
13. R. Luus, "Use of Luus–Jaakola optimization procedure for singular optimal control problems," Nonlinear Anal. **47**, 5647–5658 (2001).
14. R. Luus, "Optimization of heat exchanger networks," Ind. Eng. Chem. **32**, 2633–2635 (1993).
15. Y. P. Lee, G. P. Rangahiah, and R. Luus, "Phase and chemical equilibrium calculations by direct search optimization," Comput. Chem. Eng. **23**, 1183 (1999); http://www.ingentaconnect.com/content/els/00981354/1999/00000023/00000009/art00283.
16. S. Al-Marzoug and R. Hodgson, "Luus–Jaakola optimization procedure for multilayer optical coatings," Opt. Commun. **265**, 234–240 (2006).
17. B. Liao and R. Luus, "Comparison of the Luus–Jaakola optimization procedure and the genetic algorithm," Eng. Optimiz. **37**, 381–398 (2005).
18. R. Luus, "Determination of the region sizes for LJ optimization procedure," Hung. J. Ind. Chem. **26**, 281–286 (1998).
19. Lawrence Livermore National Laboratory optical constants database, ftp://www-phys.llnl.gov/pub/rayleigh.
20. L. G. Parratt, "Surface studies of soilds by total reflecation of x-ray," Phys. Rev. **95**, 359–369 (1954).
21. S. Yulin, T. Feigl, N. Benoit, and N. Kaiser, "EUV/soft x-ray multilayer optics," Proc. SPIE **5645**, 289–298 (2005).

5

Determination of optical constants in the EUV/soft X-ray region using the Luus-Jaakola optimization procedure

S M Al-Marzoug, R J W Hodgson. *Opt. Commun* **280**, 110 (2007)

Correction

1. In Fig. 1, the angle θ_0 is grazing angle.

2. Equation 6 should read:

$$F_j = F_{Ideal} e^{-2k_j k_{j+1} \sigma_j^2}$$

Available online at www.sciencedirect.com
ScienceDirect
Optics Communications 280 (2007) 110–113
OPTICS COMMUNICATIONS
www.elsevier.com/locate/optcom

Determination of optical constants in the EUV/soft X-ray region using the Luus-Jaakola optimization procedure

S.M. Al-Marzoug, R.J.W. Hodgson *

Department of Physics, University of Ottawa, ON, Canada K1N 6N5

Received 21 February 2007; received in revised form 19 July 2007; accepted 6 August 2007

Abstract

A Luus-Jaakola optimization procedure is described that simultaneously determines the optical constants, thickness and root mean square roughness of thin films for reflectance versus angle-of-incidences data measured in the EUV/soft X-ray region. The optimization method is applied to different films at different wavelengths. The results show that the Luus-Jaakola optimization procedure is able to determine the thickness of films and the roughness with an accuracy of less than 7%. The optical constants obtained are also in good agreement with reported values for films having an error of less than 1%.

PACS: 02.70.–c; 78.20.Ci

Keywords: Luus-Jaakola optimization; Optical constants; Reflectivity; Index of refraction

1. Introduction

Multilayer mirrors are becoming essential optical elements in applications in the soft and extreme ultraviolet (EUV) range, such as lithography, astronomy and synchrotron research. It is important to know the refractive index of the materials in these mirrors with great accuracy, since it allows successful modeling and predication of the performance of these optical elements. The thin films on transparent, slightly absorbing substrates have been extensively investigated with spectral transmittance and reflectance measurements to determine the optical constants [1–4] and many analytical and numerical methods have also been proposed to determine the optical constants [5–10]. In all these methods the input data are the values of transmittance or reflectance measured at several wavelengths. Then, using a model based on thin film optical constants, computational software fits the parameters of the model to achieve the best agreement with experimental data. Some of the methods are quite complicated and require solution by computer iteration procedures with an efficient criterion to identify the correct solution and require properly chosen initial values. The Luus-Jaakola (LJ) optimization procedure is one of the optimization methods that is largely independent of the initial conditions [11].

This latter optimization procedure has been used effectively for the optimization of complex systems such as heat exchanger networks [12,13], and it has been successfully employed for the minimization of the Gibbs free energy for single phase situations [14]. The results of Ref. [15] show that the LJ algorithm can be effectively applied to the design of standard multilayer optical coatings, resulting in fewer layers than obtained using alternative optimization methods. The LJ method and Genetic algorithms have been compared [16]. Here it was found that the LJ method is faster and offers a higher reliability in achieving the global optimum.

To improve the convergence rate of the LJ optimization procedure, Luus [17] suggested using a multi-pass procedure, where at the beginning of the process, the region size

* Corresponding author. Tel.: +1 6135625758; fax: +1 6135625190.
E-mail address: rhodgson@uottawa.ca (R.J.W. Hodgson).

0030-4018/$ - see front matter © 2007 Elsevier B.V. All rights reserved.
doi:10.1016/j.optcom.2007.08.001

for each variable is chosen to be the range over which the variable has moved during the previous pass. If the range is smaller than some tolerance ϵ, then the region size would be set equal to that tolerance. In this work we will determine the optical constants, the thickness, and the root mean square roughness of the film, using reflectance data. For this purpose, a Luus-Jaakola optimization procedure has been employed.

2. Theory

Fig. 1 shows a schematic diagram of the reflection of light from a thin homogeneous layer with a constant thickness. The thickness and the complex refractive index of the film are t and $n = n_f - ik_f$. X-rays in air are incident at the grazing angle θ_0. The incident light is transmitted through an absorbing substrate of complex refractive index $n = n_s - ik_s$. The reflection coefficient of the electric field at the jth interface is defined as

$$R_j = e^{-ik_j t_j}\left(\frac{E_{rj}}{E_{ij}}\right) \tag{1}$$

Where E_{ij} and E_{rj} are the incident and reflected electrical fields in the jth layer, respectively. In Eq. (1), k_j is the component of the wave vector normal to the coating surface in the jth layer. Since the parallel component of the wave vector is conserved and equal to $2\pi n_0 \cos\theta_0/\lambda$, k_j is given by

$$k_j = \frac{2\pi}{\lambda}\sqrt{n_j^2 - n_0^2\cos^2\theta_0} \tag{2}$$

where θ_0 is the incident angle at the interface between air and the first layer, and n_0 is the index of refraction of air. The Fresnel reflectivity of a single layer bonded on a semi-infinite substrate is [18]:

$$R = \left|\frac{F_0 + F_1\exp(-2ik_1t_1)}{1 + F_0F_1\exp(-2ik_1t_1)}\right|^2 \tag{3}$$

Here F_0 is the Fresnel coefficient of the free surface (air/film interface), F_1 the Fresnel coefficient of the film/substrate interface, k_1 is given by Eq. (2), and t is the film thickness. The expression for F_j depends on the polarization of the electromagnetic wave. For s-polarization, F_j is given by

$$F_j = \frac{k_j - k_{j+1}}{k_j + k_{j+1}} \tag{4}$$

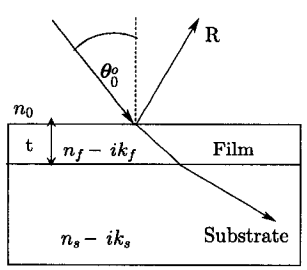

Fig. 1. Schematic diagram of a thin-film system.

whereas for p-polarization, the Fresnel reflection is

$$F_j = \frac{k_j n_j^{-2} - k_{j+1}n_{j+1}^{-2}}{k_j n_j^{-2} + k_{j+1}n_{j+1}^{-2}} \tag{5}$$

The calculation takes into account the decrease of the specular reflectivity due to the interfacial roughness by the modification of the Fresnel coefficients according to

$$F_j = F_{\text{Ideal}}e^{2k_jk_{j+1}\sigma_j} \tag{6}$$

where F_{Ideal} is the reflection coefficient from an ideal interface for either s- or p- polarization and σ is the root mean square deviation of the interface atoms with respect to a smooth interface. For unpolarized radiation the reflectivity is given by the average value of the two polarizations. Once the expression for the calculation has been specified, one would like to obtain optical information of the film (t, n_f, k_f, σ_f) from reflectivity measurements. With these parameters a theoretical reflectance spectrum can be generated and compared with the experimental one. In this case we can define the typical figure of merit (FOM):

$$\text{FOM} = \sqrt{\left[\frac{1}{N}\sum_{i=1}^{N}(R_{\text{exp}}(\theta_i) - R_{\text{comp}}(\theta_i))^2\right]} \tag{7}$$

where N is the number of points in the spectrum, R_{comp} and R_{exp} are the experimental and computed values of reflectance. The optimization algorithm will be used to minimize the value of FOM.

3. Algorithm of the Luus-Jaakola (LJ) optimization procedure

The problem of determining the optical constants of the film structure reduces to that of determining the film thicknesses t, the root mean square roughness σ_f, and the refractive index $n_f - ik_f$ of the film in the structure. The optimization procedure that is employed here does not require any auxiliary variables to be introduced in order to solve this parameter estimation problem. The set of variables in the optimization process, i.e. the film thicknesses t, σ_f, n_f and k_f, are described by a vector x consisting of a set of real numbers. The idea of the optimization is then very simple, so the standard LJ algorithm may be summarized most conveniently in the following [16]:

(1) Choose some reasonable initial point x^*; a reasonable initial region size r; and choose the number R of random points to be used at each iteration; and the number of iterations M to be used in a pass.
(2) Choose R test points through the equation $x = x^* + Dr$ where D is a diagonal matrix of randomly chosen points from the interval $[-0.5, 0.5]$, and r is the region size vector.
(3) Check each of the R test points with respect to feasibility from the domain of variables.

(4) For each feasible point evaluate the FOM as give by Eq. (7).
(5) Replace x^* by the test point that gives the smallest value for the FOM.
(6) Repeat steps 2–5 for M iterations.
(7) Reduce the region size vector r by γ through $r^{j+1} = \gamma r^j$ where γ is a region contraction factor such as 0.95, and j is the iteration index.
(8) Go to step 2 and continue for M iterations to finish a pass and examine the results.

4. Optimization results and discussion

In the present work, the LJ algorithm has been used to determine the optical constants, root mean square roughness, and thickness of different films at different wavelengths through a region of incidence angles, i.e from different reflectance spectra. Therefore, the possible solution of the problem is represented as a vector of the form,

$$x = (t_f, n_f, k_f, \sigma_f) \tag{8}$$

In all the numerical calculations, we have generated experimental data, that were obtained using the IMD software [19] as shown in Figs. 2 and 3, in order to get reflectance data. For all stacks, the interfacial roughness of experimental spectrums has been taken to be $\sigma = 0.3$ nm. The data from the IMD software are unpublished and comes from measurements made on the films. From angles of incidence 0° to 5°, we optimize these reflectance spectra by finding the solution of Eq. (8). Table 1 lists the parameters of the LJ used for the following simulations. The LJ algorithm was executed for different films as shown in Table 2. The theoretical values of the indexes of refraction were taken from Center of X-ray Optics at Lawrence Berkeley National Laboratory [20] to compare with the optimized values. In Table 2, the optical constants, the root mean square roughnesses, and the thicknesses of the films (Cr, Mo, C, Si) were simultaneously determined by applying the LJ optimization algorithm. This algorithm gave a thickness of 61.7 nm for the chromium film at $\lambda = 4.138$ nm, showing very good agreement with the actual thickness value of 60.0 nm, with a difference of <3%. However, the thickness of the molybdenum film found using the LJ algorithm is

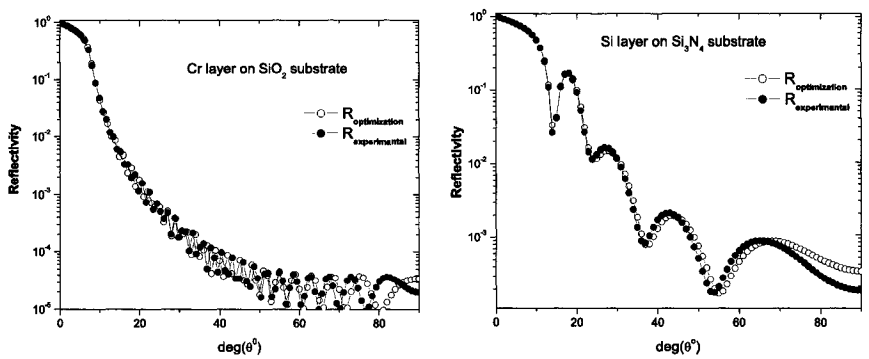

Fig. 2. Comparison between generated reflectance spectra from experimental data and reflectance spectra computed from the extracted thicknesses, roughness, n and k (left) Cr film on SiO_2 at $\lambda = 4.138$ nm and (right) Si film on Si_3N_4 substrate at $\lambda = 17.712$ nm.

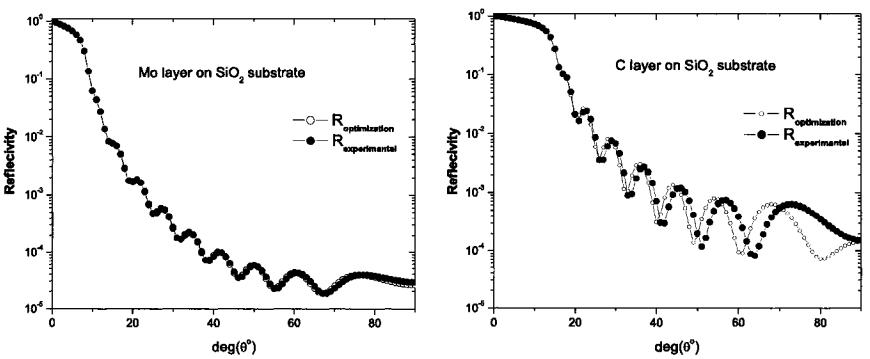

Fig. 3. Comparison between generated reflectance spectra from experimental data and reflectance spectra computed from the extracted thicknesses, roughness, n and k (left) Mo film on SiO_2 at $\lambda = 6.199$ nm and (right) C film on SiO_2 substrate at $\lambda = 12.398$ nm.

Table 1
Parameters of Luus-Jaakola (LJ) optimization procedure

Parameter	Value
No. of test points (R)	30
No. of iterations (M)	60
No. of passes (Q)	12

Table 2
Optimized normal incidence reflectances of the standard films at 13.4 nm

Film/substrate	Cr/SiO_2	Mo/SiO_2	C/SiO_2	Si/Si_3N_4
Wavelength (nm)	4.138	6.199	12.398	17.712
Thickness (optimized) (nm)	61.7	32.31	51.56	41.60
Thickness (experiment) (nm)	60	30	50	40.0
σ_f (optimized) (nm)	0.28	0.31	0.29	0.31
σ_f (experiment) (nm)	0.3	0.3	0.3	0.3
n_f (optimized)	0.9912	0.9899	0.9676	0.9824
n_f (tabulated)	0.9912	0.9899	0.9676	0.9827
k_f (optimized)	0.00243	0.00262	0.00528	0.00401
k_f (tabulated)	0.00243	0.00261	0.00529	0.00410

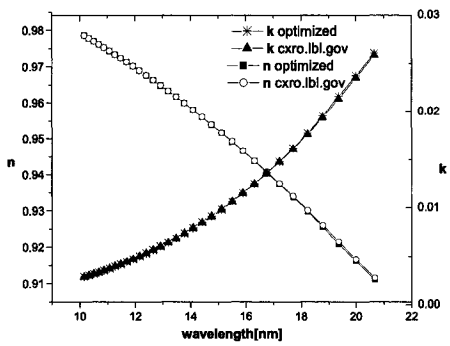

Fig. 4. Optical constants of the carbon film; constants derived in this study are compared with the data of <http://www-cxro.lbl.gov/>.

slightly worse than the other films, having an error of 8% of the actual thickness. Furthermore, the results of the thicknesses for carbon and silicon show good agreement (<5%) between the experimental and optimized values. However, the value of n and k show excellent agreement (error <1%) for all the films at different wavelengths. The root mean square roughness of Mo, C, and Si was achieved by <3% of the actual value, but for chromium film was >6%. Figs. 2 and 3 also show the reflectance spectra computed using the parameters deduced from the fit.

We also applied the LJ method to carbon film on BK7 optical glass substrates. The R–θ data were taken for soft X-rays of wavelength 10–20 nm at various angles of incidence, using the IMD software. The thickness of the carbon film and root mean square roughness were 50 and 0.3 nm. The results found for the carbon optical constants, along with optical data taken from CXRO [20], are shown in Fig. 4. The values of the optical constants for the carbon film obtained using the LJ method agree very closely with the CXRO values. Also, the average thickness of the carbon film is 50.7 nm with a standard deviation 2.7 nm and the average roughness is 0.305 nm with a standard deviation 0.06 nm.

5. Conclusion

The technique of Luus-Jaakola optimization has been successfully applied to determine the thickness of thin films, the root mean square roughness and their optical constants simultaneously. Comparison with other sources shows differences as great as 5% between our optimized data and those reported by other authors.

Acknowledgement

The authors would like to acknowledge the financial support from the Government of Saudi Arabia for this study.

References

[1] J. Manifacier, J. Gasiot, J. Fillard, J. Phys. E. 9 (1976) 1002.
[2] D. Minkov, J. Phys. D. 22 (1989) 1157.
[3] E. Khawaja, F. Bouamrane, Appl. Opt. 32 (1993) 1168.
[4] Rusli, G. Amaratunga, Appl. Opt. 34 (1995) 7914.
[5] A.V. Tikhonravov, Appl. Opt. 32 (1993) 5417.
[6] J. Cao, M. Yanagihra, M. Yamamoto, Y. Goto, T. Namioka, Appl. Opt. 33 (1994) 2013.
[7] R. Bueno, J. Trigo, J. Martinez-Duart, E. Elizalda, J. Sanz, J. Vac. Sci. Technol. A 13 (5) (1995) 2378.
[8] Y. Zheng, K. Kikuchi, Appl. Opt. 36 (1997) 6325.
[9] D. Pekker, L. Pekker, Thin Solid Films 425 (2003) 203.
[10] V. Kutavichus, V. Filippov, V. Huzouski, Appl. Opt. 45 (2006) 4547.
[11] R. Luus, Thi. Jaakola, AIChe. 19 (1973) 760.
[12] R. Luus, Nonlinear Anal. 47 (2001) 5647.
[13] R. Luus, Ind. Eng. Chem. Res. 32 (1993) 2633.
[14] Y.P. Lee, G.P. Rangahiah, R. Luus, Comp. Chem. Eng. 23 (1999) 1183.
[15] S. Al-Marzoug, R. Hodgson, Opt. Commun. 265 (2006) 234.
[16] B. Liao, R. Luus, Eng. Optim. 37 (4) (2005) 381.
[17] R. Luus, Hung. J. Ind. Chem. 26 (1998) 281.
[18] M. Born, E. Wolf, Principles of Optics, seventh ed., Cambridge University Press, Cambridge, 1999.
[19] IMD 4.1 Program for EUV and X-ray optics calcuations, D.L. Windt Available at <http://www.rxollc.com>.
[20] The Center for X-ray Optics at Lawrence Berkeley National Laboratory <http://www-cxro.lbl.gov/>.

6

Luus-Jaakola optimization procedure for phase-only sampled-fiber Bragg gratings

S M Al-Marzoug, R J W Hodgson. *Appl. Opt.* **47**, 2275 (2008)

Luus–Jaakola optimization procedure for phase-only sampled-fiber Bragg gratings

S. M. Al-Marzoug* and R. J. W. Hodgson

Department of Physics, University of Ottawa, ON K1N 6N5, Canada

*Corresponding author: salma044@uottawa.ca

Received 9 October 2007; revised 22 January 2008; accepted 8 February 2008; posted 4 March 2008 (Doc. ID 88235); published 25 April 2008

We describe a Luus–Jaakola (LJ) optimization algorithm approach for the design of wavelength division multiplexing (WDM) optical communication systems by using phase-only sampled-fiber Bragg gratings. The LJ method is used to optimize the phase grating as well as the number of segments which form the grating. The numerical example of WDM is studied. The method is easily applicable and shows promising results with low refractive index modulation. © 2008 Optical Society of America

OCIS codes: 060.2340, 230.1480, 050.2770.

1. Introduction

Fiber Bragg gratings (FBGs) are essential parts of optical communication networks and sensor applications [1–4]. Wavelength division multiplexing (WDM), based on sampled-fiber Bragg gratings (SFBGs), are of special importance since they can serve as dispersion compensators [5] and optical add–drop multiplexers (OADMs) [6]. Therefore the design of multichannel FBGs has become an important research area. Correspondingly, in order to get a higher number of channels, the effective amplitude of the refractive index modulation must be increased. Two essential techniques are employed for SFBGs, either sampling the phase of the fiber core [5,7,8] or the refractive index amplitude [9]. Wu *et al.* [8] obtained eight channels with an effective amplitude of refractive index modulation $\delta n_{\text{eff}} = 8 \times 10^{-4}$ by using sinc amplitude sampling. However, using phase-only sampling can produce eight channels with a grating length of 10 cm and $\delta n_{\text{eff}} = 4 \times 10^{-4}$ [5].

In the literature, several methods of designing multichannel FBGs using optimization algorithms have been studied, such as genetic algorithms [10,11] and simulated annealing algorithms [12,13]. These methods are complicated and lack the design flexibility for many practical applications. However, the Luus–Jaakola (LJ) optimization procedure [14] allows the number of segments in the FBG to be one of the variables in the optimization algorithm that can be optimized. This procedure has been used effectively for the optimization of complex systems, such as heat exchanger networks [15,16], and it has been successfully employed for minimization of the Gibbs free energy for single-phase situations [17]. The results of [18] show that the LJ algorithm can also be effectively applied to the design of multilayer optical coatings, resulting in fewer layers than are obtained using alterative optimization methods. The LJ method and genetic algorithm have also been compared [19]. It was found that the LJ method is faster and offers higher reliability in achieving the global optimum. In this computational study, we make use of the LJ optimization procedure to increase the number of channels by minimizing the phase shift for phase-only sampled-fiber Bragg gratings (PSFBGs) inside the sampling period as well as minimizing the number of segments in the grating.

2. Principles of Phase-Only Sampled-Fiber Bragg Grating

An FBG is produced by creating a periodic perturbation of the index of refraction along a certain length of the core of an optical fiber. When light propagates through the periodically alternating regions of high-

0003-6935/08/132275-06$15.00/0

er and lower refractive indices within the fiber, it is reflected by successive, coherent scattering from the index variations. When the reflection from a crest in the index modulation is in phase with the next one, we have maximum mode coupling or reflection. The wavelength at which maximum reflection occurs, λ_B, is called the Bragg wavelength and is given by [20]

$$\lambda_B = 2n_{\text{eff}}\Lambda, \tag{1}$$

where n_{eff} is the effective mode index of refraction of the optical fiber and Λ is the period of the grating. The periodic modulation in the refractive index of the optical fiber core can be given by the function [2,20]

$$\delta n_{\text{eff}} = \overline{\delta n_{\text{eff}}}\left\{1 + \nu\cos\left[\frac{2\pi}{\Lambda}z + \phi(z)\right]\right\}, \tag{2}$$

where $\overline{\delta n_{\text{eff}}}$ is the mean mode effective index of the refraction change and ν is the fringe visibility of the index change. The function $\phi(z)$ describes the grating chirp (i.e., the change in the grating period along the grating length) and contains the grating phase. For PSFBG, the effective index modulation can be written by using Fourier analysis as [5]

$$\delta n_{\text{eff}} = \overline{\delta n_{\text{eff}}}\left(1 + \nu\text{Re} \times \left\{\sum_m F_m \exp[i(2\pi z/\Lambda + 2\pi m z/\Lambda_s)]\right\}\right), \tag{3}$$

$$F_m = \frac{1}{M}\sum_{k=0}^{N-1}[\exp(i2\pi\phi(k))\exp(-ik2\pi m/M)],$$
$$m = 0, 1, 2, \ldots, M. \tag{4}$$

where Λ_s is the period of the sampling function that contains N segments per sampling period and M is the number of Fourier coefficients, which is assumed to be equal to the number of segments N. F_m is the Fourier coefficient that is linearly dependent on the coupling coefficient κ_m as $\kappa_m = F_m\pi\overline{\delta n_{\text{eff}}}/\lambda_B$. The channel spacing Δf of the sampled gratings is determined by the sampling period Λ_s through the following expression [21]:

$$\Delta f = \frac{c}{2n_{\text{eff}}\Lambda_s}. \tag{5}$$

The reflected spectrum for a PSFBG can be calculated by using the transfer matrix method commonly employed in multilayer optical calculations [2,20]. One begins by defining a fitness function E. In this case, for the minimization problem, the function E provides a measurement of the deviation between the target reflection spectrum and the calculated reflectivity

$$E = \sum_i |R_{\text{calc}}(\lambda_i) - R_{\text{targ}}(\lambda_i)|, \tag{6}$$

where $\{\lambda_i\}$ is the discrete set of wavelengths where the reflection spectra are evaluated. This function E becomes the figure-of-merit (FOM) function for the optimization algorithm.

3. Algorithm of the Luus–Jaakola Optimization Procedure

The problem of maximizing the number of channels reduces to that of determining the phase shift for the FBG inside the sampling period and, at the same time, minimizing the number of segments. The optimization procedure employed here does not require any auxiliary variables to be introduced in order to solve this parameter estimation problem. The set of variables in the optimization process, i.e., the grating phases and the number of segments, are described by a vector x consisting of a set of real numbers. A theoretical analysis and proof of convergence for the LJ algorithm has been published [22]. The procedure for the optimization is then very simple, so the standard LJ algorithm may be summarized most conveniently in the following [19]:

1. Choose some reasonable initial point x^*, a reasonable initial region size r, and choose the number R of random points to be used at each iteration and the number of iterations M to be used in one pass.
2. Choose R test points through the equation $x = x^* + Dr$ where D is a diagonal matrix of randomly chosen points from the interval $[-0.5, 0.5]$ and r is the region size vector.
3. Check each of the R test points with respect to feasibility from the domain of variables.
4. For each feasible point evaluate the FOM as give by Eq. (6).
5. Replace x^* by the test point that gives the smallest value for the FOM.
6. Repeat steps 2–5 for M iterations.
7. Reduce the region size vector r by γ through $r^{j+1} = \gamma r^j$, where γ is a region contraction factor, such as 0.95, and j is the iteration index.
8. Go to step two and continue for M iterations to finish a pass and examine the results.

To include the number of segments as an additional variable in the optimization process, the modification of the basic LJ optimization procedure for PSFBG may be given by the followings steps:

1. Choose a reasonable initial number of segments i^*, for example $i^* = 0.5(s_{\max} + s_{\min})$, where $s_{\max}$ is the maximum number of segments and $s_{\min}$ is the minimum number of segments allowed.
2. Choose a reasonable initial region size for the number of segments r_{segment}, for example, $r_{\text{segment}} = 10(s_{\max} - s_{\min})$.
3. Choose some reasonable initial phases p^*, for example, $p^* = 0.5(p_{\min} + p_{\max})$, where $p_{\min}$ is the

minimum phase and p_{max} is the maximum phase.

4. Choose a reasonable initial region size r, for example, $r = 4(p_{max} - p_{min})$.

5. Choose the number of random points R to be used at each iteration, the number of iterations M to be used in a pass, and the number of passes Q.

6. Choose a test point R through the equation $t = t^* + Dr_{segment}$, where D is a diagonal matrix with randomly chosen elements from the interval $[-0.5, 0.5]$.

7. Check each of the R test points with respect to feasibility with the domain of phases.

8. For every R points, choose the phase point through the equation $d = d^* + Dr$.

9. Check each of the R test points with respect to feasibility for the domain of phases.

10. For each feasible point evaluate the FOM as given by Eq. (6).

11. Replace i^* with the test point that gives the smallest value for the FOM.

12. Replace p^* with the test point that gives the smallest value for the FOM.

13. Repeat steps 2–12 for M iterations.

14. Reduce the region size vector r by γ through $r^{j+1} = \gamma r^j$, where γ is a region contraction factor of phases and j is the iteration index and reduce the region size for the number of segments by $r^{j+1}_{segment} = \alpha r^j_{segment}$, where α is a region contraction factor for segments.

15. Go to step six and continue for M iterations to finish a pass.

16. At the end of the pass, determine the region size to be used at the beginning of the next pass from the size of the variation of each variable as suggested by Luus [23], i.e., choose

$$r_i^{k+1} = |p_i^*(k) - p_i^*(k-1)|, \qquad i = 1, 2, \ldots, N, \qquad (7)$$

where $p_i^*(k)$ is the best value of p_i after k passes, $p_i^*(k-1)$ is the best value of p_i after $k-1$ passes, and N is the number of segments. To prevent the region becoming zero, if the region size as calculated from Eq. (7) is less than the region collapse parameter ε, set the region size at the beginning of the pass for that variable equal to ε.

17. If $r_{segment}$ is less than some parameter η put the region size for the next pass equal to some integer value, for example 10.

18. Continue the procedure for Q passes.

19. Run the algorithm many times and examine the results.

4. Optimization Results and Discussion

The above algorithm was utilized to design multichannel spectra gratings for high reflectivity with a design wavelength $\lambda_D = 1550$ nm and with a low refractive index modulation amplitude. On the one hand, it is required that the reflectance of the channels have a high value, wherever possible. On the other hand, it is also desirable to have the smallest possible number of segments. Table 1 lists the parameters of the LJ algorithm used for the following simulations and the grating parameters are as follows: grating length $l = 10$ cm, effective refractive index $\overline{n_{eff}} = 1.46$, refractive index modulation amplitude $\overline{\delta n_{eff}} = 4 \times 10^{-4}$, and the period of phase sampling $\Lambda_s = 1$ mm.

Table 1. Parameters for Luus-Jaakola Optimization Procedure

Parameter	Value
No. of test points (R)	30
No. of iterations (M)	60
No. of passes (Q)	10
Range of segments ($s_{min} - s_{max}$)	2–50
Range of phases ($p_{min} - p_{max}$)	$-2\pi - 2\pi$
Region contraction factor of phases (γ)	0.97
Region contraction factor of segments (α)	0.95

The results are shown in Figs. 1–8. In each case the figures show the reflection spectra of PSFBG and its phase profile. The number of WDM channels in these simulations are 14, 16, 20, and 32, respectively. The reflection spectra shown in Fig. 1 was achieved by dividing the sampling period into 10 segments. The phase profile for the 14 channel WDM is shown in Fig. 2. Its reflectance features an excellent uniformity where the reflectivity of the channels is nearly 100% and identical. In Fig. 3, the number of WDM channels is increased to 16 by dividing the sampling period into 16 segments, as seen in Fig. 4. The WDM channels are identical and the reflectance in this case is nearly 99%.

By dividing the grating phase into 20 segments, we are able to get 20 channels with reflectivities of almost 99%, as shown in Fig. 5. Producing 32 channels can be achieved by dividing the grating phase into 36 segments. For 32 channels, with $\overline{\delta n_{eff}} = 4 \times 10^{-4}$, the reflectance features are slightly worse than in the previous cases, with $R = 97\%$, as shown in Fig. 7. By using the phase profiles in Fig. 8, and increasing the value of the effective mode index of refraction to

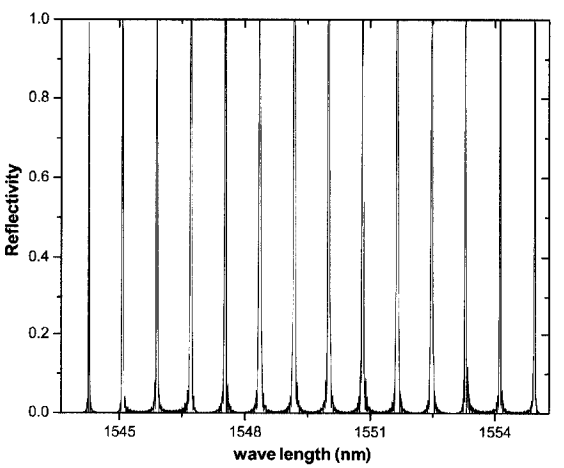

Fig. 1. Reflectivity spectrum of optimized phase profile with 10 segments.

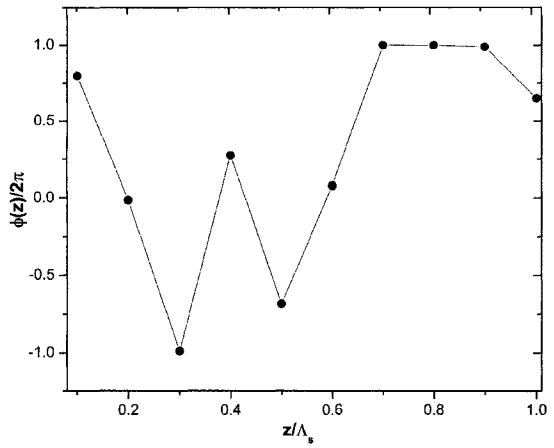

Fig. 2. Optimized phase profile with 10 segments.

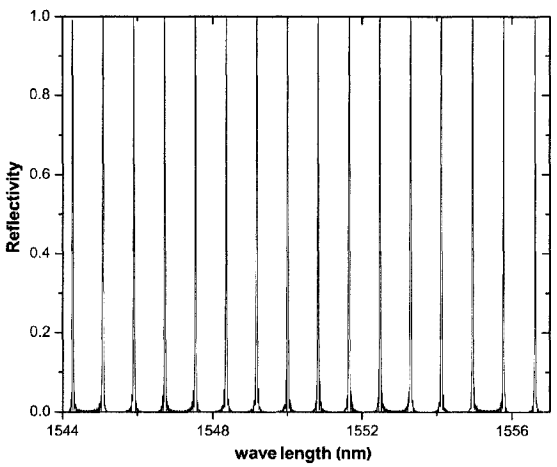

Fig. 3. Reflectivity spectrum of optimized phase profile with 16 segments.

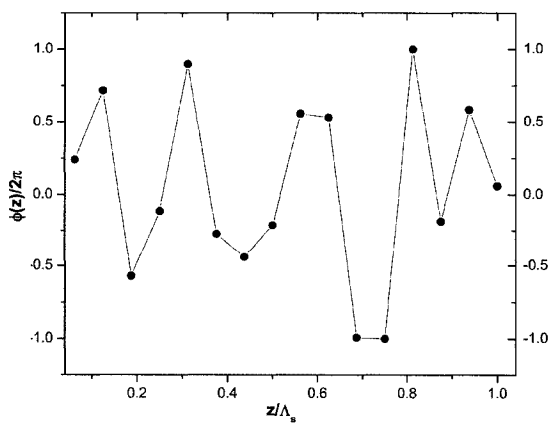

Fig. 4. Optimized phase profile with 16 segments.

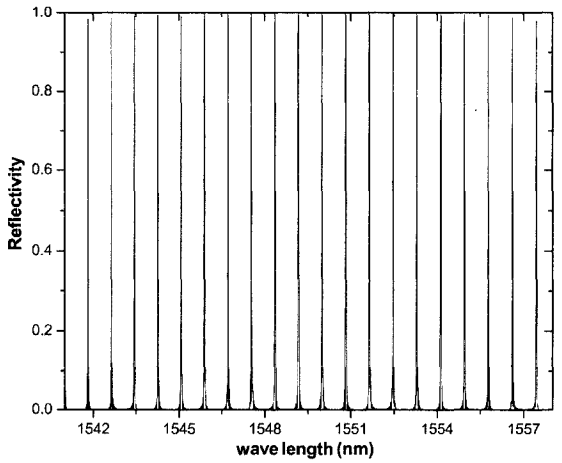

Fig. 5. Reflectivity spectrum of optimized phase profile with 20 segments.

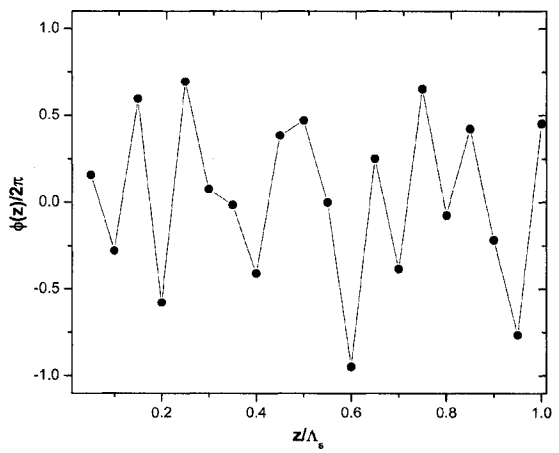

Fig. 6. Optimized phase profile with 20 segments.

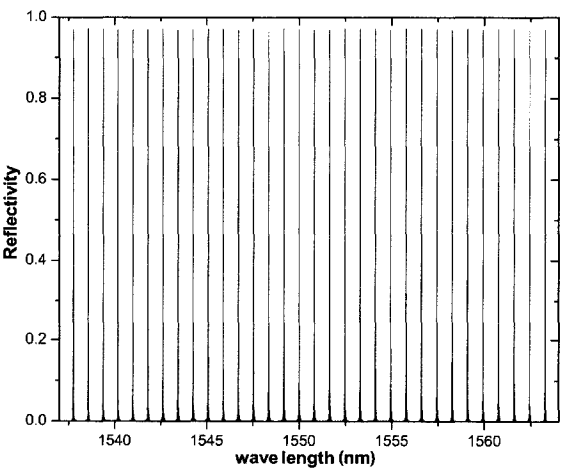

Fig. 7. Reflectivity spectrum of optimized phase profile with 36 segments.

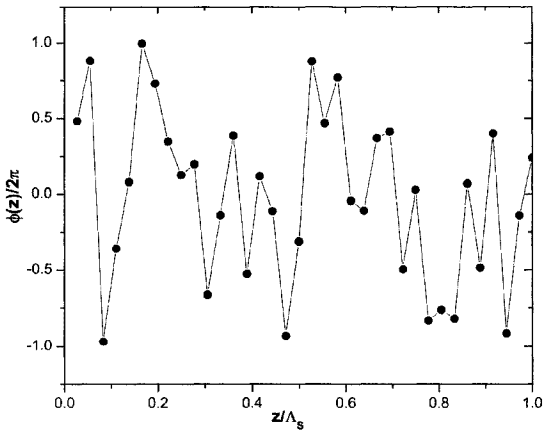

Fig. 8. Optimized phase profile with 36 segments.

$\overline{\delta n_{\text{eff}}} = 6 \times 10^{-4}$, the reflectivity is increased ($R = 98.9\%$), as shown in Fig. 9. The effectiveness of the LJ optimization procedure is confirmed by comparing the above results with those of other authors. The spectra of PSFBGs that produces 16 channels was obtained with a grating length of 10 cm and $\delta n_{\text{eff}} = 8 \times 10^{-4}$, by using 30 segments and by using a multidimensional optimization method [5]. In another study using the simulated annealing method, 20 segments were required to produce 16 channels with a grating length of 1.52 cm [12]. However, only 16 segments were needed in our case with the LJ method. This is a consequence of allowing the number of segments to be variable in the LJ method whereas, in the other methods, this number was fixed.

5. Conclusion

A new method based on the Luus–Jaakola optimization procedure and the transfer matrix method has been applied for designing multichannel spectra based on PSFBG. Simulation results show that with this method the multichannel design can be reconstructed with a minimum number of segments in the region with minimum phases. The number of channels determines the number of segments of the FBG. By increasing the number of channels, the spatial resolution can be improved but the complexity of PSFBG structure and calculation effort will also be increased. The development of this algorithm will permit the use of PSFBG for dispersion compensation of WDM optical communication systems.

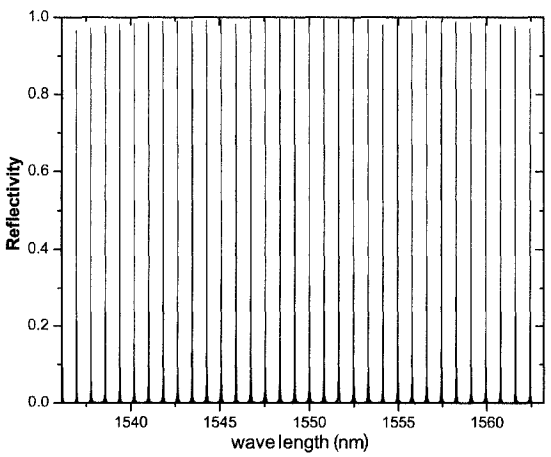

Fig. 9. Reflectivity spectrum of optimized phase profile with 36 segments and $\overline{\delta n_{\text{eff}}} = 6 \times 10^{-4}$.

The authors acknowledge the financial support of the government of Saudi Arabia for this study.

References

1. A. Paterno, N. Haramoni, J. Silva, and H. Kalinowski, "Highly reliable strain-tuning of an erbium-doped fiber laser for the interrogation of multiplexed Bragg grating sensors," Opt. Commun. **273**, 187–192 (2007).
2. K. Kashyap, *Fiber Bragg Grating* (Academic, 1999).
3. A. Othonos and K. Kally, *Fiber Bragg Gratings* (Artech House, 1999).
4. K. O. Hill and G. Meltz, "Fiber Bragg grating technology fundamentals and overview," J. Lightwave Technol. **15**, 1263–1276 (1997).
5. H. Lee and G. Agrawal, "Purely phase-sampled fiber Bragg gratings for broad-band dispersion and dispersion slope compensation," IEEE Photonics Technol. Lett. **15**, 1091–1093 (2003).
6. H. Lee and G. P. Agrawal, "Add-drop multiplexers and interleavers with broadband chromatic dispersion compensation based on purely phase-sampled fiber gratings," IEEE Photonics Technol. Lett. **16**, 635–637 (2004).
7. X. Xu, Y. Dai, X. Chen, D. Jiang, and S. Xie, "T chirped and phase-sampled fiber Bragg gratings for tunable DBR fiber laser," Opt. Express **13**, 3877–3882 (2005).
8. Q. Wu, C.-X. Yu, K. Wang, X. Xin, X. Wang, and Z. Yu, "The control of channel numbers with equal reflectivity of sinc-sampled fiber Bragg gratings," Opt. Commun. **233**, 83–88 (2004).
9. Y. Liu, Z. Yu, H. Yang, and N. Zhang, "Optimization of index modulation profile of sampling period for sampled fiber Bragg gratings," Proc. SPIE **5595**, 328 (2004).
10. A. Gill, K. Peters, and M. Studer, "Genetic algorithm for the reconstruction of Bragg grating sensor strain profiles," Meas. Sci. Technol. **15**, 1877–1884 (2004).
11. M. Liang, Q. Fang, and Y. Wang, "Fiber Bragg grating filter synthesis using the genetic algorithm," Proc. SPIE **4603**, 228 (2001).
12. I. Navruz and F. Guler, "Optimization of reflection spectra for phase-only sampled fiber Bragg gratings," Opt. Commun. **271**, 119–123 (2007).
13. P. Dong, J. Azana, and A. Kirk, "Synthesis of fiber Bragg grating parameters from reflectivity by means of a simulated annealing algorithm," Opt. Commun. **228**, 303–308 (2003).
14. R. Luus and Thi. Jaakola, "Optimization by direct search and systematic reduction of the size of search region," AIChE J. **19**, 760–766 (1973).
15. R. Luus, "Use of Luus-Jaakola optimization procedure for singular optimal control problems," Nonlinear Anal. Theory Methods Appl. **47**, 5647–5658 (2001).
16. R. Luus, "Optimization of heat exchanger networks," Ind. Eng. Chem. **32**, 2633–2635 (1993).
17. Y. P. Lee, G. P. Rangahiah, and R. Luus, "Phase and chemical equilibrium calculations by direct search optimization," Comput. Chem. Eng. **23**, 1247 (1999).

18. S. Al-Marzoug and R. Hodgson, "Luus–Jaakola optimization procedure for multilayer optical coatings," Opt. Commun. **265**, 234–240 (2006).
19. B. Liao and R. Luus, "Comparison of the Luus-Jaakola optimization procedure and the genetic algorithm," Eng. Optim. **37**, 381–398 (2005).
20. T. Erdogan, "Fiber grating spectra," J. Lightwave Technol. **15**, 1277–1294 (1997).
21. C. Sun, C. Li, and X. Yu, "Study on sampled chirped fiber gratings," Opt. Commun. **218**, 297–302 (2003).
22. G. G. Nair, "On the convergence of the LJ search method," J. Optim. Theory Applications **28**, 429–434 (1979).
23. R. Luus, "Determination of the region sizes for LJ optimization procedure," Hung. J. Ind. Chem. **26**, 281–286 (1998).

7

Conclusion

The research described in this thesis was rooted in applying the Luus-Jaakola optimization procedure to some optical problems. The LJ optimization method is simple, easy to implement, and robust in calculating the optimum. The impact of initial guess values is minimal on the optimal parameters and the optimum. Furthermore, it was illustrated that a large number of random points is not necessary. In the LJ method, the objective function is controlled directly. The parameters that give the smallest objective function are saved in the first pass after a search in the given region space. Subsequently, it proceeds into the next pass with the saved parameters, whereby the objective function is minimized along the number of passes until the optimum is reached. The central theme is the mixing of integers and real variables in the parameter optimization process. From the optimization results of multilayer coatings, the optimal solutions of Luus-Jaakola showed better multilayer performance , in terms of flatness, maximum reflectivity and the number of layers,than do existing methods.

To test the efficiency of the simple Luus-Jaakola technique, we used the Lennard Jones potential as a massively multimodal test problem. As we know, finding the equilibrated configuration of atomic clusters modeled by the Lennard-Jones potential posses a challenging task to numerical optimization strategies as the number of local minima grows exponentially with the number of atoms in the cluster. The algorithm was successful in finding the the global minima of the Lennard Jones clusters. We showed that the algorithm is a fast and highly efficient optimization tool, which can be used in optimization problems. Also, the efficiency of Luus-Jaakola was compared with the

particle swam optimization technique. A standard benchmarking function was used to compare both algorithms. We showed that the Luus-Jaakola optimization performs much better than the particle swarm technique in higher dimension optimization problems.

The multilayer mirror is another problem of higher dimension and a difficult optimization problem. In the second chapter, we modified the Luus-Jaakola optimization by mixing both integers and real variables in the space of optimization. In section 4 of this article, we applied the modification of Luus-Jaakola to the design and characterization of multilayer coatings for Soft X-rays. The modified algorithm has been used to maximize the reflectivity over a range of incident angles at fixed wavelength, and over a wavelength range at a fixed incident angle. To test the modification, we showed how such a procedure can be applied efficiently to the case of multilayer coatings to maximize the reflectivity with a smaller number of layers. From the numerical results of three multilayer thin-film problems, we demonstrated that the Luus-Jaakola approach is better than some other optimization methods like Genetic algorithms. Also, the Luus-Jaakola optimization procedure outperformed f or a mixed number of layers and thickness of each layer, combining the real variables with integer variables, based on numerical results. We showed that the reflectivity designs could be achieved with fewer layers. The main point is that the modification of the Luus-Jaakola algorithm is able to find good multilayer stack performance within a single procedure resulting in fewer layers and higher reflectivity. This reduces the amount of human effort and expertise required for analyzing different designs of multilayer mirrors. Furthermore, it reduces the probability of over looking feasible solutions. These properties make the Luus-Jaakola algorithm a promising and valuable alternative method.

Following the results from the second chapter, we applied this technique to the design of multilayer mirrors for a target application, such as an astronomical grazing-incidence hard X-ray telescope in the third chapter. As we know, a high through-put telescope is an essential instrument for astronomy. In the X-ray region, it is also needed for high sensitivity observations. In the hard X-ray region, total reflection which used in previous X-ray telescope requires extremely grazed incident angles. It means multilayer X-ray mirrors must be needed for hard X-ray telescope. We developed multilayer mirrors for hard X-ray telescopes. For astronomical use, X-ray optics requires a wide energy band and high through-put. From this point of view, performance of the X-ray reflector is most important for the X-ray telescope. Multilayer mirrors make it possible to extend the energy band to the hard X-ray region above 10 keV, in contrast to the total reflected mirror, used in previous X-ray telescopes, which limits the energy band of telescopes in the soft

X-ray band. We tried to extend the energy band of X-ray telescopes up to 40 keV using Pt/C multilayers. Platinum is one of the most suitable materials for X-ray telescopes, because it is very stable chemically and the energy of the K absorption edge is higher than the energy of the 44Ti nuclear x-ray, which is key of the mystery of supernovas. We tried to optimize the design of the multilayer mirrors for X-ray telescopes. It has to have high reflectivity for high through put and a wide energy band, for wide band observation and field of view of the telescope. Furthermore, a small number of layer pairs is required for mass production of reflectors.

We designed multilayer mirrors by modifying the Luus-Jaakola optimization procedure . Design parameters are interval energy and number of layer pairs of these multilayers. We designed 13 multilayer mirrors according to its incident angle, 0.1-0.3 degree. We achieved high reflectivity in the range between 25% and 90% using these multilayer mirrors with fewer layer pairs. By comparing our approach with the Block method, the reflectivity is improved and the number of layers is decreased.

Determination of parameters of thin films was shown in chapter four. We proposed the Luus-Jaakola method that makes it possible to determine the optical constants, the root mean square roughness and the thickness of thin films with the use of only reflectance data obtained at a single wavelength over a range of incident angles. The calculation procedure is based on the use of fairly simple relations suitable for the programmed realization and does not call for the prescription of the initial values of the determined parameters and complex methods of numerical search for minimization of the merit function.

The method provides excellent accuracy and makes it possible to uniquely solve the inverse problem of multilayer mirrors. Its applicability has been verified on some numerical models of a thin film system as presented in chapter four. The results show that the Luus-Jaakola optimization procedure is able to determine the thickness of films and the roughness with an accuracy of less than 7%. The optical constants obtained are also in good agreement with reported values for films having an error of less than 1%.

In chapter five, a new type of periodic structure with three different materials has been investigated and compared with standard multilayer mirrors from the optimization point of view. We have studied two structures to design these mirrors. These structure are multilayers with barrier zones and multilayers with three-component stacks in periodic structures. Using the modification of Luus-Jaakola approach that was introduced in the second chapter, three material structures have

been optimized in terms of thickness and number of layers. The modification of the Luus-Jaakola algorithm has proven to be extremely effective for these designs. The algorithm allows for an automated search of material combinations for the design of optimal multilayer components for specific applications and this is the subject of ongoing research. In addition, the number of layers was optimized to achieve the maximum reflectivity for every structure. We showed that the use of a third material allows an important increase of the reflectance if the order of the three materials in the stack is optimized. We have selected in a numerical study Mo, Si, C and Be materials as good candidates to produce three component multilayers in the spectral range around 13.4nm. These combinations of high reflective properties and lower number of layers can provide good potential for their use as elements in EUV collector optics. It is a simple matter to adapt the algorithm to desensitize the stack structure to use preferred materials which may be required for their inert properties in particulary harsh environments.

Phase-only sampled fiber Bragg gratings (PSFBG)is also another challenge in high dimensional optimization problem. The purpose of this problem is to obtain the maximum number of identical channels with higher reflectivity by constituting minimum possible phase shift for a PSFBG containing regularly located phase variation inside the sampling period. This problem again is one of mixing optimization variables where the number of segments is an integer and the phase shift is a real variable. For this reason, in chapter six, we used the modified Luus-Jaakola optimization procedure and transfer matrix method to minimize the number of segments with minimum phases. In this chapter, the phase sampling function is divided into fewer but enough segments to develop super structure PSFBG. When optimized the number of segments and the phase shift in FBG, multiple channels with high uniformity and fewer number of segments can be achieved. It can be predicated that the modification of Luus-Jaakola optimization procedure will become a powerful rival to other approaches to realize the purely phase only sampled fiber Bragg gratings for wavelength-division-multiplexing applications.

Final Thoughts

This thesis dealt with using Luus-Jaakola optimization procedure in some optical problems. Several advantages were introduced for optimizing multilayer mirrors and fiber Bragg gratings. Firstly, the representation employed makes it unnecessary to specify beforehand how many layers or segments will be present in a design. The algorithm can decide this, which is very efficient. Secondly,

Luus-Jaakola method is able to locate promising designs with fewer parameters. Finally, it is believed that the proposed method is an attractive and effective way for optimally designing complicated optical systems, and can be further developed to construct a powerful toolbox for practical design of many optical devices.

However, the full capability of this approach, in particular for application to hard X-rays, should be further investigated. Even the extremely simple algorithm that has been modified and presented has not yet been fully and systematically explored and the examples discussed in this thesis are examples that may possibly be improved. In particular, the algorithm should be enriched with a number of extensions from more sophisticated reproduction to the possible inclusion of local minima searching techniques into the Luus-Jaakola algorithm, achieving a so called memetic algorithm.

Appendix A

Simple Luus-Jaakola optimization procedure code

```
1  import java.io.BufferedWriter;
2  import java.io.FileWriter;
3  import java.io.IOException;
4  import java.io.PrintWriter;
5  /**
6   * A simple Luus-Jaakola optimization procedure
7   * to to minimize  Rosenbrock's function
8   */
9  public class  LJ {
10
11    private static final int TestPoints = 50;
12    private static final int MaxPass=50;
13    private static final int Parameters =12;
14    private static final double Min_Value =-2.048;
15    private static final double Max_Value =2.048;
16    private static final int NLoop = 200;
17    private FitnessFunction fit = new FitnessFunction();
18    private RandomHelper random = new RandomHelper();
19    private static final int runs=50;
20
21   // the Luus_Jaakola  loop
22    private void run() throws IOException {
23
24    Individual[] population;
25    Individual yi ,y;
26
27     double[] Region;
28     int value=NLoop*(MaxPass+1);
29     double eps=Math.pow(10,-3);
30
31     // open file to write iteration vs fitness function
32    PrintWriter it=new PrintWriter(new BufferedWriter(
33                              new FileWriter("loops.dat")));
34    //open file to write  pass vs fitness function
35    PrintWriter ps=new PrintWriter(new BufferedWriter(
36                              new FileWriter("pass.dat")));
37     double[] avF   =  new double[value];
38     double[] bestF =  new double[value];
39     for(int ii=0;ii<runs;ii++){
40     int k=0;
41  //  double[] bestF=new double[value];
42     int loopCount = 0;
43     int pass=0;
44  // initial starting values for y* and r(0)
45     Region=initialRegion();
46     yi=initialValues();
47     y=yi; //save the initial values
48  //passes loop
49        do{
```

```
50          pass++;
51
52        if(pass % 2 == 0)eps=0.5*eps;
53  //iteration loop
54        for(int lop=0;lop<NLoop;lop++) {
55          k++;
56        loopCount ++;
57
58        population = createPopulation (Region,yi);
59
60        evaluate (population, fit);
61
62  // sort the best fitness from population
63        printStats (population);
64         int best = 0;
65        double bestFitness;
66           bestFitness = population[0].getFitness();
67           for (int i=0; i<population.length; i++)
68            if (population[i].fitness < bestFitness) {
69               best = i;
70               bestFitness = population[i].fitness;
71            }
72  // write the file loops  ( iteration vs bestFitness)
73        it.println(loopCount+" "+bestFitness);
74
75  // reducing the region size vector r by the factor 0.95
76        Region=reduceRegion(Region);
77
78  // save the bestFitness for next iteration
79        yi=population[best];
80
81          bestF[k]=yi.getFitness();
82  //     printStats (population, loopCount);
83
84     } // end iteration loop
85
86  //print the pass vs bestFitness
87    ps.println(pass+" "+yi.getFitness());
88
89  // change of region size for next pass
90
91     Region=RegionPass(eps,yi,y);
92
93  // save the best fitness for next pass
94     y=yi;
95
96
97  } while (! endTest (pass));
98  for(int j=0;j<avF.length;j++)  {avF[j]+=bestF[j];}
```

```
99
100 // close both files
101 it.close();
102 ps.close();
103     System.out.println("run="+ii+" "+"BestF= "+yi.getFitness()) ;
104  }
105 PrintWriter af=new PrintWriter(new BufferedWriter( new FileWriter("avgFitness.dat"
106 for(int j=0;j<avF.length;j++)af.println(j+" "+avF[j]/runs);
107 af.close();
108 }
109
110   /**
111    * Method regionPass
112    * @return r after Pass Loop
113    * @param yi Best value of y afeter k passes
114    * @param eps  region Callapse
115    * @param yy  Best value of y after (k-1) passes
116    */
117   private double[] RegionPass( double eps, Individual yi,Individual yy)
118   {
119      double[] RegionPass=new double[Parameters];
120    for(int i=0;i<Parameters;i++)
121       {
122       RegionPass[i]=Math.abs(yi.getPos(i)-yy.getPos(i));
123         if (RegionPass[i]<=eps)RegionPass[i]=eps;
124        }
125   return RegionPass;
126   }
127
128 /**
129  * Method reduceRegion
130   * @return  Region size after j loop
131   * @param   regionBefore size befer j loop
132   */
133 private double[] reduceRegion( double[] regionBefore)
134 {
135    double[] regionAfter= new double[Parameters];
136       for(int i=0;i<Parameters;i++){
137     regionAfter[i]=0.95*regionBefore[i];}
138 return regionAfter;
139 }
140
141 /**
142  * Method initial Region  r(0)
143   * @return Region  r
144   */
145 private double[] initialRegion()
146 {
147    double[] Region=new double[Parameters];
```

```
148     for(int i=0;i<Parameters;i++)
149        {
150     Region[i]=0.5*(Max_Value-Min_Value);
151        }
152  return Region;
153  }
154
155  /*
156   * Method initial Values of point y*
157   */
158  private Individual initialValues()
159  {
160  Individual yi=new  Individual(Parameters);
161  for(int i=0;i<Parameters;i++)
162        {
163     yi.setPos(i,0.5*(Min_Value+Max_Value));
164        }
165  return yi;
166  }
167
168  /* Method  create Random points
169   */
170
171  private Individual[] createPopulation( double[] Region,
172                                 Individual yi)
173  {
174
175     Individual[] population = new Individual[TestPoints];
176     for (int i=0; i<TestPoints; i++) {
177        population[i] = createRandomIndividual (Region,yi);
178     }
179     return population;
180  }
181
182  // Create a single random individual and check
183  // the feasibility of each yi with respect to the bounds.
184     private Individual createRandomIndividual (double[] Region,
185                                        Individual yi) {
186
187     Individual individual = new Individual (Parameters);
188     for (int i=0; i<Parameters; i++) {
189        individual.setPos (i, yi.getPos(i) + (random.random() * Region[i]));
190     }
191
192     for(int i=0;i<Parameters;i++)
193     {
194        if(individual.getPos(i)<Min_Value) individual.setPos(i,Min_Value);
195        if(individual.getPos(i)>Max_Value) individual.setPos(i,Max_Value);
196     }
```

```
197     return individual;
198     }
199
200   // Evaluate an array of individuals
201     private void evaluate (Individual[] individuals, FitnessFunction fit) {
202     for (int i=0; i<individuals.length; i++) {
203       fit.evaluate (individuals[i]);
204     }
205     }
206
207     // Print some runtime statistics
208     private void printStats(Individual[] population)
209                         throws IOException {
210     int best = 0;
211     PrintWriter op=new PrintWriter(new BufferedWriter(
212                               new FileWriter("optimal.dat")));
213     double bestFitness = population[0].getFitness();
214     for (int i=0; i<population.length; i++) {
215
216       if (population[i].fitness < bestFitness) {
217         best = i;
218         bestFitness = population[i].fitness;
219       }
220
221       }
222   //Print the optimal positions in data file
223         for(int i=0;i<Parameters;i++){
224        //System.out.println(i+" = "+population[best].getGene(i));
225        op.println(population[best].getPos(i));
226           }
227        //close file optimal
228        op.close();
229   //   System.out.println("Loop " + loop + " best fitness " + bestFitness );
230
231     }
232     // End test
233     // Implemented Algorithm: finish after n loops
234
235     private boolean endTest(int pass) {
236       return(pass>=MaxPass);}
237
238     // Main class (static)
239     public static void main (String[] args) throws IOException {
240     LJ lj = new LJ();
241     lj.run();
242     }
243   }
```

```
1  /**
2   * Fitness funtion:
3   */
4  public class FitnessFunction {
5
6    /**
7     * Avaluate an individual. Compute fitness and store it in the individual
8     *
9     * @param individual an <code>Individual</code> The individual to be evaluated
10    */
11   public void evaluate (Individual individual) {
12
13     //Rosenbrock's function( n variables)
14
15      double f = 0;
16     for( int i = 0; i < (individual.postypeSize() - 1); i++ ) {
17       double p1 = individual.getPos(i) * individual.getPos(i); //  x_i^2
18       double p2 = (1 - individual.getPos(i)); //        ( 1 - x_i )
19       p2 *= p2; //                    ( 1 - x_i )^2
20       double p3 = individual.getPos(i + 1) - p1; //    ( x_{i+1} - x_i^2 )
21       p3 *= p3; //                    ( x_{i+1} - x_i^2 )^2
22
23       f += 100 * p3 + p2; //              100 ( x_{i+1} - x_i^2 )^2 + ( 1 - x_i )^2
24     }
25   individual.setFitness(f);
26   }
27 }
28
29
30
31
```

```
1  /**
2   * A simple individual
3   * Storage for the genotype and fitness information
4   *
5   */
6
7  public class Individual {
8
9     double[] pos;
10    double fitness;
11
12
13    public Individual (int size) {
14    pos = new double[size];
15    }
16
17    public double getPos (int position) {
18    return pos[position];
19    }
20
21    public void setPos (int position, double value) {
22    pos[position] = value;
23    }
24
25    public int postypeSize() {
26    return pos.length;
27    }
28
29    public double getFitness() {
30    return fitness;
31    }
32
33
34    public void setFitness (double newFitness) {
35    fitness = newFitness;
36    }
37
38 }
39
40
41
42
43
44
45
```

```
1  import java.util.Random;
2  /**
3   * Some Random Helper classes
4   */
5  public class RandomHelper {
6
7    Random rng ;
8
9    /**
10    * Creates a new <code>RandomHelper</code> instance.
11    *
12    */
13   public RandomHelper () {
14   rng = new Random (System.currentTimeMillis());
15   }
16   /**
17    * Get a random int with equal distribution
18    *
19    * @param minVal an <code>int</code> value: minimum random value (inclusive)
20    * @param maxVal an <code>int</code> value: maximum random value (exclusive)
21    * @return an <code>int</code> value: the random value
22    */
23
24    public int between (int minVal, int maxVal) {
25   if (minVal == maxVal -1) return minVal;
26
27   return (minVal + rng.nextInt (maxVal - minVal));
28   }
29
30   /**
31    * Get a random double value with equal distribution
32    *
33    * @param minVal a <code>double</code> value: minimum random value (inclusive)
34    * @param maxVal a <code>double</code> value: maximum random value (
   exclusive)
35    * @return a <code>double</code> value: the random value
36    */
37    public double between (double minVal, double maxVal) {
38   if (minVal == maxVal) return minVal;
39   return (minVal + rng.nextDouble () * (maxVal - minVal));
40   }
41
42   /**
43    * Return a random boolean with equal true-false probability
44    *
45    * @return a <code>boolean</code> value: the random boolean
46    */
47    public boolean randomDecision () {
48   return (rng.nextDouble() >= 0.5);
```

```
49    }
50
51    /**
52     * Return a random boolean with given true-probability
53     *
54     * @param prob a <code>double</code> value: probability that value is true
55     * @return a <code>boolean</code> value: the random boolean
56     */
57     public boolean randomDecision (double prob) {
58    return (prob > rng.nextDouble());
59    }
60
61    /**
62     * Get a Gaussian distributed random value with given standard deviation
63     *
64     * @param deviation a <code>double</code> value: standard deviation of Gaussian
65     * @return a <code>double</code> value: the random value
66     */
67     public double gauss (double deviation) {
68    return (deviation * rng.nextGaussian());
69    }
70
71    /**
72     * Get a Cauchy-distributed random value with given scale
73     *
74     * @param deviation a <code>double</code> value: Cauchy scale
75     * @return a <code>double</code> value: the random value
76     */
77
78     public double cauchy (double deviation) {
79
80    double u, v;
81    do {
82       u = 2.0 * rng.nextDouble() - 1.0;
83       v = 2.0 * rng.nextDouble() - 1.0;
84    }
85    while (u*u+v*v>1.0 || (u==0.0&&v==0.0));
86
87    if (u!=0)
88       return(deviation * (v/u));
89    else
90       return(0.0);
91    }
92    public double random(){
93       double u;
94       u=2.0*rng.nextDouble()-1.0;
95          return u;
96     }
97 }
```

Appendix B

Supplementary graphs of some results

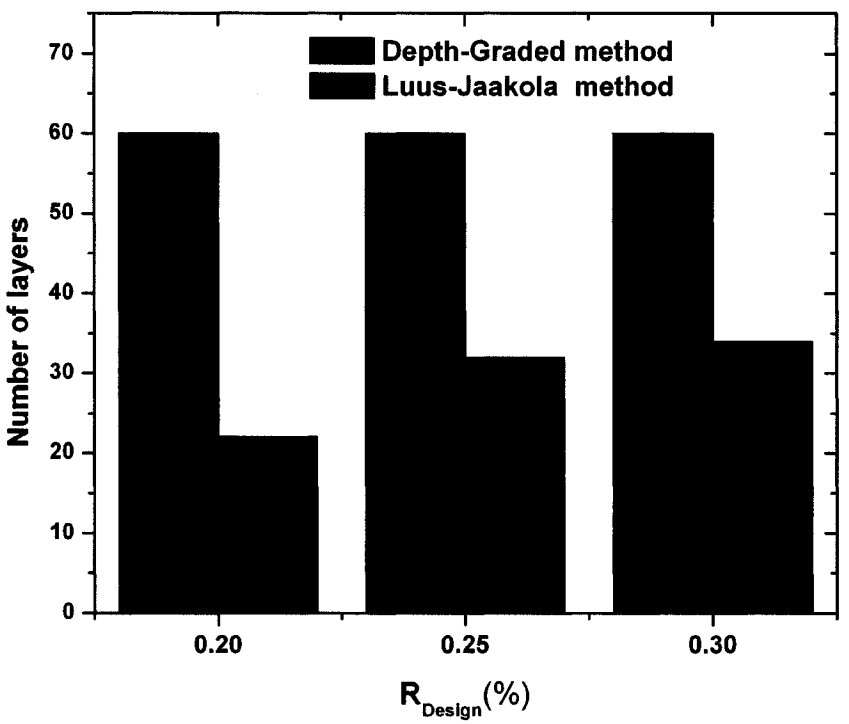

FIGURE B.1 Presenting the comparison between Luus-Jaakola method and Depth-graded method of number of layers as columns graph of Table 1 in chapter two

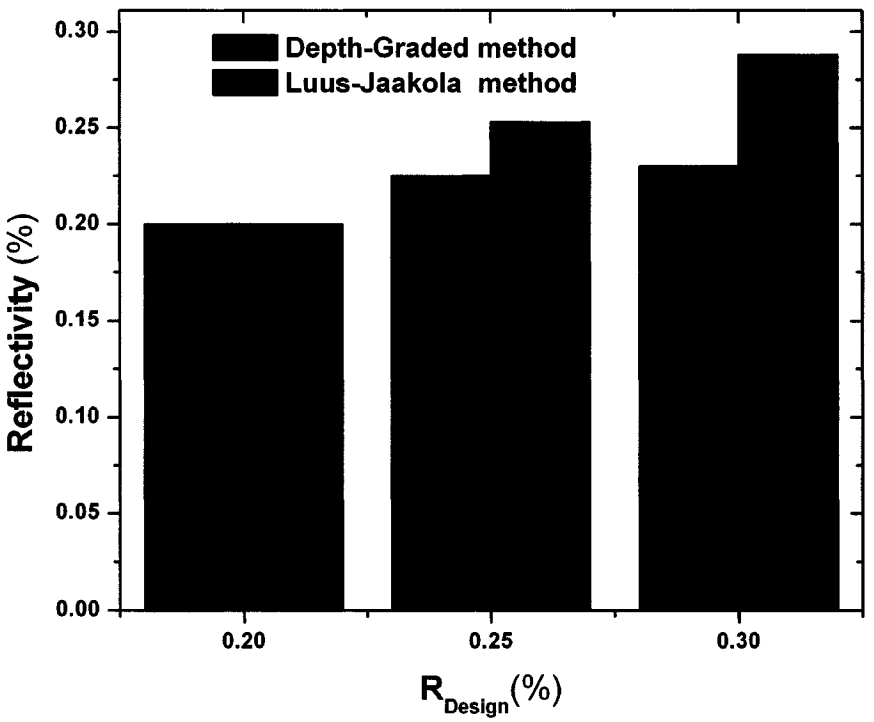

FIGURE B.2 Presenting the comparison between Luus-Jaakola method and Depth-graded method of reflectivity as columns graph of Table 1 in chapter two

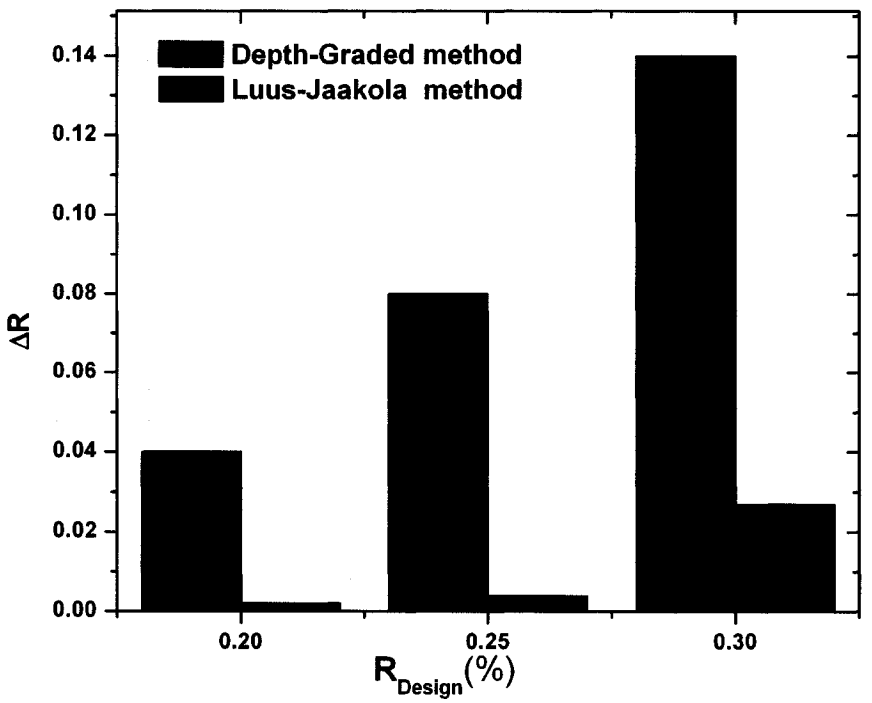

FIGURE B.3 Presenting the comparison between Luus-Jaakola method and Depth-graded method of uniformity as columns graph of Table 1 in chapter two

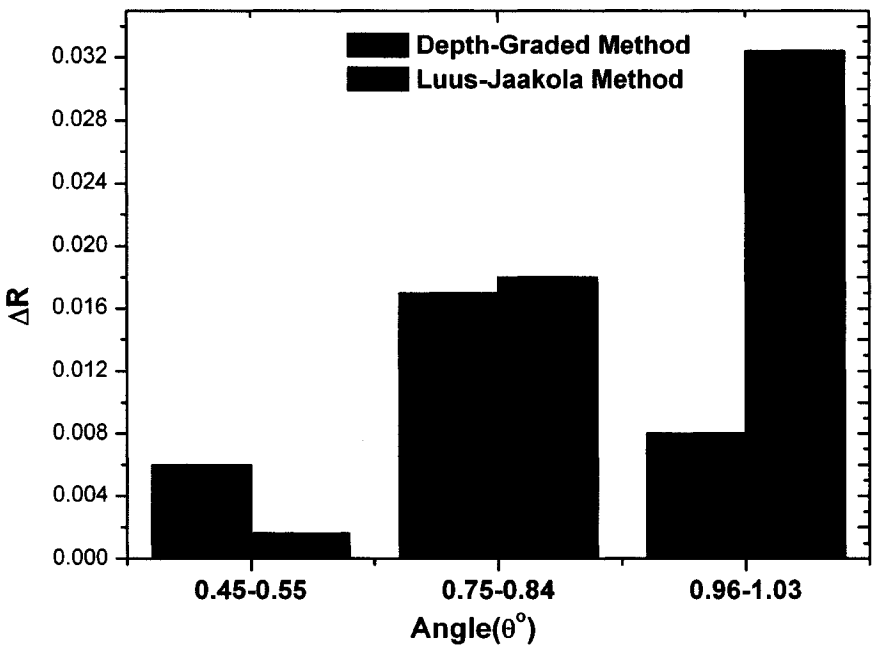

FIGURE B.4 Presenting the comparison between Luus-Jaakola method and Depth-graded method of uniformity as columns graph of Table 3 in chapter two

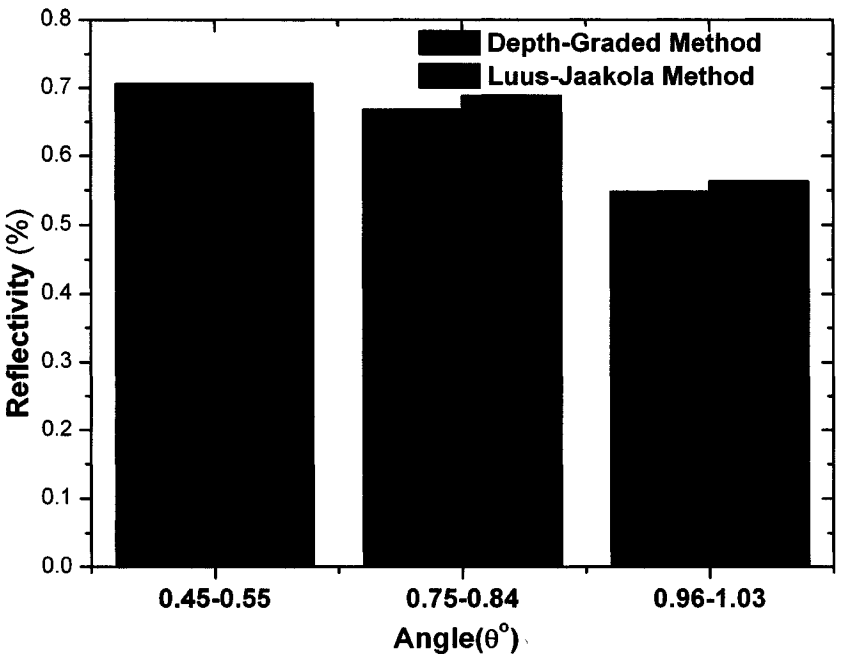

FIGURE B.5 Presenting the comparison between Luus-Jaakola method and Depth-graded method of reflectivity as columns graph of Table 3 in chapter two

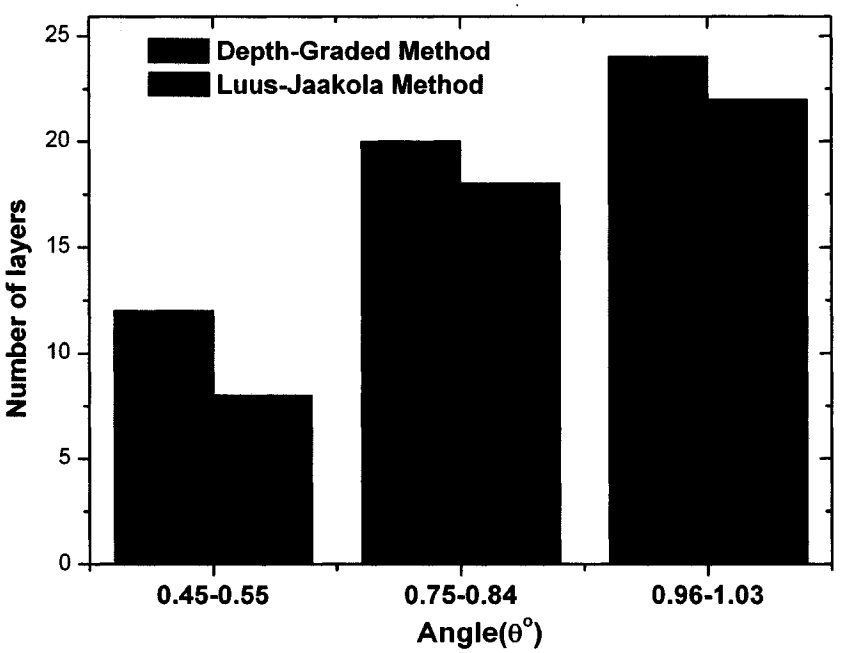

FIGURE B.6 Presenting the comparison between Luus-Jaakola method and Depth-graded method of number of layers as columns graph of Table 3 in chapter two

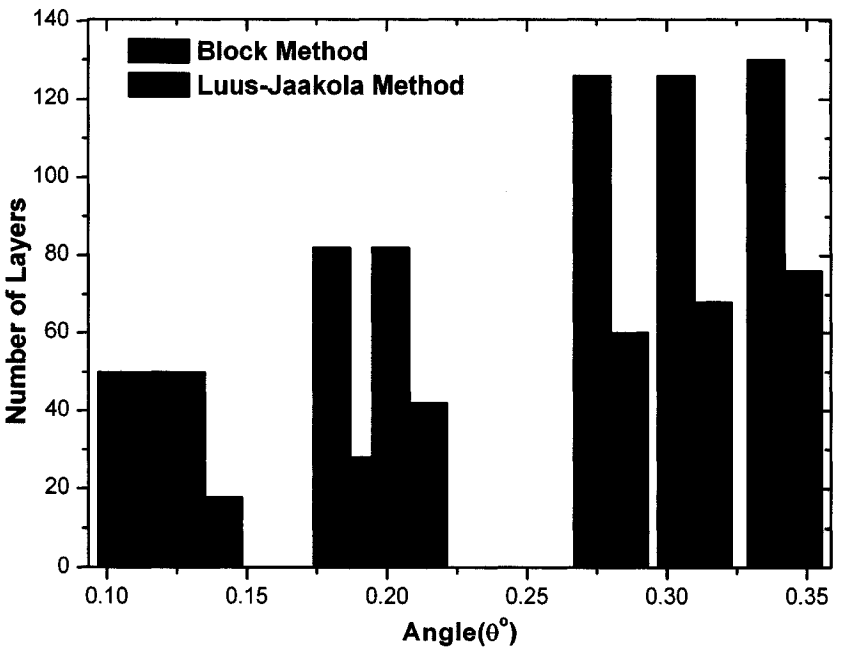

FIGURE B.7 Presenting the comparison between Luus-Jaakola method and Block method of number of layers as columns graph of Table 2 in chapter three

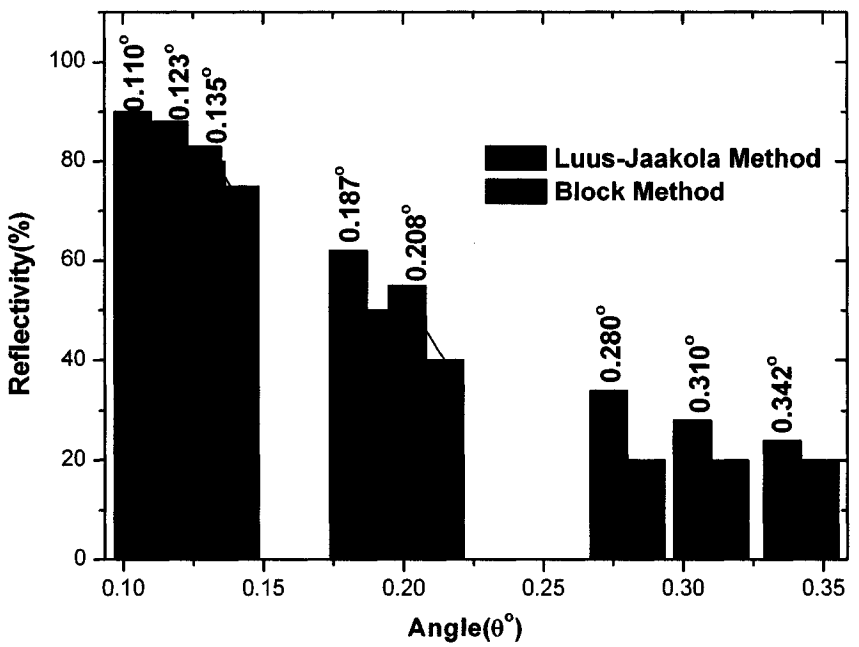

FIGURE B.8 Presenting the comparison between Luus-Jaakola method and Block method of reflectivity as columns graph of Table 2 in chapter three

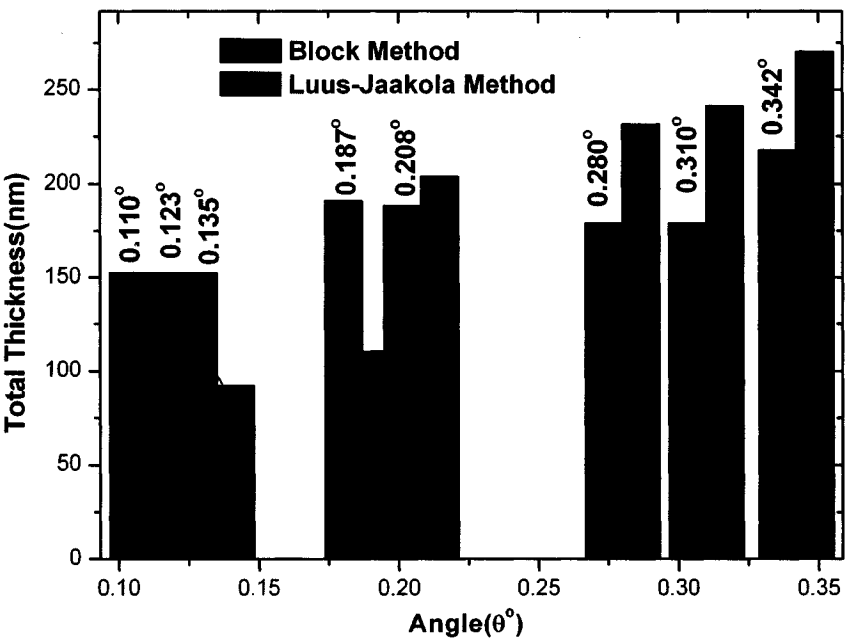

FIGURE B.9 Presenting the comparison between Luus-Jaakola method and Block method of total thickness as columns graph of Table 2 in chapter three

References

[1] R Jenkins. *Encyclolpeida in Analytical Chemistry.* John Wiley and Sons Ltd, Chichester (2000).

[2] D Attwood. *Soft X-rays and exterm ultraviolet radiation.* Cambridge University Press, Cambridge (1999).

[3] Wen-C Chianga , J G Linb , K H Hsub, D S Husseyc,and D V Baxterc. *Study of ferromagnetismŰsuperconductivity interactions in co/nb multilayers*, ***J. Magn. Magn. Mater.*** **304**, e97–e99 (2006).

[4] G Hana , Y Wua, and Y Zhengb. *Dual-synthetic magnetic force microscopy tip and its imaging performance*, ***J. Magn. Magn. Mater.*** **315**, 46–52 (2007).

[5] K Murakami, T Oshino, H Nakamura, M Ohtani, and H Nagata. *Schwarzschild microscope for carbon kalpha radiation*, ***Appl. Opt.*** **32**, 7057–000 (1993).

[6] D A Tichenor et al. *Diffraction-limited soft-x-ray projection imaging using a laser plasma source*, ***Opt. Lett.*** **16**, 1557–0000 (1990).

[7] K Yamashita et al. *Supermirror hard-x-ray telescope*, ***Appl. Opt.*** **37**, 8067–8073 (1998).

[8] D K Joensen , P Voutov , A Szentgyoryi , J Roll , P Gorenstein , P Hoghoj, and F E Christensen. *Design of grazing-incidence multilayer supermirrors for hard-x-ray reflectors*, ***Appl. Opt.*** **34**, 7935–0000 (1995).

[9] T W Barbee Jr, G E Holland, C N Boyer, C M Brown ,and R G Cruddace. *Dual-waveband operation of a multilayer-coated diffraction grating in the soft x-ray range at near-normal incidence*, ***Appl. Opt.*** **32**, 2422–2425 (1993).

[10] R W James. *The Optical Principles of the Diffraction X-rays.* Oxbow Press, Woodbridge, Connecticut (1982).

[11] H J Voorma, E Louis , N B Koster, F Bijkerk,and E Spiller. *Characterization of multilayers by fourier analysis of x-ray reflectivity*, ***J. Appl. Phys.*** **81**, 6112–0000 (1997).

[12] A V Tikhonravov , M K Trubetskov, A A Tikhonravov, and A Duparre. *Effects of interface roughness on the spectral properties of thin films and multilayers*, ***Appl. Opt.*** **42**, 5140–5148 (2003).

[13] H A Macleod. *Thin film optical filters.* McGraw-Hill, New York (1986).

[14] J A Dobrowolski. *Optical properties of films and coatings.* McGraw-Hill, New York (1995).

[15] J A Dobrowolski. *Merti function for more effective thin film calcuations*, ***Appl. Opt.* 2814**, 2824–2831 (1989).

[16] J A Aguilera et al. *Antireflection coatings fro germanium ir optics: a comparsion of numerical desgin mehtods*, ***Appl. Opt.* 27**, 2832–2840 (1998).

[17] J A Dobrowolski and R A Kemp. *Refinement of optical multilayer systems with different optimization procedures*, ***Appl. Opt.* 29**, 2876–2893 (1990).

[18] L Li and J A Dobrowolski. *Computation speeds of different optical thin-film synthesis methods*, ***Appl. Opt.* 31**, 3790–3799 (1992).

[19] A V Tikhonravov. *Some theoretical aspects of thin-film optics and their applications*, ***Appl. Opt.* 32**, 5417–5426 (1993).

[20] A V Tikhonravov. *Some theoretical aspects of thin-film optics and their applications*, ***J. Assoc, Comp. Mach* 8**, 221–229 (1961).

[21] R Luus and T H I Jaakola. *Optimization by direct search and systematic reduction of size of search region*, ***AICHE. J* 19**, 760–766 (1973).

[22] R Luus. *Determination of th region sizes for lj optimization procedure*, ***Hung. J. Ind. Chem* 26**, 281–286 (1998).

[23] R Luus. *Parameter estimation of lotka-volterra problem by direct search optimization*, ***Hung. J. Ind. Chem* 26**, 287–292 (1998).

[24] R Luus, F Hartig, and F J Keil. *Optimal drug scheduling of cancr chemotherapy by dreict search optimization*, ***Hung. J. Ind. Chem* 23**, 55–58 (1995).

[25] Y P Lee, G P Rangaiah, and R Luus. *Phase and chemical equilibrium calculations by direct search optimization*, ***Comput. Chem. Eng.* 23**, 1183–1191 (1999).

[26] E Spiller. *Soft X-rays optics*. SPIE Optical Engineering Press, Bellingham,WA (1994).

[27] P Mikulik. *X-ray reflectivity from planer and structured multialyers*. Universitè Joseph Fourier Grenoble, France (1997).

[28] L G Parrat. *Surface studies of solids by reflection of x-rays*, ***Phy. Rev.* 95**, 359–369 (1954).

[29] D K G de Boer. *Influence of the roughness profile on the specular reflectivity of x-rays and neutrons*, ***Phys. Rev. B* 49**, 5817–5820 (1994).

[30] T Yonte, J Monzón , L Sánchez-Soto , J Carinena ,and C López-Lacasta . *Understanding multilayers from a geometrical viewpoint*, ***J. Opt. Soc. Am. A*** pages 603–609 (2002).

[31] F Mezei. *Novel polarized neutron devices: supermirror and spin component amplifer*, ***Comm. on Phys.* 1**, 81–85 (1976).

[32] K D Joensen. *Design, Fabrication, and Characterization of Multilayer for Broad-band, Hard X-ray Astrophysics instrumentation*. University of Copenhagen (1995).

[33] J Schelten and K Mika. *Calculated reflectivities of supermirrors*, ***Nucl. Instrum. and Meth.* 160**, 287–294 (1978).

[34] J B Hayter and H A Mook. *Discrete thin-film multilayer design for x-ray and neutron supermirrors*, ***J. Appl. Crystallogr*** **22**, 35–41 (1989).

[35] S Yamada, T Ebisawa, N Achiwa, T kiyoshi, and S Okamoto. *Neutron-optical properties of multilayer systems*, ***Annu. Rep. Rec. Rector. Inst*** **11**, 8–27 (1978).

[36] A V Tikhonravov. *Synthesis of optical coatings using optimality conditions*, ***Physics and astronomy series*** **23**, 91–93 (1982).

[37] A N Baskakov and A V Tikhonravov. *Synthesis of two-component optical coatings*, ***Opt. Spectrosc.*** **56**, 915–919 (1984).

[38] I V Kozhevnikov, I N Bukreeva, and E Ziegler. *Theoretical study of multilayer mirrors with a wide spectral band of reflection*, ***Pros. SPIE*** **3448**, 322–331 (1998).

[39] I V Kozhevnikov, I N Bukreeva, and E Ziegler. *Design of x-ray supermirrors*, ***Nucl. Instr. Meth. A*** **460**, 424–443 (2001).

[40] K O Hill, Y Fujii, D C Johnsen, and B S Kawasaki. *Photosensitivity in optical fiber waveguides: Application to reflection filter fabrication*, ***Appl. Phys. Lett*** **32**, 647–649 (1978).

[41] D K W Lam and B K Garside. *characterisation of single-mode optical fiber filters*, ***Appl. Opt.*** **20**, 440–445 (1981).

[42] G Meltz, W W Morey, and W H Glenn. *Formation of bragg gratings in optical fibers by a transverse hlographic method*, ***Opt. Lett.*** **14**, 823–825 (1987).

[43] G A Ball, W W Morey, and H W Glen. *Standing-wave monomode erbium fiber laser*, ***IEEE Photon. Technol. Lett.*** **3**, 613–615 (1991).

[44] J A R Williams, I Bennion, K Sugden, and N J Doran. *Fiber dispersion compensation using a chirped in fiber bragg grating*, ***Electron. Lett.*** **30**, 985–987 (1994).

[45] C R Gilles and V Mizrahi. *Loww-loss add/drop multiplexers for wdm lightwave networks*, ***Proc. IOOC*** pages paper ThC2–1 (Hong Kong 1994).

[46] A D Kersey, H J Patrick,M Leblance, K P Koo, C G Askins, M A Putman, and E J Friebele. *Fiber bragg grating sensors*, ***J. Light. Techn.*** **15**, 1442–1463 (1997).

[47] R Kashyap. *Photosensitive optical fibers: devices and applications*, ***Optic. Fiber. Techn.*** **1**, 17–34 (1994).

[48] R Kashyap,R Wyatt, and R J Campbell. *Wideband gain flattened erbium fiber amplifier using photosenstivie fiber blazed grating*, ***Electron. Lett.*** **29**, 154–156 (1993).

[49] Y Tohmori, F Kano , H Ishii , Y Yoshikuni, and Y Kondo. *Wide tuning with narrow linewidth in dfb lasers with superstructure grating (ssg)*, ***Electron. Lett.*** **29**, 1350–1351 (1994).

[50] N J Frigo. *Ritenet: A passive optical network architecture based on remote interrogation of terminal equipment*, ***Optical Fiber communication Conference OFC'94*** page Post Deadline Paper PD8 (1994).

[51] Z Pan , Y W Song, C Yu, Y Wang, Q Yu, J Popelek, H Li, Y Li, and A E Willner. *Tunable chromatic dispersion compensation in 40-gb/s systems using nonlinearly chirped fiber bragg gratings*, ***J. Light. Techn.*** **20**, 2239–2246 (2002).

[52] H Li, Y Sheng, Y Li, and J E Rothenberg. *Phase-only sampled fiber bragg gratings fro high channel counts chromatic dispersion compensation*, ***J. Light. Techn.*** **21**, 2074–2083 (2003).

[53] H Lee and G P Agrawal. *Purel phase-sampled fiber bragg gratings fro broad-band dispersion and dispersion slope compensation*, ***IEEE Photon. Technol. Lett.*** **15**, 1091–1093 (2003).

[54] M Durkin, M Ibsen and M J Cole, and R I Laming. *1 m long continuously-written fiber bragg gratings fro combined second-and third-order dispersion compesnation*, ***Electron. Lett.*** **33**, 1891–1893 (1997).

[55] W H Loh, F Q Zhou,and J J Pan. *Sampled fiber grating based-dispersion slope compensator*, ***IEEE. Photon. Technol. Lett.*** **11**, 1280–1282 (1999).

[56] Y Painchaud , A Mailoux, H Chotard , E Pelletier ,and M Guy. *Multi-channel fiber bragg gratings fro dispersion and slope compensation*, ***Proc. Optical Fiber communication Conference*** (2002).

[57] M Ibsen , M K Durkin , M J Cole, and R I Laming. *Sinc-sampled fiber bragg gratings fro identical multiple wavelength operation*, ***IEEE Photon. Technol. Lett.*** **10**, 842–844 (1998).

[58] A V Buryak, K Y Kolossovski, and D Y Stepanov. *Optimization of refractive index sampling for multichannel fiber bragg gratings*, ***IEEE J. Quantum Electron.*** **39**, 91–98 (2003).

[59] J E Rothenberg, H Li, Y Li, J Popelek,Y Sheng , Y Wang , R B Wilcox, and J Zweiback. *Dammann fiber bragg grtings and phase-only sampling for high channel counts*, ***IEEE Photon. Technol. Lett.*** **14**, 1309–1311 (2002).

[60] R Kashyap. *Fiber Bragg gratings*. Academic Press, San Diego (1999).

[61] A Yariv. *Copled-mode theory for guided-wave optics*, ***IEEE J. Quantum Electron*** **QE-9**, 919–933 (1973).

[62] T Erdogan. *Fiber grating spectra*, ***J. Light. Techn.*** **15**, 1227–1294 (1997).

[63] C Sun , C Li , and X Yu. *Study on sampled chirped fiber gratings*, ***Opt. Commun.*** **218**, 297–302 (2003).

[64] M Yamada and K Sakuda. *Anaysis of almost-periodic distribuated feedback slab waveguide via a fundamenal matrix appproach*, ***Appl. Opt.*** **26**, 3474–3478 (1987).

[65] B Liao and R Luus. *Comparison of the luus-jaakola optimization procedure and the genetic algorithm*, ***Eng. Optimization*** **37**, 381–398 (2005).

[66] G G Nair. *On the convergence of the lj search method*, ***J. Optim. Theory and applications*** **28**, 429–439 (1979).

[67] F H Stillinger. *Exponential multplicity of inherent structures* **59**, 48–51 (1999).

[68] C Barrón, S Gómez, D Romero, and A Saavedra. *A genetic algorithm for lennard-jones atomic clusters*, ***Appl. Math. Lett.*** **12**, 85–90 (1999).

[69] D M Deaven , N Tit, J R Morris, and K M Ho. *Structural optimization of lennard-jones clusters by a genetic algorithm*, ***Chem. Phys. Lett.*** **256**, 195–2000 (1996).

[70] M D Wolf and U Landman. *Genetic algorithm for structural cluster optimization*, ***J. Phys. Chem. A*** **102**, 6129–6137 (1998).

[71] L T Wales. *Minimum-energy configurations of atomic clusters: new results obtained by simulated annealing*, ***Chem. Phys. Lett.*** **133**, 405–410 (1987).

[72] D J Wales and J P K Doye. *Global optimization by basin-hopping and the lowest energy structures of lennard-jones clusters containing up to 110 atoms*, ***J. Phys. Chem. A*** **101**, 5111–5116 (1997).

[73] J Kennedy and R Eberhart. *Particle swarm optimization*, ***Proceeding of the IEEE International Joint Conference on Neutral Networks*** **IV**, 1942–1948 (1995).

[74] Y Shi and R Eberhart. *A modified particle swarm optimizer*, ***Proceeding of the IEEE International Joint Conference on Evolutinary Computation*** pages 69–73 (1998).

[75] R Eberhart and Y Shi. *Particle swarm optimization: developments, applications and resources*, ***Proceeding of the IEEE International Joint Conference on Evolutinary Computation*** pages 81–86 (2001).

[76] J Kennedy. *The particle swarm: soical adaptation of knowledge*, ***Proceeding of the IEEE International Conference on Evolutinary Computation*** pages 303–308 (1997).